UNIVERSIDADE FEDERAL DE VIÇOSA

Forest fire danger modeling in Portugal

Vicente Paulo Santana Neto
Doctor Scientiae

VIÇOSA - MINAS GERAIS
2026

VICENTE PAULO SANTANA NETO

Forest fire danger modeling in Portugal

Thesis submitted to the Forest Science Graduate Program of the Universidade Federal de Viçosa in partial fulfillment of the requirements for the degree of *Doctor Scientiae*.

Adviser: Jose Marinaldo Gleriani

Co-adviser: Fillipe T. Pereira Torres

VIÇOSA - MINAS GERAIS
2026

Ficha catalográfica elaborada pela Biblioteca Central da Universidade Federal de Viçosa - Campus Viçosa

T
S232f
2026

Santana Neto, Vicente Paulo, 1995-
Forest fire danger modelling in Portugal / Vicente Paulo Santana Neto. – Viçosa, MG, 2026.
1 tese eletrônica (104 f.): il. (algumas color.).

Texto em inglês.
Orientador: José Marinaldo Gleriani.
Tese (doutorado) - Universidade Federal de Viçosa, Departamento de Engenharia Florestal, 2026.
Inclui bibliografia.
DOI: https://doi.org/10.47328/ufvbbt.2026.409
Modo de acesso: World Wide Web.

1. Incêndios florestais - Prevenção - Simulação por computador. 2. Incêndios florestais - Portugal. 3. Aprendizado do computador. I. Gleriani, José Marinaldo, 1966-. II. Universidade Federal de Viçosa. Departamento de Engenharia Florestal. Programa de Pós-Graduação em Ciência Florestal. III. Título.

GDFC adapt. CDD 634.94320113

Bibliotecário(a) responsável: Euzébio Luiz Pinto CRB-6/3317

VICENTE PAULO SANTANA NETO

Forest fire danger modeling in Portugal

Thesis submitted to the Forest Science Graduate Program of the Universidade Federal de Viçosa in partial fulfillment of the requirements for the degree of *Doctor Scientiae*.

APPROVED: June 29, 2026.

Assent:

Vicente Paulo Santana Neto
Author

Jose Marinaldo Gleriani
Adviser

Essa tese foi assinada digitalmente pelo autor em 07/07/2026 às 16:53:33 e pelo orientador em 07/07/2026 às 19:02:11. As assinaturas têm validade legal, conforme o disposto na Medida Provisória 2.200-2/2001 e na Resolução nº 37/2012 do CONARQ. Para conferir a autenticidade, acesse https://siadoc.ufv.br/validar-documento. No campo 'Código de registro', informe o código **LJF2.RLNH.A6XY** e clique no botão 'Validar documento'.

À minhas filhas de quatro patas Safira e Pérola, por serem a luz nos meus dias mais escuros, e serem minha ponte entre os dois mundos,
Dedico com amor.

ACKNOWLEDGMENTS

To my mother, Luciene, the most important person in my entire life. Thank you for bringing me into the world, supporting, guiding, and raising me with unconditional love.

To my fiancée and future wife, Suellen, for being the light that brightens my days, the color that brings life to my world, and the safe haven that keeps me grounded. For being my greatest companion and friend, the person who listens to, cares for, and loves me every day and night.

To my grandmother, Helena, for being my first and most incredible teacher, and for all her love and affection.

To my little dogs, Safira and Mário, for their eternal love and companionship. To my beloved Pérola, my great companion, for loving and watching over me wherever she is. And to my first daughter, Belinha, for showing me an animal's infinite love and pointing me to this path of animal protection.

To my father, Márcio, for his love and bringing me into this world. To my father at heart, Mário, for raising and loving me as a son. To my brother, for his companionship and being my great childhood role model.

To my aunts, uncles, and cousins, Heleno, Flávia, Geraldo, Caio, and Arthur, and all other family members, for the good times, love, and affection always dedicated to me. To my stepmother, Alessandra, for being so good to me and my father.

To my goddaughters at heart, Helena and Yara, for being so incredible and making my life happier.

To my advisor, Dr. José Marinaldo Gleriani, for his exquisite guidance and the solid friendship we built. To my co-advisor, Dr. Fillipe Tamiozzo Pereira Torres, for his guidance and all opportunities given to me.

To the examining board for dedicating their time to this work: to Profa. Dra. Adélia de Jesus Nobre Nunes, for her guidance and caring for me like a son during my time in Portugal. To my eternal advisor and friend, Prof. Dr. Fausto Weimar Acerbi Júnior, for being my great role model as a professor and researcher. To Prof. Dr. Alexandre Simões Lorenzon, for contributing to my growth as a researcher during my master's.

To my great friend Igor Sanches, who helped me immensely in preparing the Graphical Abstracts. To my great friend Jeffin, for being a fundamental partner in happy and difficult times, always present. To my friend Matheus Silveira, for being a great friend, admirable professional, and excellent coworker.

To my friends João Mokdeci, Mariana Cruz, Polyanne Coelho, Bruna Queiroz, Candinha, Bianca and Luis, Alessandro and Isabela, and Samuel, and others not mentioned, for providing happy moments and making this journey lighter. To the friends I met in Portugal, Gabriela Veroes, Renato Spigarello, Erick Ferreira, Everton Kozenieski, Maurizio Zambaldi, and the rest, for being my family away from home. To Thaynele, my psychologist, for taking care of my mind for years with such dedication.

To the Universidade Federal de Viçosa, for the opportunity to pursue graduate studies; to all professors, and the staff of the Departamento de Engenharia Florestal. And to the Centro de Estudos em Geografia e Ordenamento do Território (CEGOT), for the infrastructure provided during my sandwich doctorate, financed by national funds through the Fundação para a Ciência e a Tecnologia (FCT) under reference UIDB/04084/2025.

This work has been sponsored by the following Brazilian research agencies: Coordination for the Improvement of Higher Education Personnel (CAPES; Financing code 001), Minas Gerais State Foundation for Research Aid (FAPEMIG) and National Council of Scientific and Technological Development (CNPq).

"Fate is inexorable. Wyrd bið ful aræd. Fate is uncaressed, unkind, and unyielding, but a man must still walk his path."

Bernard Cornwell, The Last Kingdom

ABSTRACT

NETO, Vicente Paulo Santana, D.Sc., Universidade Federal de Viçosa, June, 2026. **Forest fire danger modeling in Portugal**. Adviser: Jose Marinaldo Gleriani. Co-adviser: Fillipe Tamiozzo Pereira Torres.

Wildfires represent a significant socio-ecological threat worldwide, with severe impacts in the Mediterranean region, particularly in Portugal. Accurate modeling of wildfire susceptibility and hazard is crucial for preventive planning and effective mitigation. This thesis aimed to advance the spatial and temporal assessment of wildfires in central Portugal by employing geoprocessing and machine learning approaches. The central research problem stems from the need to overcome the limitations of traditional models, which frequently rely on static annual averages and overlook the seasonal dynamics of driving factors and the protective effect of fuel memory. The global methodology of the thesis was divided into two complementary approaches: the first focused on wildfire susceptibility mapping using the Random Forest algorithm with 13 socio-environmental variables;the second investigated fire hazard through seasonally-disaggregated models generated via a data-driven Spatial Multi-Criteria Evaluation (SMCE) and Simple Additive Weighting (SAW) approach, and tested the incorporation of fuel age via the Fire Return Interval (FRI). Consolidated results demonstrated that susceptibility models achieved high predictive accuracy (AUC of 84.68%) by identifying the specific contribution of structural variables. Furthermore, evidence showed that seasonally disaggregated models (High, Medium, and Low seasons) systematically outperform overall annual models. A fundamental conclusion of this thesis is that, during the critical periods of the high-fire season, extreme weather conditions override the constraints imposed by fuel memory (recently burned areas), refuting the hypothesis that the FRI strictly limits fire spread. These findings highlight the absolute need to integrate both structural spatial drivers and dynamic seasonal components for more resilient wildfire management.

Keywords: machine learning; fire susceptibility; fire probability; fire return interval (fri)

RESUMO

NETO, Vicente Paulo Santana, D.Sc., Universidade Federal de Viçosa, junho de 2026. **Modelagem do perigo de incêndios florestais em Portugal**. Orientador: Jose Marinaldo Gleriani. Coorientador: Fillipe Tamiozzo Pereira Torres.

Os incêndios florestais representam uma ameaça socioecológica significativa em todo o mundo, com impactos severos na região do Mediterrâneo, especialmente em Portugal. A modelagem precisa da suscetibilidade e do perigo de incêndios é fundamental para o planejamento e a mitigação destes eventos extremos. Esta tese teve como objetivo geral avançar na avaliação espacial e temporal dos incêndios florestais na região central de Portugal, empregando abordagens de geoprocessamento e aprendizado de máquina. O problema central da pesquisa baseia-se na necessidade de superar as limitações dos modelos tradicionais, que frequentemente utilizam médias anuais estáticas e negligenciam a dinâmica sazonal dos fatores causais e o efeito limitante da memória do combustível. A metodologia global da tese dividiu-se em duas abordagens complementares: a primeira focou no mapeamento da suscetibilidade ao fogo utilizando o algoritmo Random Forest alimentado por 13 variáveis socioambientais; a segunda investigou o perigo de incêndio por meio de modelos sazonalmente desagregados (Alta, Média e Baixa estação), gerados via Avaliação Multicritério Espacial (SMCE) guiada por dados e ponderação aditiva (SAW), e testou a incorporação da idade do combustível, via Intervalo de Retorno do Fogo (FRI). Os resultados consolidados demonstraram que os modelos de suscetibilidade obtiveram alta precisão preditiva (AUC de 84,68%) ao identificar a contribuição específica de variáveis estruturais. Em adição, evidenciou-se que modelos de perigo desagregados por estação superam o desempenho dos modelos anuais globais. Uma conclusão fundamental da tese é que, durante os períodos críticos da estação de alto risco, as condições meteorológicas extremas anulam a restrição imposta pela memória do combustível, refutando a hipótese de que o FRI restringe intrinsecamente a propagação do fogo. Estes resultados destacam a necessidade de integrar fatores espaciais estruturais e dinâmicas sazonais para um gerenciamento mais resiliente dos incêndios florestais.

Palavras-chave: aprendizado de máquina; susceptibilidade de incêndios; probabilidade de incêndios; intervalo de retorno do fogo (irf)

SUMMARY

GENERAL INTRODUCTION

Wildfires are a globally important and integral part of many ecosystems, playing key roles in ecosystem dynamics and the retention of species that have evolved in response to fire (Pausas and Keeley, 2019). From an ecological perspective, fire disturbances generate open habitats that enable the evolution of a diversity of shade-intolerant plants and animals (Pausas and Keeley, 2019). However, wildfires are also perceived as undesirable and uncontrolled events, representing hazardous phenomena that pose severe risks to human safety and the environment (Leuenberger et al., 2018). When fire regimes exceed historical bounds, they become a major cause of soil degradation through nutrient volatilization and increased susceptibility to erosion (Agbeshie et al., 2022). Furthermore, fire is a primary driver of biodiversity loss, depletion of terrestrial ecosystem productivity, and the exhaustion of forest carbon stocks (Sannigrahi et al., 2020). Beyond immediate terrestrial impacts, the arrival of heavy rains following a fire often triggers intense hydro-geomorphic processes, including flash floods and the pollution of adjacent water bodies due to ash and sediment transport (Marquez Torres et al., 2023).

The Mediterranean Basin is Europe's primary fire hotspot, where the landscape is characterized by an extensive wildland-urban interface (WUI) that increases the probability of human-caused ignitions (San-Miguel-Ayanz et al., 2013). In Portugal, wildfires are a recurring hazard, with records indicating an annual average of 147,000 ha burned between 2000 and 2018 (Oliveira et al., 2021). The catastrophic potential of this fire regime was demonstrated in 2017, when mega-fires resulted in massive socio-economic impacts, destruction of forest carbon sequestration capacity, and tragic human casualties (Turco et al., 2019). Rational wildfire defense and suppression plans require, first and foremost, accurate estimates of the differential susceptibility of the land to wildfires in relation to the specific characteristics of the territory (Jaafari et al., 2018).

To assess the susceptibility and hazard of wildland fires in specific regions, it is necessary to comprehensively consider the local natural environment, climate conditions, and anthropogenic activities (Yue et al., 2023). Most traditional hazard models, however, are limited by the use of spatially coarse climatic data, rather than local fire weather variables, which are often significant drivers of fire area and severity (Zald and Dunn, 2018). Furthermore, static annual assessments fail to reflect the seasonal impacts of wildfires on ecosystems, as ecological value and fire susceptibility vary dynamically over time (Tang et al., 2022). The development of predictive models is also hindered by the massive effort required in the assembly, validation, and linkage of longitudinal historical fire databases across governmental agencies (Xi et al., 2019).

Despite significant progress in risk research, current susceptibility models often lack detailed analysis regarding the specific contributions of variables and the mechanisms behind model decisions (Yue et al., 2023). Many studies in the field have proposed initial approximations based on expert evaluations, which are inherently subjective, or have used static frameworks that become obsolete without regular renewal (Arrogante-Funes et al., 2022; Marquez Torres et al., 2023). Therefore, there is a clear need for advanced, dynamic modeling approaches that account for the complexity of socio-ecological systems and the heterogeneity of fuel characteristics (Vigna et al., 2021; Jenkins et al., 2020).

Addressing these methodological needs, the general objective of this thesis is to advance the spatial and temporal assessment of wildfire susceptibility and hazard in central Portugal (Santana Neto et al., 2025). This research utilizes machine learning approaches spatial multi-criteria evaluation to quantify the specific contributions of biophysical and anthropogenic drivers to fire occurrence, while overcoming traditional static modeling limitations through seasonal disaggregation and the integration of historical fire metrics. To achieve this, the comprehensive susceptibility assessment developed in Chapter 1 serves as the fundamental baseline for Chapter 2. By establishing the inherent spatial propensity to fire, it provides the necessary geographical framework to subsequently integrate temporal dynamics and historical fire regimes into the season-specific hazard models. By transitioning from annual averages to dynamic, season-specific hazard assessments, this work provides an improved predictive framework for more effective and resilient forest fire management.

REFERENCES

Caúla, R.H., Oliveira-Júnior, J.F., Lyra, G.B., Delgado, R.C., Heilbron Filho, P.F.L., 2015. Overview of fire foci causes and locations in Brazil based on meteorological satellite data from 1998 to 2011. Environmental Earth Sciences 74, 1497–1508. https://doi.org/10.1007/s12665-015-4142-z

Duguy, B., Paula, S., Pausas, J.G., Alloza, J.A., Gimeno, T., Vallejo, R.V., 2013. Effects of Climate and Extreme Events on Wildfire Regime and Their Ecological Impacts, in: Navarra, A., Tubiana, L. (Eds.), Regional Assessment of Climate Change in the Mediterranean, Advances in Global Change Research. Springer Netherlands, Dordrecht, pp. 101–134. https://doi.org/10.1007/978-94-007-5772-1_6

Eugenio, F.C., Dos Santos, A.R., Fiedler, N.C., Ribeiro, G.A., Da Silva, A.G., Dos Santos, Á.B., Paneto, G.G., Schettino, V.R., 2016. Applying GIS to develop a model for forest fire risk: A case study in Espírito Santo, Brazil. Journal of Environmental Management 173, 65–71. https://doi.org/10.1016/j.jenvman.2016.02.021

Fu, Y.H., Zhao, H., Piao, S., Peaucelle, M., Peng, S., Zhou, G., Ciais, P., Huang, M., Menzel, A., Peñuelas, J., Song, Y., Vitasse, Y., Zeng, Z., Janssens, I.A., 2015. Declining global warming effects on the phenology of spring leaf unfolding. Nature 526. https://doi.org/10.1038/nature15402

Gimingham, C.H., Johnson, E.A., 1993. Fire and Vegetation Dynamics: Studies from the North American Boreal Forest. The Journal of Ecology 81, 384. https://doi.org/10.2307/2261510

IPCC, 2013. Summary for policymakers, Managing the Risks of Extreme Events and Disasters to Advance Climate Change Adaptation: Special Report of the Intergovernmental Panel on Climate Change. https://doi.org/10.1017/CBO9781139177245.003

IPCC, 2007. Climate Change 2007: Impacts, Adaptation and Vulnerability. Contribution of Working Group II to the Fourth Assessment Report of the Intergovernmental Panel on Climate Change. Journal of Environmental Quality. https://doi.org/10.2134/jeq2008.0015br

Moreno, J., Vallejo, R., Chuvieco, E., 2013. Current fire regimes, impacts and the likely changes-VI: Euro Mediterranean. Vegetation Fires and Global Change: Challenges for Concerted International Action 115–131.

Moreno, J.M.; Urbieta, I.R.; Bedia, J.; Gutierrez, J.M.; Vallejo, V.R., 2015. Los incendios forestales en España ante al cambio climático, in: Los Bosques y La Biodiversidad Frente al Cambio Climático: Impactos, Vulnerabilidad y Adaptación En España. pp. 395–405.

Nunes, A., Lourenço, L., Bento-Gonçalves, A., Vieira, A., 2013. Três décadas de incêndios florestais em Portugal: incidência regional e principais fatores responsáveis. GeoJou 133–143. https://doi.org/10.14195/0871-1623_32_12

Peters, G.P., Andrew, R.M., Boden, T., Canadell, J.G., Ciais, P., Le Quéré, C., Marland, G., Raupach, M.R., Wilson, C., 2013. The challenge to keep global warming below 2 °C. Nature Clim Change 3, 4–6. https://doi.org/10.1038/nclimate1783

Pirovani, D.B., Pezzopane, J.E.M., Xavier, A.C., Pezzopane, J.R.M., de Jesus Júnior, W.C., Machuca, M.A.H., dos Santos, G.M.A.D.A., da Silva, S.F., de Almeida, S.L.H., de Oliveira Peluzio, T.M., Eugenio, F.C., Moreira, T.R., Alexandre, R.S., dos Santos, A.R., 2018. Climate change impacts on the aptitude area of forest species. Ecological Indicators 95. https://doi.org/10.1016/j.ecolind.2018.08.002

Romps, D.M., Seeley, J.T., Vollaro, D., Molinari, J., 2014. Projected increase in lightning strikes in the united states due to global warming. Science 346, 851–854. https://doi.org/10.1126/science.1259100

San-Miguel-Ayanz, J., Moreno, J.M., Camia, A., 2013. Analysis of large fires in European Mediterranean landscapes: Lessons learned and perspectives. Forest Ecology and Management 294, 11–22. https://doi.org/10.1016/j.foreco.2012.10.050

Swetnam, T.W., 1993. Fire history and climate change in giant sequoia groves. Science 262, 885–889. https://doi.org/10.1126/science.262.5135.885

CHAPTER I

Assessing wildfire susceptibility and driving variables in Portugal using machine learning approach

Published in the **Journal for Nature Conservation**
DOI: https://doi.org/10.1016/j.jnc.2025.126956

Vicente Paulo Santana Neto[a], Adelia de Jesus Nobre Nunes[b], Fillipe Tamiozzo Pereira Torres[a], José Marinaldo Gleriani[a], Diogo Nepomuceno Cosenza[a].

[a] Universidade Federal de Viçosa/UFV, Departamento de Engenharia Florestal,
Rua Purdue - Campus UFV, 36570-900, Viçosa – MG, Brasil.
[b] Universidade de Coimbra, Faculdade de Letras, Departamento de Geografia e Turismo
Colégio de S. Jerónimo, 3004-530, Coimbra, Portugal.

Journal for Nature Conservation 86 (2025) 126956

Contents lists available at ScienceDirect

Journal for Nature Conservation

journal homepage: www.elsevier.com/locate/jnc

Assessing wildfire susceptibility and driving variables in Portugal using machine learning approach

Vicente Paulo Santana Neto [a,*], Adelia de Jesus Nobre Nunes [b], Fillipe Tamiozzo Pereira Torres [a], José Marinaldo Gleriani [a], Diogo Nepomuceno Cosenza [a]

[a] *Universidade Federal de Viçosa/UFV, Departamento de Engenharia Florestal, Rua Purdue - Campus UFV, 36570-900 Viçosa, MG, Brazil*
[b] *Universidade de Coimbra, Faculdade de Letras, Departamento de Geografia e Turismo, Colégio de S. Jerónimo, 3004-530 Coimbra, Portugal*

ARTICLE INFO

Keywords:
Burning susceptibility mapping
Random forest
GIS
Central Portugal
Remote sensing
Land variables
AUC

ABSTRACT

Wildfires fulfill various social and ecological functions, potentially causing loss and destruction of resources, lives, and urban infrastructure, as well as modifying the landscape and contributing to climate change. The objective of the work is to generate a fire susceptibility map for central Portugal using the Random Forest method, and to evaluate the importance of variables in the model and select those that contribute most to the accuracy of the susceptibility map. For the model, 13 social or environmental variables and the history of fires in the region were used for fire modeling with Random Forest, where only 10 were considered important for the model. For validation, the Kappa and accuracy of the fire occurrence classification model, Area Under the Curve (AUC), and burned area relative to susceptibility classes were calculated. The best model presented a Kappa of 0.641, AUC of 84.68%, and showed that the burned area increased with the increase in wildfire susceptibility. Population density and firefighter density were the most important variables, while environmental ones proved to be an important support for fire modeling. Thus, the results enable assisting in the suppression and prevention of fires, mainly in the furthest inland and less populous regions of the area, while advancing the understanding of fire regimes and playing a crucial role in protecting biodiversity by identifying ecosystems susceptible to wildfires.

1. Introduction

Wildfires serve numerous social and ecological functions, including creating open habitats that support shade-intolerant plants and animals, regulating fire intensity and pest control, preventing catastrophic fires, supporting cultural and recreational practices, promoting habitat heterogeneity by enhancing biodiversity and ecosystem resilience, and improving genetic variability and species diversity (Pausas & Keeley, 2019); however, they can cause loss and destruction of resources, human lives, and urban infrastructure (Tran et al., 2024). They also act as a landscape modifier, altering the existing ecosystem function (Camargo et al., 2018; Costa et al., 2022) and impacting the soil and water quality and characteristics (Nitzsche et al., 2024; Nunes & Lourenço, 2017; Ribeiro et al., 2021; Sequeira et al., 2020). In addition, they can be responsible for high CO_2 emissions, thus contributing to climate change, and the consequent increase in fires due to the rise in global temperature (Costa et al., 2023; Stephens et al., 2020).

Mediterranean countries face the challenge of large-scale wildfires annually, with Portugal recording the highest average annual number of fires among them (Bergonse et al., 2022). The central region of Portugal is characterized by a diverse topography and vegetation and is particularly susceptible to wildfires (Nunes et al., 2016, 2023b, 2023a). Indeed, this susceptibility has led to 26,560 km^2 of burned areas in the period from 1975 to 2022, totaling an annual average of 565 km2 (ICNF, 2023). This is equivalent to 2 % of the country's territory each year. For instance, in 2017 Portugal experienced extreme weather conditions that favored a large wildfire, causing 113 fatalities (Turco et al., 2019). Similarly, a wildfire in Castelo Branco in 2019 resulted in dozens of injured people (Calheiros et al., 2022; Santana Neto et al., 2022).

Wildfires can have natural causes, but they are primarily caused by anthropogenic factors such as arson, the burning of debris, smoking, campfires, railways and equipment use (Oliveira et al., 2012; Santana Neto et al., 2022). To predict and prevent wildfires, addressing human causes directly linked to land use is crucial; however, it remains a

* Corresponding author.
E-mail addresses: vipsneto@gmail.com, vicentepneto@ufv.br (V.P. Santana Neto), adeliajnnunes@gmail.com, adelia.nunes@fl.uc.pt (A.J. Nobre Nunes), tamiozzo@ufv.br (F.T. Pereira Torres), gleriani@gmail.com, gleriani@ufv.br (J.M. Gleriani), diogo.cosenza@ufv.br (D.N. Cosenza).

https://doi.org/10.1016/j.jnc.2025.126956
Received 20 January 2025; Received in revised form 23 April 2025; Accepted 23 April 2025
Available online 3 May 2025
1617-1381/© 2025 Elsevier GmbH. All rights are reserved, including those for text and data mining, AI training, and similar technologies.

complex and challenging task. Therefore, understanding the spatial relationships among the natural drivers of fires can provide valuable information about their frequency and the areas potentially threatened by fires (Sari, 2024).

Risk, ignition, susceptibility and fire hazard maps are crucial tools for land management and planning since they allow the identification of areas prone to wildfires (Akıncı & Akıncı, 2023; Milanović et al., 2021; Nunes et al., 2023a). According to Bachmann and Allgöwer (2001), wildfire risk is defined as the likelihood of a wildfire occurring in a certain location under specified conditions, as well as the predicted effects on impacted areas. Ignition maps specifically identify areas with a high likelihood of fire initiation (Santos et al., 2022).

Susceptibility refers to the area's natural tendency to experience or support wildfires due to factors like elevation, slope, and vegetation cover, while fire hazard refers to the overall likelihood of wildfires occurring, taking into account potential ignition sources and environmental conditions. By integrating susceptibility with the probability of wildfire occurrence, the concept of hazard is established (Parente & Pereira, 2016; Verde & Zêzere, 2010).

Furthermore, the susceptibility map provides valuable insights into areas naturally predisposed to wildfires, emphasizing environmental factors such as elevation, slope, and vegetation cover. Wildfires were often related to anthropic factors, indicating that human-related variables (such as population density) should be considered. Several authors state that these variables are intrinsic to the territory, reflecting enduring characteristics due to their relative stability over time (Parente & Pereira, 2016; Santos et al., 2022; Verde & Zêzere, 2010).

These maps are important tools for developing prevention and mitigation strategies, which significantly contribute to the reduction of wildfire risks (Tran et al., 2024). There are various methods for creating fire susceptibility maps, such as the Analytical Hierarchical Process (AHP) (Kayet et al., 2020; Nunes et al., 2023b), parametric models (Oliveira et al., 2012; Santana Neto et al., 2022; Xiao et al., 2015), and machine learning models (Akıncı & Akıncı, 2023; Iban & Sekertekin, 2022; Pourghasemi et al., 2020). Of these methods, the Random Forest machine learning method (Breiman, 2001) stands out for its ability to process large volumes of data and identify complex patterns accurately (Akıncı & Akıncı, 2023; Iban & Sekertekin, 2022; Milanović et al., 2023; Santana Neto et al., 2022; Yue et al., 2023).

Despite its widespread use in literature, the Random Forest approach frequently becomes a black-box, making model analysis and interpretation more challenging. Furthermore, the failure to account for the temporal variation of certain variables, as well as the exclusion of anthropogenic variables closely related to fires (such as population density and firefighter density), may jeopardize the efficiency and correlation of the results with the real world. Incorporating these parameters is critical for increasing the robustness and practical usability of the produced models.

The study's hypothesis is that both socioeconomic (such as population density and firefighter density) and biophysical variables of the territory (such as elevation, temperature, and precipitation) influence fire susceptibility, with higher values indicating a higher susceptibility to forest fires. On the other hand, it is proposed that the interaction of these variables, rather than the isolation of each factor, is critical for accurately modeling the risk of forest fires and understanding their dynamics in the region. Finally, we hypothesize that the combined method of machine learning and GIS to produce forest fire susceptibility maps improves the results accuracy.

Considering the above hypothesis, the main objectives of this research are to develop a fire susceptibility map for central Portugal using the Random Forest method and to assess the significance of various variables in predicting forest fire occurrences. This study is distinguished by the use of Shapley analysis to interpret the contributions of the variables, with a particular emphasis on population and firefighter density as novel and distinguishing factors in comparison to the existing literature. The study's goal is to show how incorporating these unusual anthropogenic factors into wildfire susceptibility research can have a significant impact on the model's results. By identifying and quantifying the impact of these variables, the study hopes to improve understanding of forest fire dynamics and provide valuable insights for developing more effective fire prevention and management strategies in the region.

2. Material and methods

2.1. Study area

The Central Region of Portugal spans 28,199 km^2 with 100 municipalities varying in population density, geomorphology, and climate (Nunes et al., 2023b) (Fig. 1). Altitudes range from the Central Cordillera mountains to coastal areas. Summer temperatures average 16–33.7 °C, precipitation 14–194 mm, and wind speeds 3.26–7.71 m/s at 20 m height (Costa & Estanqueiro, 2023; IPMA, 2009a; 2009b). Population density ranges from uninhabited areas to 535.81 inhabitants/ha, concentrated in district capitals (INE, 2022). Firefighter density declined from 0 to 640.96/km^2 in 1998 to 4.42–360.06/km^2 by 2021, with outliers like Espinho (INE, 2024).

Bergonse et al. (2023) describes four distinct fire regimes in Central Portugal, based on variations in burned area extent, wildfire frequency, and temporal concentration. The first regime features the smallest and most temporally concentrated burned areas, along with the lowest wildfire frequency. The second regime involves more extensive burned areas and higher wildfire frequency than the first, with less temporal concentration. The third regime is characterized by the most extensive burned areas and the highest wildfire frequency, with fires spread over time. In contrast, the fourth regime has slightly less extensive burned areas but a much lower wildfire frequency, with the burned areas being more temporally concentrated.

There was also a change in land use and cover, with emphasis on the reduction of coniferous forests and an increase of eucalyptus forests in the region (Fig. 2). Additionally, the other land cover and use (LCU) classes underwent minor area changes in relation to those mentioned above (DGTerritório, 2022).

2.2. Variables description

For wildfire modeling, georeferenced polygons of burned areas (1990–2022) were used, partially aligned with Portugal's census data (1991, 2001, 2011, 2021). Wildfires are mapped via GPS surveys (Tedim et al., 2013) and Sentinel-2 images (10-meter resolution), detecting fires over 10 ha through vegetation and heat algorithms. Refer to ICNF (2023) for further details. The year 2017 was excluded due to the abnormal behavior of fires in the study area caused by extreme weather conditions that favored them (Turco et al., 2019).

The data obtained from the fire images were utilized in the machine learning model as a response variable, classified binomially into "occurrence" and "no occurrence", and georeferenced images of environmental, social, and climatic factors were used as explanatory (Table 1).

Data from the demographic censuses of the National Institute of Statistics (INE, 2022) containing population numbers from 1991, 2001, 2011, and 2021 were applied for modeling. For details on the census methodology, refer to INE (2022). The data were converted into population density (inhabitants per hectare).

Information about the number of firefighters from 1998, 2001, 2007, 2009, 2012, 2018, and 2021 were used (INE, 2013; 2024). Just like the

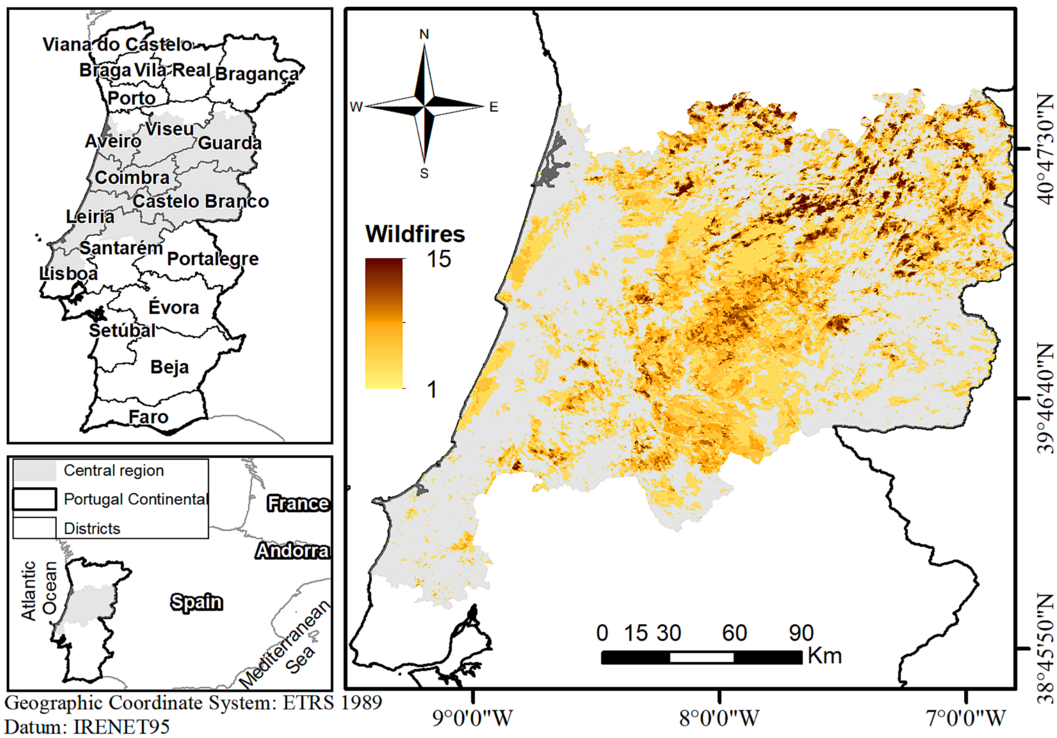

Fig. 1. On the upper left, a map of the central region and its surroundings, with a district division and identification. On the lower left, the location of mainland Portugal in relation to the European continent. On the right, the study area and the number of fires from 1975 to 2022 (ICNF, 2023).

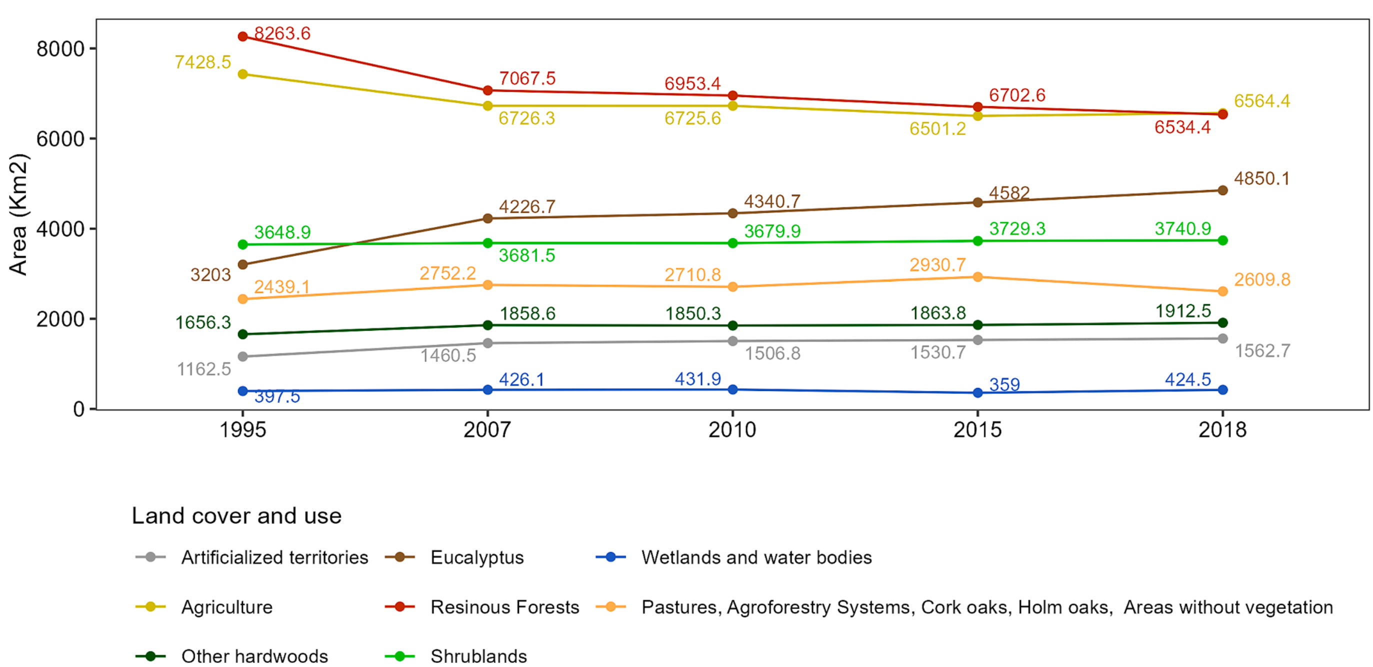

Fig. 2. Changes in Land Cover and Use in Central Portugal from 1995 to 2018.

Table 1
Geospatial explanatory variables applied in the modeling of fire susceptibility.

Name	Acronym (unit)	Description	Scale / Resolution	Source
Population density	POP (Count/ha)	Number of habitants per hectare	County municipality level	(INE, 2022)
Firefighter density	FFD (Count/ha)	Number of firefighters per hectare	County municipality level	(INE, 2013; 2024)
Land cover and use	LCU	Type of land cover and/or use	Minimum cartographic unit: 1 ha / Minimum distance between lines: 20 m / Scale: 1:25,000	(DGTerritório, 2022)
Euclidean distance from agricultural areas	EDA (km)	Euclidean distance from agricultural areas	Minimum cartographic unit: 1 ha / Minimum distance between lines: 20 m / Scale: 1:25,000	(DGTerritório, 2022)
Average of the maximum summer temperature	TMAX (°C)	Average of the maximum temperature of each summer day	100 m	(IPMA, 2009a)
Accumulated precipitation in the summer	PREC (mm)	Accumulated precipitation in the summer	100 m	(IPMA, 2009c)
Number of days with temperature above 25 °C	T25 (°C)	Number of days with temperature above 25 °C	100 m	(IPMA, 2009c)
Number of days with precipitation above 10 mm	P10	Number of days with precipitation above 10 mm	100 m	(IPMA, 2009d)
Elevation	ELV (m)	Altitude relative to sea level	10 m	(ASF, 2024)
Slope	SLP (°)	Slope of relief, in degrees	10 m	(ASF, 2024)
Solar Radiation	RAD (Whm^2)	Incident solar radiation on a point	10 m	(ASF, 2024)
Aspect	ASP	Orientation of the slopes according to cardinal points	10 m	(ASF, 2024)
Average wind speed	AWS (m/s)	Wind speed measured at 20 m height	500 m	(Costa & Estanqueiro, 2023)

population's variable, these data were normalized per area, converting the number of firefighters per covered area (FFD), to ensure representativeness. For further methodological details, refer to INE (2013; 2024).

Land cover and use (LCU) maps from 1995, 2007, 2010, 2015, and 2018 were utilized in this study. For details regarding their methodology, refer to DGTerritório (2022). The maps were regrouped into eight categories based on technical expertise: Artificialized territories; Agriculture; Pastures, Agroforestry Systems, Cork oaks, Holm oaks, and Areas without vegetation; Other hardwoods; Eucalyptus; Resinous Forests; Shrublands; and Wetlands and water bodies. Additionally, the Euclidean Distance of Agriculture areas (EDA) variable was developed using the agriculture category.

The data related to the topography of the region were derived from ALOS PALSAR digital elevation model (ASF, 2024). From this image, the Elevation (ELV), Slope (SLP), Slope Orientation or Aspect (ASP), and Solar Radiation (RAD) were generated.

For climate characterization, maps of summer maximum air temperature (TMAX) and total summer precipitation (PREC), averaged over 1971–2000, were used (IPMA, 2009a, 2009b). Additionally, the annual number of days with maximum air temperature ≥ 25 °C (T25) and the number of days with precipitation ≥ 10 mm (P10) were included for the same period (IPMA, 2009c; IPMA, 2009d). Further methodological details can be found in Cunha et al. (2010).

Lastly, a map of the average wind speed in m/s (AWS) of Continental Portugal at a reference height of 20 m and a spatial resolution of 500 m was used (Costa & Estanqueiro, 2023).

2.3. *Data processing*

2.3.1. *Sampling*

Maps were processed in *ArcMap 10.8* (ESRI, 2011), cropped to the central region of Portugal, and resampled to a 30 m pixel size. Binary fire data, excluding occurrences under one hectare, were used, as small fires account for a minor share of the total burned area (Calheiros et al., 2022). Data were divided into eleven three-year groups (Table 2), with time-varying variables assigned to the nearest available date and constant variables repeated across all groups.

The data sampling for the modeling was conducted in the R environment (R Core Team, 2024), where the maps of each group were overlapped and converted into a dataframe, with each row corresponding to a pixel. Subsequently, all eleven data frames (groups) were consolidated and randomly sampled to represent 0.02 % of the total map

Table 2
Division of fire occurrence and variable groups, considering the temporality of the variables. POP: Populational density; FFD: Firefighter density; LCU: Land cover and use; EDA: Euclidean distance from agricultural areas.

Group	Wildfires	POP	FFD	LCU	EDA	Other variables
1	2020–2022	2021	2021	2018	2018	Constant
2	2017–2019	2021	2018	2018	2018	
3	2014–2016	2011	2015	2015	2015	
4	2011–2013	2011	2012	2010	2010	
5	2008–2010	2011	2009	2010	2010	
6	2005–2007	2011	2007	2007	2007	
7	2002–2004	2001	2001	2007	2007	
8	1999–2001	2001	2001	1995	1995	
9	1996–1998	2001	1998	1995	1995	
10	1993–1995	1991	1998	1995	1995	
11	1990–1992	1991	1998	1995	1995	

pixels. This step was taken to reduce computational demands and ensure efficient data processing.

To maintain the representativeness of the samples, the proportion between the samples was determined based on the occurrence ratio of burned areas (from 1990 to 2022, excluding 2017) and unburned areas. Thus, the total burned area corresponded to approximately 14,146 km^2 (43 % of Central Portugal area) considering the recurrence of burns by area (e.g., 10-hectare polygons that burned twice will be counted as 20 ha of wildfire), and 18,575 km^2 (57 %) of unburned area. Afterwards, the sample data was split into training and test data, corresponding to 75 % and 25 % of the sample, respectively. The Pearson correlation between the variables was then computed, also in R environment.

2.3.2. *Wildfires modeling*

The *Random Forest* (Breiman, 2001) model was trained using the fire occurrence as the response, which was derived from historical data from 1990 to 2022 (except 2017), and the other variables as explanatory. We set the following model parameters: mtry = 4 and ntree = 1000, while the others were set to the package default. We set mtry = 4 because it closely approximates the square root of the number of variables (13), as recommended by Huang and Boutros (2016).

The work was carried out in two stages. First, a model was generated using all explanatory variables, and the importance of each variable was calculated using the VIP package (Greenwell & Boehmke, 2020). Subsequently, a second model was created, excluding the variables that had less than 50 % relative importance as determined in the first model. The importance of each variable was quantified using the Gini impurity function, aggregating their importance across all trees in the model and normalizing them such that the most influential variable reaches a value of one (100 %) (Milanović et al., 2021; Nembrini et al., 2018).

While the previous method was applied to validate the model and assess the importance of the variables, the SHAP (Shapley Additive Explanation) approach was employed to interpret and analyze the relationships between variables and the occurrence of wildfires. The SHAP method, based on game theory (Shapley, 1953), quantifies each feature's contribution to a model's output (Lundberg & Lee, 2017). Shapley values are calculated (Ann A) by comparing prediction differences with and without a feature, weighted by the subset size and averaged (Yue et al., 2023). This approach interprets machine learning models by assessing whether features positively or negatively impact predictions, unlike traditional feature importance (Iban & Sekertekin, 2022; Kannangara et al., 2022; Kavzoglu et al., 2021; Yue et al., 2023).

2.3.3. *Model validation and susceptibility map assessment*

The models were validated in three stages. Firstly, both models (all variables included; only > 50 % importance variables) were used to predict wildfires. The predictions were compared to the actual fire data. These steps were repeated three times to obtain an average value for the overall accuracy and Cohen's Kappa (κ) of the models.

The selected model was then employed to predict the fire susceptibility image. This involved calculating the probability of each pixel being classified as either 0 (indicating no burn) or 1 (indicating a burn). The explanatory variables used in this process were the georeferenced images from Group 4 (as detailed in Table 2). For validation, a binary image was generated through the reclassification of the fire occurrences image from 2011 to 2022 (Groups 1 to 4) in ArcMap 10.8 software (ESRI, 2011).

Subsequently, the Area Under the Curve (AUC) was calculated using the fire susceptibility and validation images, synthesizing the receiver operating characteristic (ROC) (Bradley, 1997). It measures model

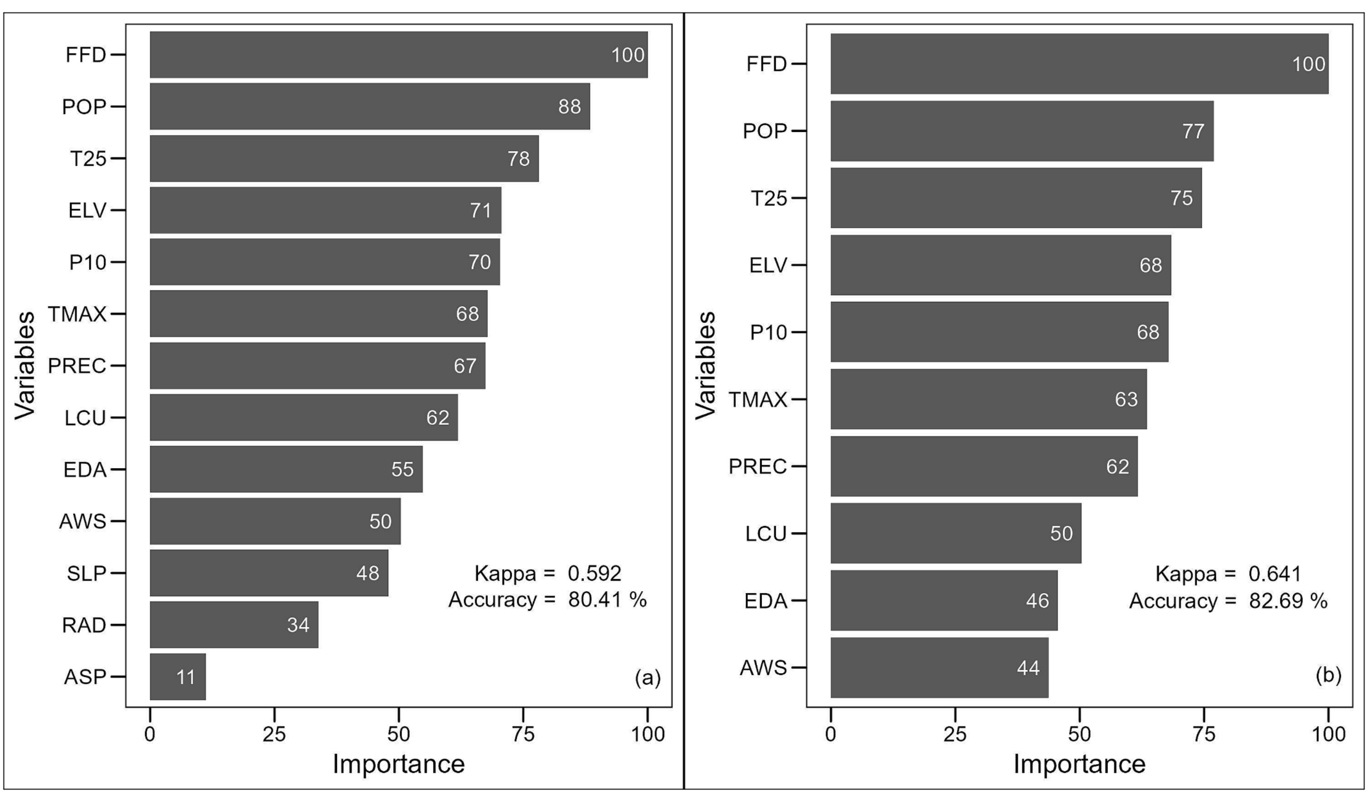

Fig. 3. Variable importance, accuracy, and Kappa value, considering the removal of variables with importance below 50 % (a) All variables included, (b) Without the variables Aspect (ASP) and Solar Radiation (RAD). Where, FFD: Firefighter density; POP: Population density; T25: Number of days with temperature above 25 °C; P10: Number of days with precipitation above 10 mm; ELV: Elevation; TMAX: Average of the maximum temperature in summer; PREC: Accumulated precipitation in the summer; LCU: Land cover and use; EDA: Euclidean distance from agricultural areas; AWS: Average wind speed; SLP: Slope; RAD: Solar Radiation; ASP: Aspect.

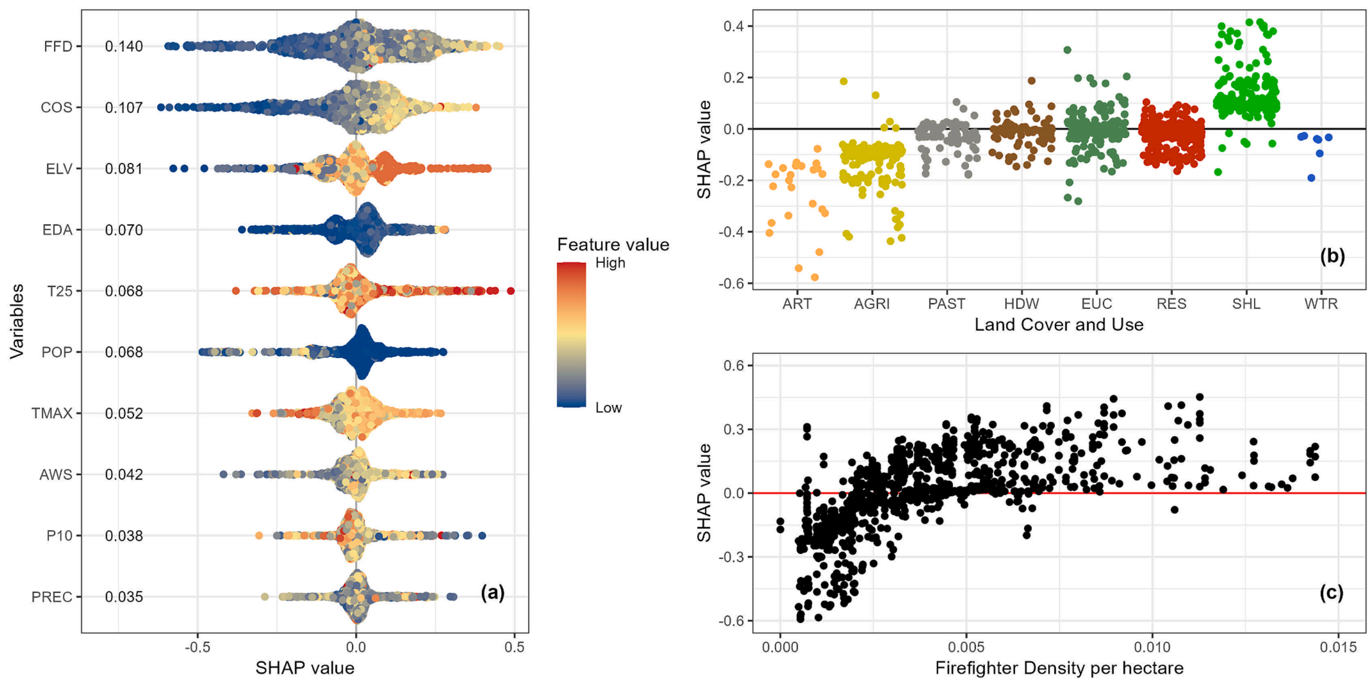

Fig. 4. (a) Shapley Additive explanation values, considering the removal of variables with importance below 50 %. (b) SHAP values for Land Cover and Use classes. Where, FFD: Firefighter density; POP: Population density; T25: Number of days with temperature above 25 °C; P10: Number of days with precipitation above 10 mm; ELV: Elevation; TMAX: Average of the maximum temperature in summer; PREC: Accumulated precipitation in the summer; LCU: Land cover and use; EDA: Euclidean distance from agricultural areas; AWS: Average wind speed; ART: Artificialized Territories; AGRI: Agriculture; PAST: Pastures, Agroforestry Systems, Cork oaks, Holm oaks, Areas without vegetation; HDW: Other Hardwoods; EUC: Eucalyptus; RES: Resinous Forests; SHL: Shrublands; WTR: Wetlands and water bodies. (c) SHAP Values for Firefighter Density.

quality, indicating the probability that burned areas have higher fire probabilities than unburned areas (Nunes & Lourenço, 2017; Santana Neto et al., 2022; 2023). AUC values are categorized as inadequate (<0.6), unsatisfactory (0.7–0.8), moderate (0.8–0.9), good, or excellent (>0.9) (Akıncı et al., 2024; Shang et al., 2020).

To facilitate a comparison of burn susceptibility with actual data, the susceptibility image was segmented into five classes: very low, low, moderate, high, and very high. For each of these classes, the relative area that burned during the validation period (in comparison to the total area of the class) was calculated.

2.3.4. *Actual wildfire susceptibility image*

After the model validation, a prediction of fire susceptibility was carried out using the most recent data from the study (Group 1) using the same method as that applied for the previous susceptibility map. Furthermore, we calculated the average fire susceptibility for each district within the central region of Portugal.

3. Results

The correlation matrix (Annex B) displays the relationships between the variables. PREC shows a positive correlation with P10 (0.7) and a negative correlation with TMAX (−0.65), indicating that higher

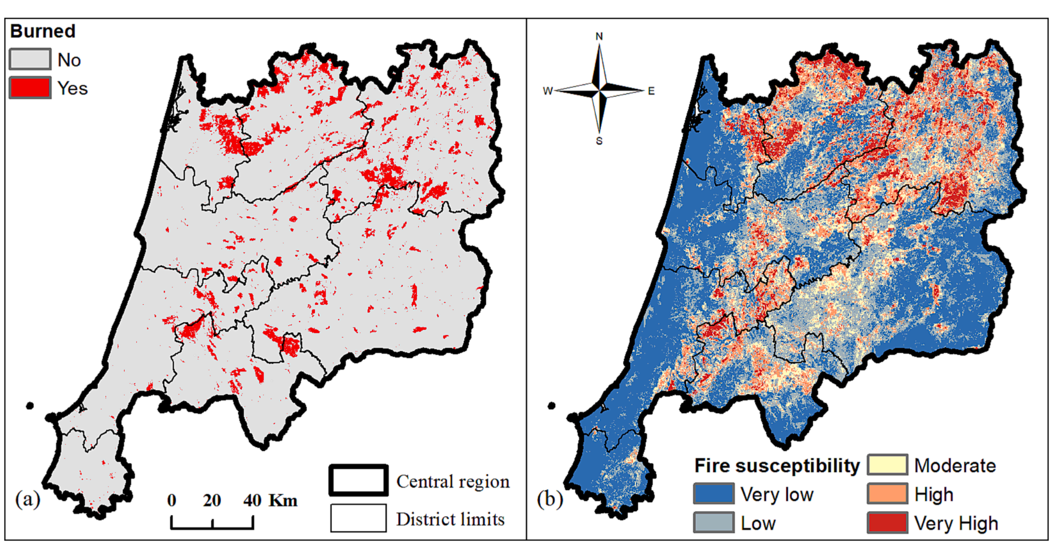

Fig. 5. (a) Fire occurrence image from the years 2011–2022; (b) Susceptibility image based on the variables from Group 4.

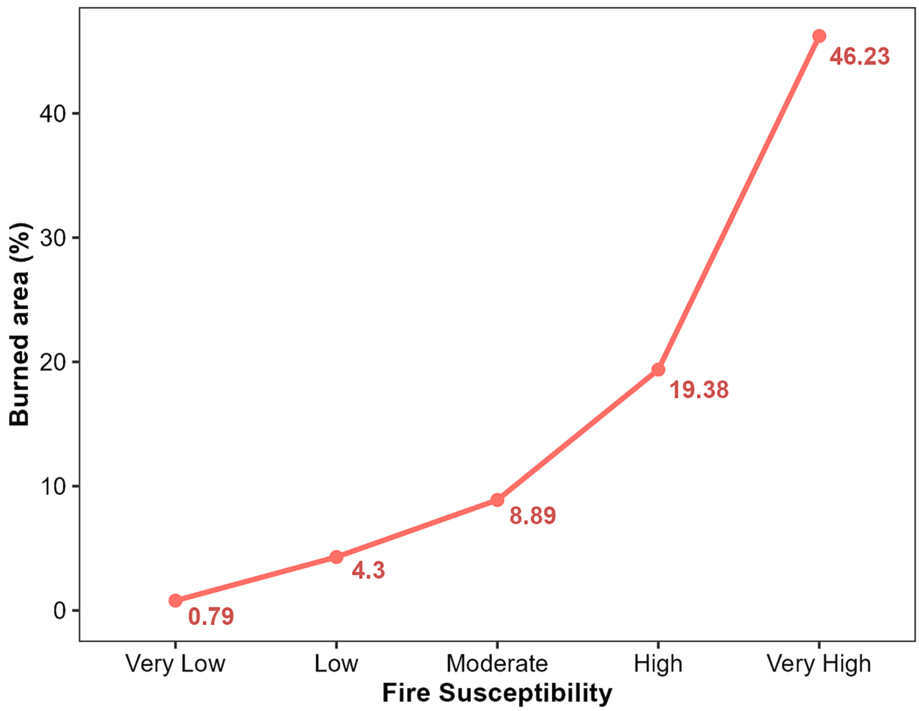

Fig. 6. Relative burned area from 2011 to 2022 (except 2017) by susceptibility class defined by the random forest model using data from Group 4.

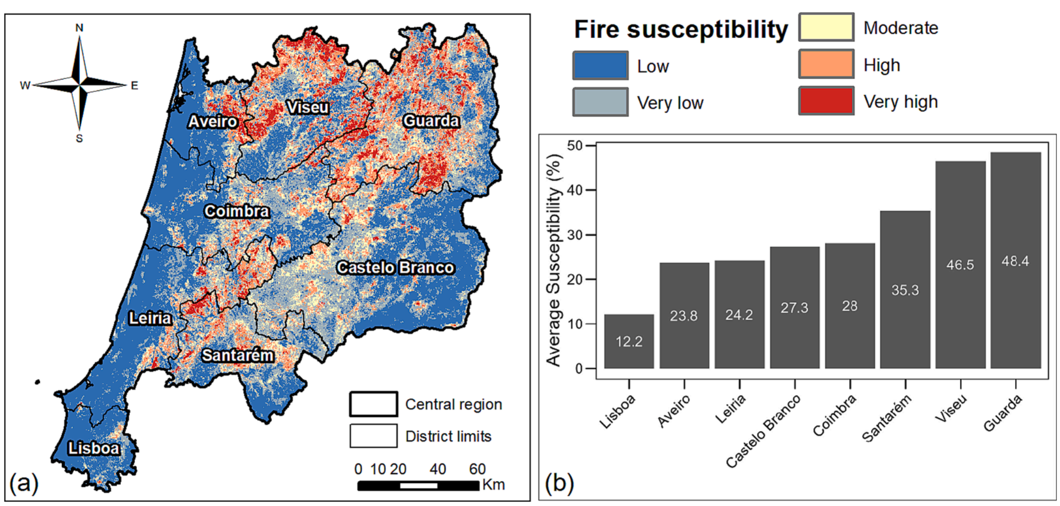

Fig. 7. (a) Fire susceptibility image based on the most recent data (Group (1). (b) Average fire susceptibility (%) in the area of the districts located in the central region of Portugal.

precipitation is associated with more days of precipitation above 10 mm and lower average maximum summer temperatures. Other correlations exhibit weaker values, suggesting negligible or low levels of association between the remaining variables.

The models showed a higher importance for the variables of firefighter density (FFD), population (POP), and number of days with temperature above 25 °C (T25) (Fig. 3). On the other hand, the radiation (RAD) and aspect (ASP) variables showed a relative importance below the others. Nevertheless, removing these less important variables resulted in improved Cohen's Kappa (κ) and overall accuracy, leading to the selection of this streamlined model for the next validation stage.

Fig. 4 illustrates the directional influence of effects and the importance of each variable in predicting wildfire susceptibility. On the horizontal axis, we observe the Shapley values, with larger values signifying a more significant impact on prediction outcomes. Positive Shapley values correspond to a positive influence, while negative values indicate a negative influence. The color scheme further enhances our understanding: red denotes high attribute values, while blue represents low attribute values. For example, when FFD and Elevation values are high, Shapley values tend to be large, suggesting that increased FFD and Elevation are associated with a higher likelihood of wildfire occurrence.

Less prominently but still relevant, both agricultural distance (EDA) and the number of days with temperatures exceeding 25 °C (T25) exhibited similar behavior as the previously cited. Conversely, population density showed an inverse relationship with wildfire susceptibility. The remaining continuous variables had SHAP values closer to zero, indicating their lesser relevance to the model being distributed uniformly along the X-axis, making it challenging to confirm the direction in which these variables contribute to susceptibility.

Regarding the SHAP values for the categorical variable LCU (Fig. 4b), a substantial positive contribution is observed from the shrublands class, while the water bodies, artificialized, and agricultural classes exhibit opposite behaviors. The other LCU classes do not demonstrate significant relevance in contributing to the variable's impact on the model.

Thus, the real burned area image used for validation (Groups 1–4, except 2017) presented a predominance of wildfires in the north and northeast regions of the study area (Fig. 5a). Similarly, the predicted burning susceptibility image, based on Group 4 (Table 2), exhibited a comparable pattern but also indicated some high susceptibility areas in the southern part of the area (Fig. 5b) and a very low susceptibility in the southeastern region.

When comparing the susceptibility image generated with the real fire data, an AUC of 84.68 % was calculated (Annex C).

The burned area increased exponentially with the increase in susceptibility. About 46.23 % of the area considered Very High susceptibility to fires was burned, while only 0.79 % of the area classified as Very Low susceptibility burned (Fig. 6). This indicates a consistent correlation between the fire susceptibility of an area and the extent of the burned area.

The fire susceptibility map developed using the most recent data from this study (as per Group (1), Table 2) reveals significant insights (Fig. 7). Notably, the districts of Guarda and Viseu, situated in the northern part of the region, exhibit a high susceptibility to fires. Conversely, Lisboa and Aveiro, which are located closer to the coast, demonstrate a lower average susceptibility to fires. Furthermore, it's worth noting that the eastern region of Castelo Branco demonstrates remarkably low susceptibility.

4. Discussion

4.1. Variables assessment

4.1.1. Firefighter and population density

The findings indicate that firefighter presence is a highly influential factor in the model, holding the highest importance value. The analysis shows a positive correlation between wildfire occurrences and the number of deployed firefighters, which is consistent with the results of Piñol et al. (2005) The authors states that the higher firefighting capacities resulted in a slightly higher proportion of large fires. Notably, in areas with firefighter densities between 0 and 0.5 firefighters/km2 the probability of fire incidents increases, but this probability tends to stabilize beyond that range.

This stabilization likely reflects strategic firefighter allocation, where regions with higher historical fire incidence receive more resources. Such allocation suggests that fire prevention measures are already being implemented in these areas. However, these findings contrast with earlier research, which commonly links concentrated firefighter deployment with a reduction in burned areas (Félix & Lourenço, 2017; Nunes et al., 2023b). On the other hand, inadequate or excessive fire suppression policies, particularly in fire-dependent ecosystems, can disrupt the natural fire regime. This disruption leads to the accumulation of combustible material, which significantly increases the area's susceptibility to wildfires (Fidelis et al., 2018; Tedim et al., 2018; Ponce-Calderón et al., 2021).

However, population density shows a negative correlation with burn areas. Our study highlights an elevated occurrence of big and extreme fires in regions with smaller populations. This observation can be attributed to several factors. Regions with larger populations tend to have lower fuel density, reducing fire susceptibility. Although Central Portugal features an extensive Wildland-Urban Interface—spanning 60,373 km in 2023, with 15,000 km comprising built-up areas directly adjacent to fuel sources (Nunes et al., 2023a, 2023b)—making it more susceptible to human-induced fire ignition, the region benefits from stricter regulations, accessible firefighting services, and advanced fire detection systems that enable swift response and containment (Oliveira et al., 2018; Piñol et al., 2005).

Also, distinct land use patterns, reduced flammable vegetation, and limited agricultural activities—major wildfire triggers in rural regions—further minimize fire risk. Additionally, the diminished reliance on traditional fire practices in urban settings decreases the likelihood of extensive outbreaks (Bergonse et al., 2021a; Catry et al., 2009; Rodríguez-Trejo et al., 2022).

In Portugal, coastal areas are characterized by high population density and urbanization, allied to higher precipitation and lower temperatures, while mountainous, rural, and interior regions of the center exhibit low population density and a dispersed housing pattern, with a predominance of isolated buildings and abandoned shrublands (Nunes et al., 2023b). This land cover, driven by low profitability and insufficient incentives for its management, persists particularly during periods when fuel management near houses and settlements was not mandated (Calviño-Cancela et al., 2016; Nunes et al., 2023a).

As a result, residents in these regions face heightened risks due to inadequate maintenance of structures and fuel management practices (Oliveira & Zêzere, 2020). Furthermore, low population density complicates access to fire suppression and surveillance resources, increasing wildfire risks and exacerbating their impacts (Fernandes et al., 2016a; Moreira et al., 2010; Oliveira et al., 2021.

4.1.2. Temperature and precipitation

The elements of temperature and precipitation also influenced in the model. The study reveals that, irrespective of maximum temperature, days exceeding 25 °C—alongside other factors—are sufficient for fire occurrence. Additionally, heavy rainfall (above 10 mm) increases soil moisture and reduces fire susceptibility. However, when considering cumulative effects globally, the impact remains less certain due to evaporation in areas affected by lighter rains. It is known that wildfires tend to increase under extreme weather conditions (Calheiros et al., 2022). The relationship between temperature and precipitation significantly influences fire occurrence. High temperatures and low precipitation are critical factors that increase forest vulnerability to fires, impacting atmospheric air mass, soil moisture, and evapotranspiration, which directly affect fuel flammability (Mansoor et al., 2022; Sari, 2021).

These variables can exert diverse effects based on their combination. For example, increased spring precipitation contributes to fuel formation, while the combination of summer's high temperatures and low precipitation favors forest fires due to the thermal and water stress on living fuels and the dryness of dead fuels. (Bergonse et al., 2022; Calheiros et al., 2022; Romano & Ursino, 2020).

Moreover, it is crucial to emphasize that climate change not only impacts the quantity and quality of vital resources—such as water, minerals, and diverse species of plants, animals, and fungi (Voggesser et al., 2013)—but also increases the likelihood of extreme humidity or drought conditions. These changes can significantly alter ecosystems and disrupt human lives (Ponce-Calderón et al., 2021).

4.1.3. Elevation

Elevation has significant practical implications. These include influencing factors such as wind speed, precipitation, temperature, sunlight intensity, and therefore the types, quantity, and moisture of available fuels, all of which play a crucial role in fire behavior and occurrence (Iban & Sekertekin, 2022; Jaafari et al., 2018; Nunes et al., 2016; Oliveira & Zêzere, 2020; Tran et al., 2024; Verde & Zêzere, 2010). Thus, numerous studies have shown an escalation in the extent of the burned area correlating with an increase in altitude up to a limited height (Bergonse et al., 2021a; Bergonse et al., 2021b; Marques et al., 2011; Nunes et al., 2023a; Oliveira & Zêzere, 2020).

This research aligns with this pattern, as we found that higher elevations demonstrated heightened susceptibility to wildfires. Furthermore, high altitudes are associated with livestock activities and lower population density, which play a significant role in the ignition of wildfires (Catry et al., 2009). The negligence in fire management techniques, stemming from the loss of cultural knowledge linked to these livestock activities, further heightens the risk of wildfires (Ponce-Calderón et al., 2022).

4.1.4. Land use and land cover and distance from agriculture area

Another factor of paramount importance for wildfire behavior is land use and land cover (LCU). The type and availability of fuel influence the likelihood of fire occurrence, just as different land uses influence the distribution and propagation of fires (Bergonse et al., 2021a; Calheiros et al., 2022; Oliveira & Zêzere, 2020). Numerous studies indicate that scrubland is the type of land cover most susceptible to fires in Portugal (Bergonse et al., 2022; Carmo et al., 2011; Marques et al., 2011; Santana Neto et al., 2022), which aligns with our findings. This can be explained by a combination of factors: the fuel has a high fire propagation rate because its properties include highly flammable resins and essential oils, and it is common in rugged terrains; the incidence of ignitions is more frequent, for instance, for scrubland clearance for conversion into pastures, which often leads to fires spreading into adjacent forest areas; and the priority given to firefighting is lower due to the low economic value attributed to it (Marques et al., 2011; Moreira et al., 2009).

The results indicate that urban, agricultural, and agroforestry areas presented a lower susceptibility to fires, which is in concordance with other studies (Bergonse et al., 2021; Fernandes, Monteiro-Henriques, Guiomar, Loureiro, & Barros, 2016; Bergonse et al., 2022Oliveira & Zêzere, 2020). On one hand, they can act as ignition sources, especially in urban-forest interface regions, thereby facilitating the rapid spread of fires (Nunes et al., 2016; Tran et al., 2024). However, the presence of people living in these areas can support the rapid detection and combating of fires (Oliveira et al., 2022).

Agricultural areas, subject to rigorous management practices, owe their effectiveness more to human intervention than inherent plant species characteristics, as suggested by Oliveira et al. (2021). Additionally, these agricultural zones adjacent to settlements can act as natural firebreaks, limiting fire spread, although extreme conditions may occasionally override the typical selectivity of fire based on land cover type (Barros & Pereira, 2014).

4.1.5. Average wind speed

While the average wind speed (AWS) variable was less relevant in the model, it exerts considerable influence in the practical scenario, theoretically exhibiting a positive association with the spread of wildfires (Tran et al., 2024; Xiao et al., 2015). Wind supplies oxygen, introduces a new source of fuel to the fire, and spreads the flames to reach new fuels (Costa et al., 2011; Pourtaghi et al., 2015).

4.1.6. Slope, aspect and solar radiation (RAD)

Lastly, with the removal of the variables Slope (SLP), Aspect (ASP), and Solar radiation (RAD), the model exhibited greater accuracy and a higher Kappa value. The removal of these variables could reduce the model's ability to capture the complexity of the phenomenon. Additionally, it is important to remember that the accuracy of a model does not always reflect its long-term validity or its ability to generalize in real and heterogeneous scenarios. Future studies should consider including these variables and conducting additional field validations to ensure the model better captures the factors influencing wildfires.

The inclusion of the slope variable in our study stems from its theoretical role in promoting upward fire propagation through the heating of combustible materials, being positively associated with wildfire spread (Carmo et al., 2011; Costa et al., 2011; Leuenberger et al., 2018; Oliveira & Zêzere, 2020; Tran et al., 2024). The slope also influences land cover types and, consequently, the availability of fuel (Bergonse et al., 2021b). However, its relatively lower importance in our model likely results from its irregular distribution within the region, consistent with findings by Bergonse et al. (2022).

The inability of the Aspect and Solar radiation variables to enhance the wildfire susceptibility model aligns with the findings reported by Oliveira et al. (2021) and Iban and Sekertekin (2022). Those two variables are directly related and were evaluated due to their influence on heating fuel (Santana Neto et al., 2023). For instance, in the northern hemisphere, southern slopes tend to receive greater exposure to direct sunlight, which results in higher temperatures and so dries the combustible material (Akıncı & Akıncı, 2023; Sari, 2021), thereby facilitating the ignition and propagation of fires (Sayad et al., 2019; Tran et al., 2024).

4.2. Wildfire susceptibility map

It is well-known that susceptibility maps aim to identify regions with higher susceptibility to fires, taking into account various socio-environmental and historical aspects. These maps are designed to support fire prevention and suppression strategies (Tran et al., 2024) while advancing the understanding of fire regimes (Bergonse et al., 2023). Additionally, they play a crucial role in protecting biodiversity by identifying ecosystems susceptible to wildfires, such as carbon-rich forests and pollinator habitats (Marquez Torres et al., 2023; Torres & Paz, 2024). Consequently, developing more efficient maps becomes crucial for effectively guiding these efforts (Santana Neto et al., 2022).

Thus, the initially calculated model presented a Kappa value of 0.592. However, after removing the less important variables, this value increased to 0.641, representing moderate agreement. The model's behavior is in line with the study by Jaafari et al. (2018), which shows that reducing variables can lead to better Kappa values in wildfire prediction.

Furthermore, the susceptibility map exhibited an AUC of 83.81 %, which is considered a good performance (Akıncı et al., 2024; Shang et al., 2020). Several studies that employed the Random Forest method also achieved an AUC above 80 % (Akıncı & Akıncı, 2023; Iban & Sekertekin, 2022; Milanović et al., 2023, 2021; Yue et al., 2023), demonstrating the method's high adoption and efficiency. Not only that, the curve represented in Fig. 6 was consistent with expectations, where higher susceptibilities presented a larger relative burned area, showing similarity with other fire studies that used the same algorithm (*Random Forest*) in different areas (Leuenberger et al., 2018; Santana Neto et al., 2022). This method is favored due to its ability to construct multiple decision trees during the training, while also demonstrating robustness against outliers and noisy data (Oliveira et al., 2012; Rodrigues & De la Riva, 2014; Santana Neto et al., 2022; Su et al., 2018).

Thus, it can be noted that the distribution of fire susceptibility in Fig. 3b was primarily influenced by social factors, as previously discussed. Areas with larger populations (closer to the coast) exhibited lower susceptibility, while the more central regions and the northeastern part of the study area showed higher susceptibility. This result is similar to other studies conducted in the same region (Nunes et al., 2023a; Oliveira et al., 2021).

The spatial pattern of fires in the central part of the study area remains stable, but there's an overall decrease in fire susceptibility across the region. This could be due to the significant consumption of available fuel by the widespread fires of 2017 (Calheiros et al., 2022; Santana Neto et al., 2022), which would still be in a recovery phase during the period identified by Group (1) (De Zea Bermudez et al., 2009), given that biomass accumulation is a crucial factor for fire occurrence (Pandey et al., 2023).

4.3. Environmental impacts

Wildfires in Portugal not only cause the direct destruction of many individuals, including those of conservation concern, but also generate conditions conducive to the invasion of non-native species (Rossetti et al., 2022). For example, Aguiar et al. (2021) reported a dramatic rise in the number and development of *Acacia melanoxylon* seedlings, as well as sprouts from root suckers and burnt stools. Furthermore, post-fire episodes promote dwarf shrubs and other low vegetation, modifying the landscape's physiognomy (Bastos et al., 2011).

In addition, wildfires cause soil degradation, considerably influencing the post-fire environment. For example, the removal of vegetation cover makes landscapes highly susceptible to soil erosion (Nunes & Lourenço, 2017). Furthermore, wildfires reduce soil organic matter and produce contaminants such as charcoal and pyrogenic polycyclic aromatic hydrocarbons (PAHs). These substances offer environmental and ecological risks, being the second recognized as human carcinogen (Ribeiro et al., 2021). As a result, the combined effects of wildfire-induced alterations and faster soil erosion promote sediment transport into aquatic systems, reducing water quality and raising major environmental issues (Nunes & Lourenço, 2017). Additionally, wildfires disrupt fish assemblages, causing shifts in population dynamics and long-lasting ecological impacts (Monaghan et al., 2016).

4.4. Directions for future research and study limitations

It is important that new studies are conducted periodically, as some variables tend to change over time (Tran et al., 2024). In order to develop even more precise models, it is crucial to have access to more accurate and updated data of the defined variables, such as climatic data, in addition to the inclusion of new variables related to population (Oliveira & Zêzere, 2020), like socio-economic and cultural characteristics. Additionally, it is essential to recognize the importance of pyrobiocultural territories, which have been shaped through traditional practices over time. These territories, which integrate local cultural knowledge and fire management practices, offer valuable insights for better understanding the dynamics of fire occurrence and prevention (Ponce-Calderón et al., 2022). Incorporating these cultural aspects into future studies could significantly improve the accuracy of models and contribute to more sustainable fire management strategies. Furthermore, images with higher spatial resolutions and considering seasonality could result in more accurate models, thereby providing better materials for fire prevention and suppression strategies.

5. Conclusions

The study evaluated the importance of variables in the creation of a wildfire susceptibility map, highlighting a stronger correlation between the presence of firefighters and depopulation. However, when environmental variables are analyzed together, they provide crucial support for wildfire modeling.

Furthermore, our study reveals that, in Central Portugal, regions at higher elevations tend to exhibit greater susceptibility to wildfires. Notably, when examining climatic factors, we observed that their relevance becomes more pronounced when considering lower thresholds—specifically, the number of days with elevated temperatures and precipitation (above 25 °C and 10 mm, respectively), suggesting that the use of general data (mean temperature or accumulated precipitation) may not fully reflect its true impact on wildfire susceptibility.

In addition, the spatial distribution of high levels of susceptibility to fires remains unchanged, with a focus on the northern region of the study area. Ultimately, the results can assist with directing efforts towards fire suppression and prevention in order to protect people, assets, and nature, highlighting a greater need for attention to the further inland and less populous regions of the study area, especially those with higher elevation and more shrublands, particularly in the districts of Guarda, Viseu, and Santarém.

Moreover, the study emphasizes the need for periodic updates and improved model accuracy by incorporating higher-resolution data, socio-economic and cultural factors, and seasonality. Recognizing pyrobiocultural territories and integrating local fire management practices can also enhance understanding and sustainability. The findings can lead future fire management strategies, particularly in less populated and inland regions, where targeted interventions may be most needed, in order to protect nature and people's lives.

Funding

This study was financed in part by the Coordenação de Aperfeiçoamento de Pessoal de Nível Superior-Brasil (CAPES)-Finance Code 001. This work also received support from the Centre of Studies in Geography and Spatial Planning (CEGOT), funded by national funds through the Foundation for Science and Technology (FCT) under the reference UIDB/04084/2025.

CRediT authorship contribution statement

Vicente Paulo Santana Neto: Writing – review & editing, Writing – original draft, Visualization, Validation, Software, Resources, Project administration, Methodology, Investigation, Funding acquisition, Formal analysis, Data curation, Conceptualization. **Adelia de Jesus Nobre Nunes:** Writing – review & editing, Supervision, Resources, Methodology, Conceptualization. **Fillipe Tamiozzo Pereira Torres:** Writing – review & editing, Supervision, Methodology, Conceptualization. **José Marinaldo Gleriani:** Writing – review & editing, Supervision. **Diogo Nepomuceno Cosenza:** Writing – review & editing, Visualization, Validation, Software.

Declaration of competing interest

The authors declare that they have no known competing financial interests or personal relationships that could have appeared to influence the work reported in this paper.

Acknowledgements

I extend my heartfelt thanks to designer Igor Sanches Marini for his invaluable support in crafting the Graphical Abstract of the article, and to MSc. Carlos Daniel Vicente Pinto for his assistance in providing some data utilized in our study.

Appendix A. Equation for shapley additive explanation

$$\phi_j = \frac{1}{M}\sum\nolimits_{i=1}^{M}\sum\nolimits_{S\subseteq x_i/j}\frac{|S|!(|x_i| - |S| - 1)!}{|x_i|!}\left(f_{S\cup j}(x_i) - f_S(x_i)\right) \tag{1}$$

where x_i represents the i-th sample; j represents one of the features; S represents the subset of features that does not include feature S; $f_S(x_i)$ represents the model's prediction output after removing feature S; $f_{S\cup j}(x_i)$ represents the model prediction outputs after adding feature j; and M is the number of samples. The Shapley value is the contribution of feature j to the prediction output for sample x_i, which is calculated as the difference between the prediction outputs with and without feature j, multiplied by the weight of the sample subset when feature j is considered, and then averaged (Yue et al., 2023).

Annex B. . Matrix correlation between explanation variables. Where, FFD: Firefighter density; POP: Population density; T25: Number of days with temperature above 25 °C; ELV: Elevation; P10: Number of days with precipitation above 10 mm; TMAX: Average of the maximum temperature in summer; PREC: Accumulated precipitation in the summer; SLP: Slope; RAD: Solar radiation.

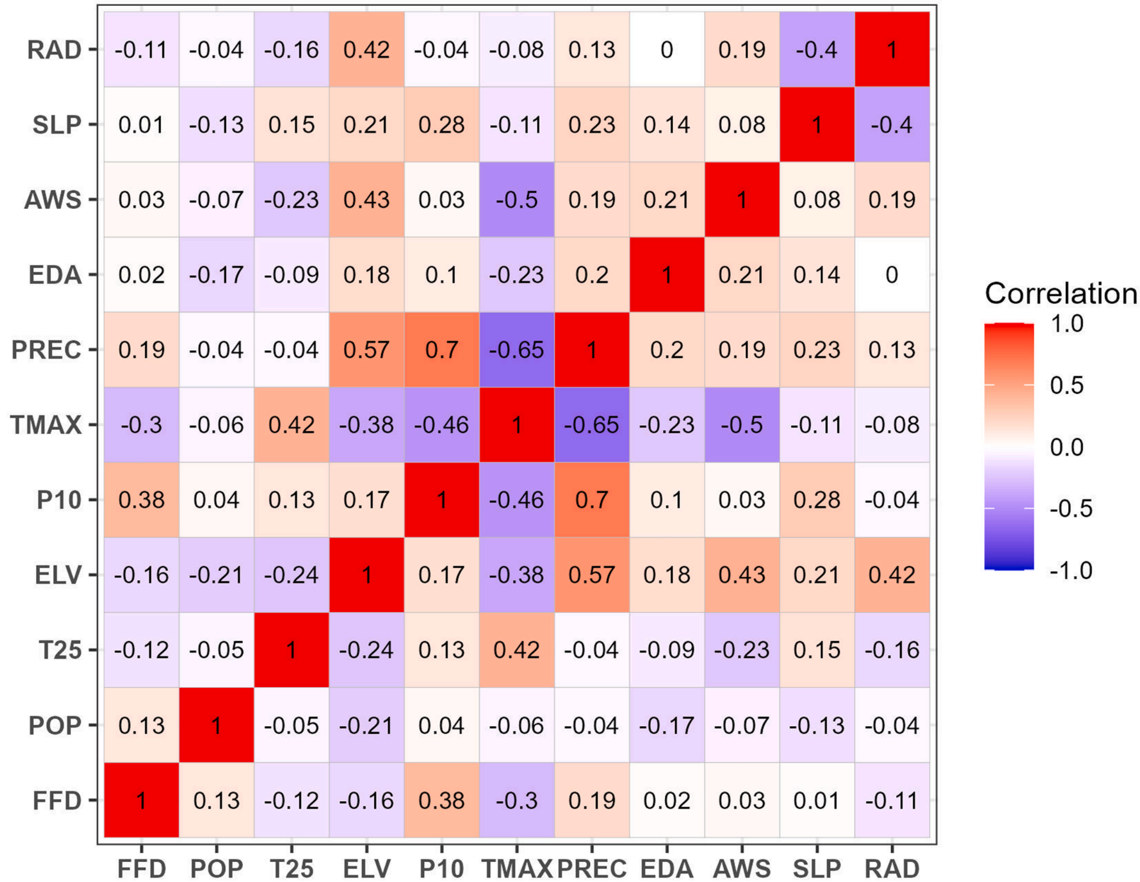

Annex C. . ROC Curve and AUC for the predicted burning susceptibility map compared to real fire data based on Group 4

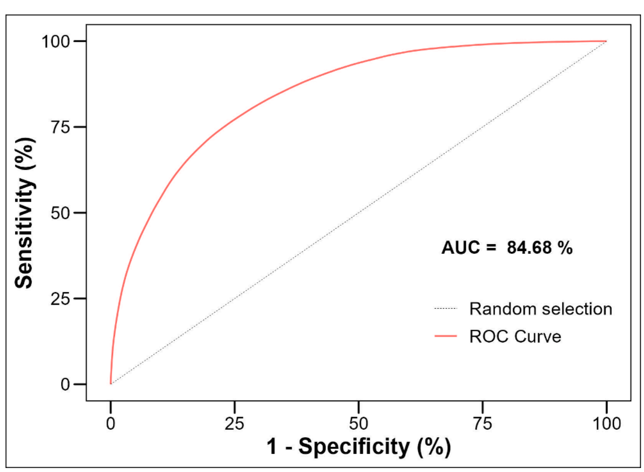

Data availability

Data will be made available on request.

References

Aguiar, F. C., Rodrigues, C., Pina, J. P., & Soares, P. (2021). Regeneration of riparian and maritime pine forests after a large wildfire on the largest public forest of Portugal. *Forests, 12*(4), 477. https://doi.org/10.3390/f12040477

Akıncı, H. A., & Akıncı, H. (2023). Machine learning based forest fire susceptibility assessment of Manavgat district (Antalya), Turkey. *Earth Science Informatics, 16*, 397–414. https://doi.org/10.1007/s12145-023-00953-5

Akıncı, H. A., Akıncı, H., & Zeybek, M. (2024). Comparison of diverse machine learning algorithms for forest fire susceptibility mapping in Antalya, Turkey. *Advances in Space Research, 74*, 647–667. https://doi.org/10.1016/j.asr.2024.04.018

Bachmann, A., & Allgöwer, B. (2001). A consistent wildland fire risk terminology is needed! *Fire Management Today, 61*, 28–33.

Barros, A. M. G., & Pereira, J. M. C. (2014). Wildfire selectivity for land cover type: Does size matter? *PLoS One1, 9*. https://doi.org/10.1371/journal.pone.0084760

Bastos, A., Gouveia, C. M., DaCamara, C. C., & Trigo, R. M. (2011). Modelling post-fire vegetation recovery in Portugal. *Biogeosciences, 8*(12), 3593–3607. https://doi.org/10.5194/bg-8-3593-2011

Bergonse, R., Oliveira, S., Gonçalves, A., Nunes, S., da Câmara, C., & Zêzere, J. L. (2021). A combined structural and seasonal approach to assess wildfire susceptibility and hazard in summertime. *Natural Hazards, 106*, 2545–2573. https://doi.org/10.1007/s11069-021-04554-7

Bergonse, R., Oliveira, S., Gonçalves, A., Nunes, S., DaCamara, C., & Zêzere, J. L. (2021). Predicting burnt areas during the summer season in Portugal by combining wildfire susceptibility and spring meteorological conditions. *Geomatics Nature Hazards Risk, 12*, 1039–1057. https://doi.org/10.1080/19475705.2021.1909664

ASF, (2024). ASF Data Search [WWW Document]. URL: https://search.asf.alaska.edu (accessed 3.1.24).

Bergonse, R., Oliveira, S., Zêzere, J.L., Moreira, F., Ribeiro, P.F., Leal, M., Lima e Santos, J.M. (2022). Biophysical controls over fire regime properties in Central Portugal. Science of the Total Environment 810, 152314. Doi: 10.1016/j.scitotenv.2021.152314.

Bergonse, R., Oliveira, S., Zêzere, J. L., Moreira, F., Ribeiro, P. F., Leal, M., & Santos, J. M. L. (2023). Differentiating fire regimes and their biophysical drivers in central Portugal. Article 3 *Fire, 6*(3). https://doi.org/10.3390/fire6030112.

Bradley, A. P. (1997). The use of the area under the ROC curve in the evaluation of machine learning algorithms. *Pattern Recognition, 30*, 1145–1159. https://doi.org/10.1016/S0031-3203(96)00142-2

Breiman, L. (2001). Random Forests.

Calheiros, T., Benali, A., Pereira, M., Silva, J., & Nunes, J. (2022). Drivers of extreme burnt area in Portugal: Fire weather and vegetation. *Natural Hazards and Earth System Sciences, 22*, 4019–4037. https://doi.org/10.5194/nhess-22-4019-2022

Calviño-Cancela, M., Chas-Amil, M. L., García-Martínez, E. D., & Touza, J. (2016). Wildfire risk associated with different vegetation types within and outside wildland-urban interfaces. *Forest Ecology and Management, 372*, 1–9. https://doi.org/10.1016/j.foreco.2016.04.002

Camargo, A. C. L., Barrio, R. O. L., de Camargo, N. F., Mendonça, A. F., Ribeiro, J. F., Rodrigues, C. M. F., & Vieira, E. M. (2018). Fire affects the occurrence of small mammals at distinct spatial scales in a neotropical savanna. *European Journal of Wildlife Research, 64*. https://doi.org/10.1007/s10344-018-1224-8

Carmo, M., Moreira, F., Casimiro, P., & Vaz, P. (2011). Land use and topography influences on wildfire occurrence in northern Portugal. *Landscape and Urban Planning, 100*, 169–176. https://doi.org/10.1016/j.landurbplan.2010.11.017

Catry, F. X., Rego, F. C., Bação, F. L., & Moreira, F. (2009). Modeling and mapping wildfire ignition risk in Portugal. *International Journal of Wildland Fire (IJWF), 18*, 921–931. https://doi.org/10.1071/WF07123

Costa, L., Thonicke, K., Poulter, B., & Badeck, F. (2011). Sensitivity of Portuguese forest fires to climatic, human, and landscape variables: Subnational differences between fire drivers in extreme fire years and decadal averages. *Regional Environmental Change, 11*, 543–551. https://doi.org/10.1007/s10113-010-0169-6

Costa, A. das G., Torres, F.T.P., Lima, G.S., de Melo, F.R., Rodrigues, V.B., Neto, V.P.S., Fernandes, T.V., Costa, A. das G., Torres, F.T.P., Lima, G.S., de Melo, F.R., Rodrigues, V.B., Santana Neto, V.P., Fernandes, T.V. (2022). Fire influence on the ants community in savanic and forest environments of the Cerrado biome. Floresta e Ambient. 29, 1–10. Doi: 10.1590/2179-8087-FLORAM-2022-0025.

Costa, A. das G., Torres, F.T.P., Lima, G.S., de Melo, F.R., Torres, C.M.M.E., Schettini, B.L.S., Santana Neto, V.P., de Faria, A.L.L. (2023). Influence of fire on woody vegetation of savanna and forest formations in the Cerrado biome. J. For. Res. 34, 1207–1216. Doi: 10.1007/s11676-022-01573-3.

Costa, P.S., Estanqueiro, A. (2023). Mapa do Atlas do Potencial Eólico Onshore de Portugal Continental.

Cunha, S., Silva, A., Santo Coelho, F.E., Nunes, L.F., Pires, V., Mendes, L., Cota, T., Belo, M., Neto, J., Mendes, M. (2010). Atlas Climático de Portugal Continental 1971-2000: Modelação SIG da Precipitação e da Temperatura do Ar.

De Zea Bermudez, P., Mendes, J., Pereira, J. M. C., Turkman, K. F., & Vasconcelos, M. J. P. (2009). Spatial and temporal extremes of wildfire sizes in Portugal (1984-2004). *International Journal of Wildland Fire, 18*, 983–991. https://doi.org/10.1071/WF07044

DGTerritório, 2022. Especificações técnicas da Carta de uso e Ocupação do Solo de Portugal Continental para 1995, 2007, 2010, 2015 e 2018, Relatório Técnico.

ESRI (2011). ArcGIS Desktop: Release 10.8.

Félix, F., & Lourenço, L. (2017). O tempo de resposta do ataque inicial a incêndios florestais nos espaços mais sensíveis de Portugal: O exemplo prático da serra da Lousã. *Territorium, 187–211*. https://doi.org/10.14195/1647-7723_24_14

Fernandes, P. M., Pacheco, A. P., Almeida, R., & Claro, J. (2016.). The role of fire-suppression force in limiting the spread of extremely large forest fires in Portugal. *European Journal of Forest Research, 135*, 253–262. https://doi.org/10.1007/s10342-015-0933-8

Fernandes, P. M., Monteiro-Henriques, T., Guiomar, N., Loureiro, C., & Barros, A. M. G. (2016). Bottom-Up Variables Govern Large-Fire Size in Portugal. *Ecosystems, 19*, 1362–1375. https://doi.org/10.1007/s10021-016-0010-2

Fidelis, A., Alvarado, S. T., Barradas, A. C. S., & Pivello, V. R. (2018). The year 2017: Megafires and management in the cerrado. *Fire, 1*(3), 1–11. https://doi.org/10.3390/fire1030049

Greenwell, B. M., & Boehmke, B. C. (2020). Variable importance plots – An introduction to the vip package. *R J., 12*, 343–366.

Huang, B. F. F., & Boutros, P. C. (2016). The parameter sensitivity of random forests. *BMC Bioinformatics, 17*, 331. https://doi.org/10.1186/s12859-016-1228-x

Iban, M. C., & Sekertekin, A. (2022). Machine learning based wildfire susceptibility mapping using remotely sensed fire data and GIS: A case study of Adana and Mersin provinces, Turkey. *Ecol. Inform., 69*, Article 101647. https://doi.org/10.1016/j.ecoinf.2022.101647

ICNF, 2023. Territórios ardidos [WWW Document]. URL: https://sig.icnf.pt/portal/home/item.html?id=983c4e6c4d5b4666b258a3ad5f3ea5af (accessed 2.27.24).

INE (2013). Inquérito às entidades detentoras de corpos de bombeiros. URL: https://smi.ine.pt/Indicador/Detalhes/16650?LANG=PT (accessed 3.26.25).

INE (2022). Base Geográfica de Referenciação da Informação de Portugal. URL: https://mapas.ine.pt/download/index2011.phtml (accessed 3.26.25).

INE (2024). Inquérito às entidades detentoras de corpos de bombeiros. URL: https://smi.ine.pt/Indicador/Detalhes/12174?LANG=PT (accessed 3.26.25).

IPMA (2009a). Média Temperatura Máxima do Ar, Verão, normal 1971-2000 [WWW Document]. URL: https://snig.dgterritorio.gov.pt/rndg/srv/por/catalog.search#/metadata/PT100-ho19712000-jja-avgr-txavgr-cdg (accessed 2.27.24).

IPMA (2009b). Precipitação Total, Verão, normal 1971-2000 [WWW Document]. URL: https://snig.dgterritorio.gov.pt/rndg/srv/por/catalog.search#/metadata/PT100-ho19712000-jja-avgr-pravgr-cdg?tab=responsible (accessed 2.27.24).

IPMA (2009c). Número de dias Temperatura Máxima do Ar ≥25°C, normal 1971-2000 [WWW Document]. URL: https://snig.dgterritorio.gov.pt/rndg/srv/por/catalog.search#/metadata/PT100-ho19712000-aaa-avgr-txna25-cdg (accessed 2.27.24).

IPMA (2009d). Número de dias com Precipitação ≥10mm, normal 1971-2000 [WWW Document]. URL: https://snig.dgterritorio.gov.pt/rndg/srv/por/catalog.search#/metadata/PT100-ho19712000-aaa-avgr-prna10-cdg (accessed 2.27.24).

Jaafari, A., Zenner, E. K., & Pham, B. T. (2018). Wildfire spatial pattern analysis in the Zagros Mountains, Iran: A comparative study of decision tree-based classifiers. *Ecol. Inform., 43*, 200–211. https://doi.org/10.1016/j.ecoinf.2017.12.006

Kannangara, K. K. P. M., Zhou, W., Ding, Z., & Hong, Z. (2022). Investigation of feature contribution to shield tunneling-induced settlement using Shapley additive explanations method. *Journal of Rock Mechanics and Geotechnical Engineering, 14*, 1052–1063. https://doi.org/10.1016/j.jrmge.2022.01.002

Kavzoglu, T., Teke, A., & Yilmaz, E. O. (2021). Shared blocks-based ensemble deep learning for shallow landslide susceptibility mapping. *Remote Sens., 13*. https://doi.org/10.3390/rs13234776

Kayet, N., Chakrabarty, A., Pathak, K., Sahoo, S., Dutta, T., & Hatai, B. K. (2020). Comparative analysis of multi-criteria probabilistic FR and AHP models for forest fire risk (FFR) mapping in Melghat Tiger Reserve (MTR) forest. *Journal of Forest Research, 31*, 565–579. https://doi.org/10.1007/s11676-018-0826-z

Leuenberger, M., Parente, J., Tonini, M., Pereira, M.G., Kanevski, M. (2018). Wildfire susceptibility mapping: Deterministic vs. stochastic approaches. 101, 194–203. Doi: 10.1016/j.envsoft.2017.12.019.

Lundberg, S.M., Lee, S.I. (2017). A unified approach to interpreting model predictions. Adv. Neural Inf. Process. Syst. 2017-December, 4766–4775.

Mansoor, S., Farooq, I., Kachroo, M. M., Mahmoud, A. E. D., Fawzy, M., Popescu, S. M., … Ahmad, P. (2022). Elevation in wildfire frequencies with respect to the climate change. *Journal of Environmental Management, 301*, Article 113769. https://doi.org/10.1016/j.jenvman.2021.113769

Marques, S., Borges, J. G., Garcia-Gonzalo, J., Moreira, F., Carreiras, J. M. B., Oliveira, M. M., Cantarinha, A., Botequim, B., & Pereira, J. M. C. (2011). Characterization of wildfires in Portugal. *European Journal of Forest Research, 130*, 775–784. https://doi.org/10.1007/s10342-010-0470-4

Marquez Torres, A., Signorello, G., Kumar, S., Adamo, G., Villa, F., & Balbi, S. (2023). Fire risk: An integrated modelling approach. Doi: 10.5194/egusphere-2023-138.

Milanović, S., Milanović, S. D., Marković, N., Pamučar, D., Gigović, L., & Kostić, P. (2021). Forest fire probability mapping in eastern Serbia: Logistic regression versus random forest method. *Forests, 12*, 1–17. https://doi.org/10.3390/f12010005

Milanović, S., Kaczmarowski, J., Ciesielski, M., Trailović, Z., Mielcarek, M., Szczygieł, R., Kwiatkowski, M., Bałazy, R., Zasada, M., & Milanović, S. D. (2023). Modeling and mapping of forest fire occurrence in the lower silesian voivodeship of poland based on machine learning methods. *Forests, 14*. https://doi.org/10.3390/f14010046

Monaghan, K. A., Machado, A. L., Wrona, F. J., & Soares, A. M. V. M. (2016). The impact of wildfire on stream fishes in an Atlantic-Mediterranean climate: Evidence from an 18-year chronosequence. *Knowledge and Management of Aquatic Ecosystems, 417*, 28. https://doi.org/10.1051/kmae/2016015

Moreira, F., Catry, F. X., Rego, F., & Bacao, F. (2010). Size-dependent pattern of wildfire ignitions in Portugal: When do ignitions turn into big fires? *Landscape Ecology, 25*, 1405–1417. https://doi.org/10.1007/s10980-010-9491-0

Moreira, F., Vaz, P., Catry, F., & Silva, J. S. (2009). Regional variations in wildfire susceptibility of land-cover types in Portugal: Implications for landscape management to minimize fire hazard. *Int. J. Wildl. Fire, 18*, 563–574. https://doi.org/10.1071/WF07098

Nembrini, S., König, I. R., & Wright, M. N. (2018). The revival of the Gini importance? *Bioinformatics, 34*, 3711–3718. https://doi.org/10.1093/bioinformatics/bty373

Nitzsche, N., Nunes, J. P., & Parente, J. (2024). Assessing post-fire water quality changes in reservoirs: Insights from a large dataset in Portugal. *Science of The Total Environment, 912*, Article 169463. https://doi.org/10.1016/j.scitotenv.2023.169463

Nunes, A. N., Lourenço, L., & Meira, A. C. C. (2016). Exploring spatial patterns and drivers of forest fires in Portugal (1980–2014). *The Science of the Total Environment, 573*, 1190–1202. https://doi.org/10.1016/j.scitotenv.2016.03.121

Nunes, A. N., & Lourenço, L. (2017). Increased vulnerability to wildfires and post fire hydro-geomorphic processes in Portuguese mountain regions: What has changed? *Open Agriculture, 2*(1), 70–82. https://doi.org/10.1515/opag-2017-0008

Nunes, A. N., Figueiredo, A., Pinto, C., & Lourenço, L. (2023). Assessing wildfire hazard in the wildland–urban interfaces (WUIs) of central Portugal. *Forests, 14*. https://doi.org/10.3390/f14061106

Nunes, A. N., Figueiredo, A., Pinto, C. D., & Lourenço, L. (2023). An Evaluation of wildfire vulnerability in the wildland–urban interfaces of central Portugal using the analytic network process. *Fire, 6*. https://doi.org/10.3390/fire6050194

Oliveira, S., Oehler, F., San-Miguel-Ayanz, J., Camia, A., & Pereira, J. M. C. (2012). Modeling spatial patterns of fire occurrence in Mediterranean Europe using multiple regression and random forest. *Forest Ecology and Management, 275*, 117–129. https://doi.org/10.1016/j.foreco.2012.03.003

Oliveira, S., Félix, F., Nunes, A., Lourenço, L., Laneve, G., & Sebastián-López, A. (2018). Mapping wildfire vulnerability in Mediterranean Europe. Testing a stepwise approach for operational purposes. *Journal of Environmental Management, 206*, 158–169. https://doi.org/10.1016/j.jenvman.2017.10.003

Oliveira, S., & Zêzere, J. L. (2020). Assessing the biophysical and social drivers of burned area distribution at the local scale. *Journal of Environmental Management, 264*. https://doi.org/10.1016/j.jenvman.2020.110449

Oliveira, S., Gonçalves, A., & Zêzere, J. L. (2021). Reassessing wildfire susceptibility and hazard for mainland Portugal. *The Science of the Total Environment, 762*, Article 143121. https://doi.org/10.1016/j.scitotenv.2020.143121

Oliveira, M. R., Ferreira, B. H. S., Souza, E. B., Lopes, A. A., Bolzan, F. P., Roque, F. O., Pott, A., Pereira, A. M. M., Garcia, L. C., Damasceno, G. A., Costa, A., Rocha, M., Xavier, S., Ferraz, R. A., & Ribeiro, D. B. (2022). Indigenous brigades change the spatial patterns of wildfires, and the influence of climate on fire regimes. *Journal of Applied Ecology, 59*(5), 1279–1290. https://doi.org/10.1111/1365-2664.14139

Pandey, P., Huidobro, G., Lopes, L.F., Ganteaume, A., Ascoli, D., Colaco, C., Xanthopoulos, G., Giannaros, T.M., Gazzard, R., Boustras, G., Steelman, T., Charlton, V., Ferguson, E., Kirschner, J., Little, K., Stoof, C., Nikolakis, W., Fernández-Blanco, C.R., Ribotta, C., Lambrechts, H., Fernandez, M., Dossi, S. (2023). A global outlook on increasing wildfire risk: Current policy situation and future pathways. Trees, For. People 14. Doi: 10.1016/j.tfp.2023.100431.

Parente, J., & Pereira, M. G. (2016). Structural fire risk: The case of Portugal. *Science of the Total Environment, 573*, 883–893. https://doi.org/10.1016/j.scitotenv.2016.08.164

Pausas, J. G., & Keeley, J. E. (2019). Wildfires as an ecosystem service. *Frontiers in Ecology and the Environment, 17*, 289–295. https://doi.org/10.1002/fee.2044

Piñol, J., Beven, K., & Viegas, D. X. (2005). Modelling the effect of fire-exclusion and prescribed fire on wildfire size in Mediterranean ecosystems. *Ecological Modelling, 183*, 397–409. https://doi.org/10.1016/j.ecolmodel.2004.09.001

Ponce-Calderón LP, Rodríguez-Trejo DA, Villanueva-Díaz J, Bilbao BA, Álvarez-Gordillo GDC y Vera-Cortés G. (2021). Historical fire ecology and its effect on vegetation dynamics of the Lagunas de Montebello National Park, Chiapas, México. iForest 14: 548-559. http://doi.org/10.3832/ifor3682-014.

Ponce-Calderón, L. P., Limón-Aguirre, F., Rodríguez, I., Rodríguez-Trejo, D. A., Bilbao, B. A., Álvarez-Gordillo, G. D. C., & Villanueva-Díaz, J. (2022). Fire management in pyrobiocultural landscapes, Chiapas, Mexico. *Tropical Forest Issues, 61*, 53–59. https://doi.org/10.55515/ABWJ7126

Pourghasemi, H. R., Gayen, A., Lasaponara, R., & Tiefenbacher, J. P. (2020). Application of learning vector quantization and different machine learning techniques to assessing forest fire influence factors and spatial modelling. *Environmental Research, 184*, Article 109321. https://doi.org/10.1016/j.envres.2020.109321

Pourtaghi, Z. S., Pourghasemi, H. R., & Rossi, M. (2015). Forest fire susceptibility mapping in the Minudasht forests, Golestan Province, Iran. *Environmental Earth Sciences, 73*, 1515–1533. https://doi.org/10.1007/s12665-014-3502-4

R Core Team, 2024. The R Project for Statistical Computing.

Ribeiro, J., Marques, J. E., Mansilha, C., & Flores, D. (2021). Wildfires effects on organic matter of soils from Caramulo Mountain (Portugal): Environmental implications. *Environmental Science and Pollution Research, 28*(1), 819–831. https://doi.org/10.1007/s11356-020-10520-w

Rodrigues, M., & De la Riva, J. (2014). An insight into machine-learning algorithms to model human-caused wildfire occurrence. *Environmental Modelling & Software: With Environment Data News, 57*, 192–201. https://doi.org/10.1016/j.envsoft.2014.03.003

Rodríguez-Trejo, D. A., Ponce-Calderón, L. P., Tchikoué, H., Martínez-Domínguez, R., Martínez-Muñoz, P., & Pulido-Luna, J. A. (2022). Towards integrated fire management in Mexico's Megalopolis region: A diagnosis. *Tropical Forest Issues, 61*, 80–86. https://doi.org/10.55515/NWAM8441

Romano, N., & Ursino, N. (2020). Forest fire regime in a mediterranean ecosystem: Unraveling the mutual interrelations between rainfall seasonality, soil moisture, drought persistence, and biomass dynamics. *Fire, 3*, 1–20. https://doi.org/10.3390/fire3030049

Rossetti, I., Cogoni, D., Calderisi, G., & Fenu, G. (2022). Short-term effects and vegetation response after a Megafire in a Mediterranean area. *Land, 11*(12), 2328. https://doi.org/10.3390/land11122328

Santana Neto, V. P., Leite, R. V., dos Santos, V. J., Castro, J. D. S., Torres, F. T. P., & Calijuri, M. L. (2022). Burning susceptibility modeling to reduce wildfire impacts: a GIS and multivariate statistics approach. *Floresta e Ambient., 29*, 1–12. https://doi.org/10.1590/2179-8087-FLORAM-2021-0078

Santana Neto, V. P., Soares, D. M., da Silva, T. C., & Torres, F. T. P. (2023). Assessment of two methods on zoning wildfire propagation in Itacolomi State Park, Minas Gerais State, Brazil. *Pesqui. Florest. Bras., 43*, 1–12. https://doi.org/10.4336/2023.pfb.43e202102227

Santos, L., Lopes, V., & Baptista, C. (2022). MDIR monthly ignition risk maps, an integrated open-source strategy for wildfire prevention. *Forests, 13*, 408. https://doi.org/10.3390/f13030408

Sari, F. (2021). Forest fire susceptibility mapping via multi-criteria decision analysis techniques for Mugla, Turkey: A comparative analysis of VIKOR and TOPSIS. *Forest Ecology and Management, 480*, Article 118644. https://doi.org/10.1016/j.foreco.2020.118644

Sari, F. (2024). Assessment of the effects of different variable weights on wildfire susceptibility. *European Journal of Forest Research*. https://doi.org/10.1007/s10342-023-01643-z

Sayad, Y. O., Mousannif, H., & Al Moatassime, H. (2019). Predictive modeling of wildfires: A new dataset and machine learning approach. *Fire Safety Journal, 104*, 130–146. https://doi.org/10.1016/j.firesaf.2019.01.006

Sequeira, M. D., Castilho, A. M., Dinis, P. A., & Tavares, A. O. (2020). Impact assessment and geochemical background analysis of surface water quality of catchments affected by the 2017 Portugal wildfires. *Water, 12*(10), 2742. https://doi.org/10.3390/w12102742

Shang, C., Wulder, M. A., Coops, N. C., & White, J. C. (2020). Spatially-Explicit Prediction of Wildfire Burn Probability Using Remotely-Sensed and Ancillary Data. *Canadian Journal of Remote Sensing*, 1–17. https://doi.org/10.1080/07038992.2020.1788385

Shapley, L. S. (1953). Stochastic games. *Proceedings of the National Academy of Sciences, 39*, 1095–1100. https://doi.org/10.1073/pnas.39.10.1095

Stephens, S. L., Westerling, A. L. R., Hurteau, M. D., Peery, M. Z., Schultz, C. A., & Thompson, S. (2020). Fire and climate change: Conserving seasonally dry forests is still possible. *Frontiers in Ecology and the Environment, 18*, 354–360. https://doi.org/10.1002/fee.2218

Su, Z., Hu, H., Wang, G., Ma, Y., Yang, X., & Guo, F. (2018). Using GIS and random forests to identify fire drivers in a forest city, Yichun, China. Geomatics. *Nature Hazards Risk, 9*, 1207–1229. https://doi.org/10.1080/19475705.2018.1505667

Tedim, F., Remelgado, R., Martins, J., Carvalho, S. (2013). Os grandes incêndios florestais em Portugal: desafios para a gestão do risco, in: Grandes Incêndios Florestais, Erosão, Degradação e Medidas de Recuperação Dos Solos. António Bento Gonçalves e António Vieira, NIGP – Núcleo de Investigação em Geografia e Planeamento Universidade do Minho, pp. 75–86.

Tedim, F., Leone, V., Amraoui, M., Bouillon, C., Coughlan, M., Delogu, G., … Xanthopoulos, G. (2018). Defining Extreme Wildfire Events: Difficulties, Challenges, and Impacts. *Fire, 1*(1), 9. https://doi.org/10.3390/fire1010009

Torres, A. M., & Paz, D. B. (2024). Advanced wildfire risk mapping: a novel global approach using AI and socio-ecological data (EGU24-16436). EGU24. *Copernicus Meetings*.. https://doi.org/10.5194/egusphere-egu24-16436

Tran, T. T. K., Janizadeh, S., Bateni, S. M., Jun, C., Kim, D., Trauernicht, C., Rezaie, F., Giambelluca, T. W., & Panahi, M. (2024). Improving the prediction of wildfire susceptibility on Hawai'i Island, Hawai'i, using explainable hybrid machine learning models. *Journal of Environmental Management, 351*, Article 119724. https://doi.org/10.1016/j.jenvman.2023.119724

Turco, M., Jerez, S., Augusto, S., Tarín-Carrasco, P., Ratola, N., Jiménez-Guerrero, P., & Trigo, R. M. (2019). Climate drivers of the 2017 devastating fires in Portugal. *Scientific Reports, 9*(1), 13886. https://doi.org/10.1038/s41598-019-50281-2

Verde, J. C., & Zêzere, J. L. (2010). Assessment and validation of wildfire susceptibility and hazard in Portugal. *Natural Hazards and Earth System Sciences, 10*, 485–497. https://doi.org/10.5194/nhess-10-485-2010

Voggesser, G., Lynn, K., Daigle, J., Lake, F. K., & Ranco, D. (2013). Cultural impacts to tribes from climate change influences on forests. *Climatic Change, 120*(3), 615–626. https://doi.org/10.1007/s10584-013-0733-4

Xiao, Y., Zhang, X., & Ji, P. (2015). Modeling forest fire occurrences using count-data mixed models in Qiannan autonomous prefecture of Guizhou Province in China. *PLoS One1, 10*. https://doi.org/10.1371/journal.pone.0120621

Yue, W., Ren, C., Liang, Y., Liang, J., Lin, X., Yin, A., & Wei, Z. (2023). Assessment of wildfire susceptibility and wildfire threats to ecological environment and urban development based on GIS and multi-source data: A Case study of Guilin, China. *Remote Sens., 15*. https://doi.org/10.3390/rs15102659

Chapter II

Weather Overrides Fuel Memory: Seasonal Dynamics of Fire Hazard and the Limits of the Fire Return Interval

Submitted to **Science of The Total Environment**

Vicente Paulo Santana Neto[a], José Marinaldo Gleriani[a], Fillipe Tamiozzo Pereira Torres[a], Adelia de Jesus Nobre Nunes[b], Igor Sanches Marini[c]

[a] Universidade Federal de Viçosa/UFV, Departamento de Engenharia Florestal,

Rua Purdue - Campus UFV, 36570-900, Viçosa – MG, Brasil.

[b] Universidade de Coimbra, Faculdade de Letras, Departamento de Geografia e Turismo

Colégio de S. Jerónimo, 3004-530, Coimbra, Portugal.

[c] Universidade Federal de Juiz de Fora/UFJF, Instituto de Arte e Design, Rua José Lourenço Kelmer, São Pedro, Juiz de Fora – MG, Brasil.

Weather Overrides Fuel Memory: Seasonal Dynamics of Fire Hazard and the Limits of the Fire Return Interval

Graphical Abstract

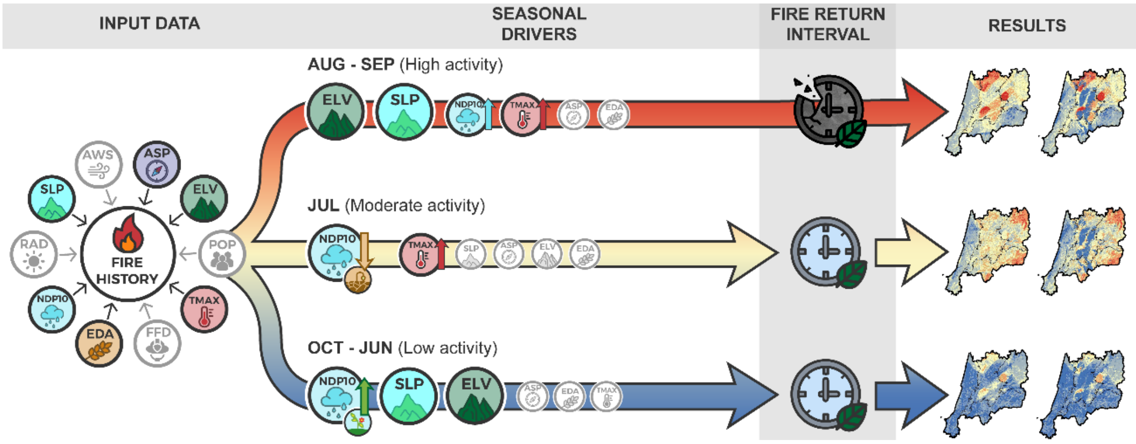

ABSTRACT

Wildfire regimes in Mediterranean hotspots like Portugal are driven by anthropogenic factors and fuel build-up, causing severe socio-economic impacts. Traditional hazard models, reliant on annual averages, often fail to capture the distinct seasonal dynamics governing these fire regimes. This study evaluated two hypotheses in Central Portugal: 1) that seasonally-disaggregated models outperform an overall annual model; and 2) that incorporating fuel age, via the Fire Return Interval (FRI), enhances predictive accuracy. Three fire seasons (High: Aug-Sep; Medium: Jul; Low: Oct-Jun) were statistically defined. Hazard maps were generated using a data-driven Spatial Multi-Criteria Evaluation (SMCE) and Simple Additive Weighting (SAW) approach. The FRI was calculated as the 10th percentile (P10) of re-burn intervals (1990-2024) per land cover class and geoclimatic zone; a temporal mask based on this threshold was applied to assign zero hazard to recently burned areas. All models were validated against independent 2019–2024 fire perimeters using the Area Under the Curve (AUC) method. The first hypothesis was partially validated: the seasonal High (AUC=0.81) and Low (AUC=0.80) models outperformed the Overall (AUC=0.77). We found dominant hazard drivers shifted seasonally: the July model (AUC=0.58) was linked to drought (low NDP10), whereas the High, Low, and Overall models were driven by topography and high fuel load (proxied by high NDP10). However, the second hypothesis was refuted for the critical period, as the FRI mask decreased predictive performance in the Overall and High-season models. The findings indicate that while seasonality is essential for differentiating hazard drivers, this "fuel memory" is overridden by extreme weather conditions. Management strategies based solely on historical burn patterns are, therefore, insufficient to mitigate hazard in extreme events.

Keywords: Portugal, Pyrogeography, Danger, Spatial Multi-Criteria Evaluation, Topography, Mediterranean, Recurrence

1 Introduction

Wildfire causes are broadly categorized into two main groups: natural and human. While natural ignitions are primarily driven by lightning (U.S. National Park Service, 2018), the overwhelming majority of ignitions are of anthropogenic origin. These result largely from negligence—such as uncontrolled agricultural burning and poorly extinguished campfires—or intentional acts (Nunes et al., 2021). In Portugal, arson and the misuse of fire collectively account for approximately 83% of occurrences with determined causes (AGIF, 2025).

The consequences of wildfires are extensive and devastating, entailing profound environmental, social, and economic impacts (Fidalgo and Fernandes, 2023). Ecologically, they drive habitat destruction, biodiversity loss, soil degradation and erosion, and massive greenhouse gas emissions into the atmosphere (Camargo et al., 2018; Costa et al., 2022; NASA Science, 2025). Socially, they result in loss of life, destruction of housing and infrastructure, and severe public health issues due to smoke inhalation, which can lead to increased mortality from cardiovascular and respiratory diseases (Reid et al., 2016; Tran et al., 2024). In Portugal, in 2024 alone, forest fires caused 16 fatalities and forest damages estimated at 67 million euros (AGIF, 2025).

Global wildfire dynamics present a complex and paradoxical picture. Contrary to common perception, the total global burned area has declined in recent decades, with Portugal recording the lowest number of fires since records began (AGIF, 2025; Doerr and Santín, 2016; Jones et al., 2022). This trend is largely driven by the conversion of fire-prone ecosystems, such as savannas and grasslands, into agricultural land, leading to landscape fragmentation and the disruption of fuel continuity (Jones et al., 2022; Shen et al., 2025).

However, this global trend masks a divergent reality: a significant increase in fire frequency and intensity within forest ecosystems, particularly in Southern Europe (Carmo et al., 2022). Portugal stands out as a "hotspot," with a burned area of approximately 265,560 km² during the 1975–2022 period, totaling an annual average of 565 km² (ICNF, 2024; Santana Neto et al., 2025). In extreme years such as 2003, 2005, and 2017, the burned area in Portugal exceeded that of all other Southern European countries combined (Carmo et al., 2022).

This regional intensification is unequivocally driven by climate change, which creates hotter, drier, and windier meteorological conditions—known as "fire weather" (Barbero et al., 2020; Jones et al., 2022). Factors such as increased vapor pressure deficit (VPD) and reduced fuel moisture are direct determinants of fire propagation (Haas et al., 2024). Human activity modulates the impact of these climatic conditions, influencing ignitions as well as fuel structure and characteristics through suppression policies that lead to fuel accumulation (Bowman et al., 2011; Shen et al., 2025).

The fire regime in Portugal exhibits three primary characteristics. First, it displays marked seasonality, with the majority of fires concentrated in the summer months (July to September) (Silva et al., 2023); Second, it demonstrates extreme interannual variability, strongly correlated with climatic variability such as severe droughts and heatwaves (DaCamara, 2024; Pereira et al., 2013). Finally, its vulnerability is accentuated by a confluence of structural factors: a climate characterized by hot, dry summers, a landscape dominated by flammable forests, and a history of socioeconomic changes—such as rural abandonment—that have led to fuel accumulation (Oliveira and Zêzere, 2020).

For effective territorial management, it is crucial to distinguish between fire diagnostic concepts which, although related, are not synonymous. Analysis begins with susceptibility, the landscape's intrinsic propensity to burn, dictated by slowly changing factors such as relief and vegetation (Luu et al., 2024; Mihajlovski and Zhiyanski, 2025; Santana Neto et al., 2025; Verde and Zêzere, 2010). This is complemented by ignition, which identifies locations where a fire is most predisposed to start (Santos et al., 2022).

Hazard combines these two elements, representing the probability and susceptibility of an area to wildfire, serving as the foundation for strategic planning (Parente and Pereira, 2016). The final concept is risk, which translates hazard into expected losses by considering the vulnerability of exposed elements (Bachmann and Allgöwer, 2001; Jappiot et al., 2009; Parente and Pereira, 2016; Verde and Zêzere, 2010).

Based on these definitions, this study adopts hazard as the central metric, focusing on strategic territorial planning. This choice is justified because hazard advances beyond susceptibility by incorporating the probability of fire occurrence (Trucchia et al., 2023). the primary innovation of this work lies in surpassing the traditional, typically annual approach, which masks crucial temporal dynamics (Yue et al., 2025). By refining the analysis with a seasonal dimension, it becomes possible to differentiate the factors driving fire throughout the year, generating more effective territorial management strategies (Januário and Minuzzi, 2020; Torres et al., 2024; Wang et al., 2023).

To enhance the precision of this seasonal hazard analysis, integrating fuel dynamics—directly influenced by historical fire frequency—is fundamental. In this context, the Fire Return Interval (FRI)—the average time between fires at a specific location—becomes an essential metric, often determined by methods such as dendrochronology to establish a historical baseline (Frost, 1998; Parks et al., 2025). This metric is crucial for defining wildfire hazard, as intervals significantly longer than the historical baseline lead to fuel accumulation and a "fire deficit" condition, increasing the risk of catastrophic fires (Merriam et al., 2022; Parks et al., 2025).

The FRI varies significantly across regions; in Portugal, for instance, it is shorter in the north due to practices such as pastoral burning (Mateus and Fernandes, 2014; Oliveira and Fernandes, 2023), directly influencing forest management decisions, such as species selection for planting (Mateus and Fernandes, 2014). Furthermore, the realization that total suppression policies, without proper fuel management, prove ineffective against large wildfires under extreme meteorological conditions reinforces the importance of mapping high-hazard areas and prioritizing management actions aimed at restoring landscape resilience.

Existing hazard models, including the official methodology in Portugal, rely on annual data aggregation that masks distinct seasonal fire dynamics (DGTerritório, 2022a). An aggregated model is forced to derive an average relationship that fails to faithfully represent the different fire regimes throughout the year—such as those driven by human factors versus those dominated by climate—resulting in a sub-optimized planning tool.

The innovative proposal of this work is to overcome this limitation by disaggregating the temporal analysis. The study posits that identifying distinct fire seasons and applying a seasonal Fire Return Interval (FRI) metric significantly increases the accuracy of hazard models. Additionally, it is postulated that the predictive factors of greatest importance differ between seasons, with socioeconomic and climatic variables assuming distinct weights.

To test these hypotheses, the general objective is to develop and validate hazard assessment models that incorporate fire regime seasonality. Specific objectives include the objective characterization of fire seasons, the calculation of a seasonal FRI, the development of distinct hazard models for each season, and the comparison of their performance against a reference annual model, culminating in the production of more precise and dynamic hazard maps.

2 Material and Methods

2.1 Study area

The landscape of the Central Region of Portugal, covering an area of 28,199 km², is characterized by remarkable geomorphological and climatic heterogeneity, featuring topography that extends from the Central Mountain Range to the coastal zone (Nunes et al., 2023b) (Figura 1). Average summer climatic conditions—pivotal drivers of fire spread—range from 16 to 33.7 °C in temperature, 14 to 194 mm in accumulated precipitation, and 3.26 to 7.71 m/s in wind speed (Costa and Estanqueiro, 2023; IPMA, 2009a, 2009b).

Human intervention and occupation within this landscape manifest in diverse forms. Administratively divided into 100 municipalities, the region exhibits marked variation in population density, ranging from uninhabited areas to peaks of 535.81 inhabitants/ha in major urban centers (INE, 2022). Concurrently, the landscape has been shaped by land cover changes between 1990 and 2018, driven notably by the replacement of coniferous forests with eucalyptus plantations, while shifts in other land use classes remained less significant (DGTerritório, 2022b; Santana Neto et al., 2025). Firefighting personnel levels have also shifted over time, decreasing from 10,652 in 1998 to 7,800 in 2023 (PORDATA, 2025).

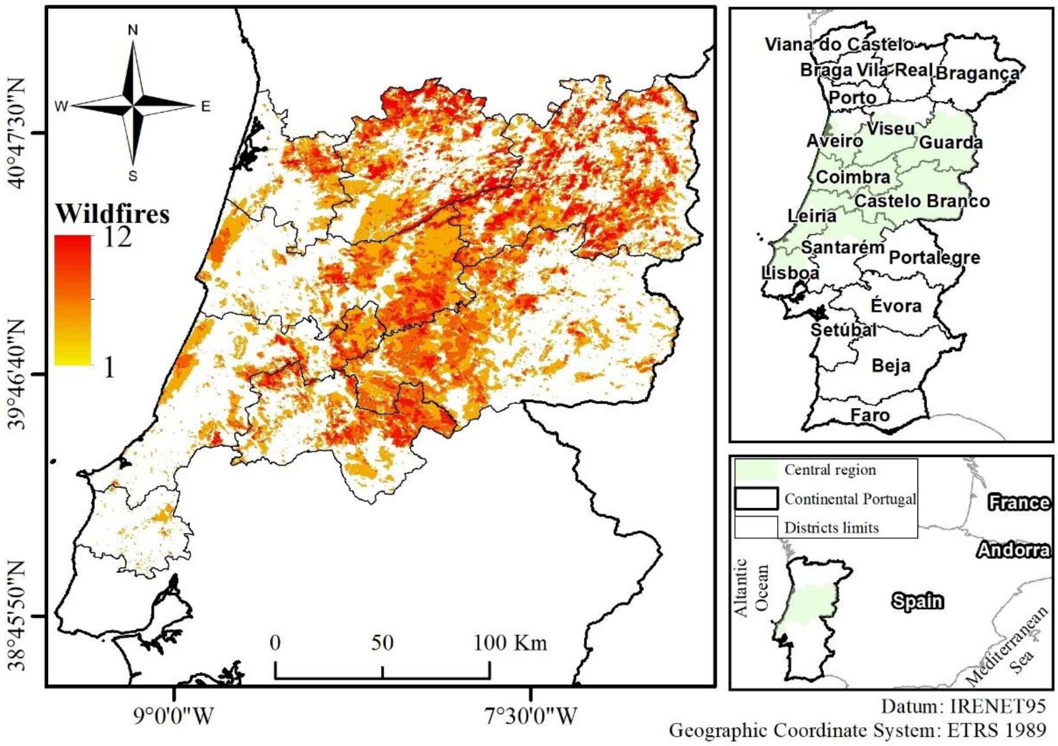

Figure 1. Location of the study area and the number of wildfires recorded between 1990 and 2024 (ICNF, 2024). The inset maps on the right provide regional context, detailing district divisions (top) and the location of mainland Portugal within Europe (bottom).

Within the study area, the southern region is characterized by hotter summers, low precipitation, and steep relief in its central portion (ASF, 2024; IPMA, 2009c, 2009a). The eastern zone, while similarly dry, features higher altitudes, most notably the *Serra da Estrela* mountain range, where a colder and wetter microclimate constitutes a significant exception. Conversely, the central/northern region combines steep slopes with high precipitation, whereas the western coastal zone—the most populous area (INE, 2022), —contrasts with flat terrain, mild temperatures, and low precipitation, except in its northernmost reaches.

2.2 Spatiotemporal Characterization of Fire Regimes

2.2.1 Geoclimatic Stratification

To analyze the spatial variability of fire regimes, the region was stratified into geoclimatic zones. Input variables included elevation and the climatic variables number of days with precipitation greater than 10 mm and number of days with temperature above 25°C, which were identified as the best predictors for fire susceptibility by Santana Neto (2025).

The variable values were extracted onto a hexagonal grid. Following standardization, the Ward.D2 hierarchical clustering method was applied. This method groups data by minimizing the increase in internal variance to create compact and homogeneous clusters (Murtagh and Legendre, 2014). The optimal number of clusters was determined using the Within-Cluster Sum of Squares (WCSS) method. The result was then spatially refined by merging polygons smaller than 500 km^2 with their neighboring zones—a threshold defined through visual analysis—thereby consolidating the final geoclimatic zones.

2.2.2 Statistical Definition of Fire Seasons

To avoid a subjective definition, a multivariate statistical approach was employed. To determine the month of occurrence for each event, the fire database was complemented by spatiotemporal matching between the burned area polygons and the ICNF forest fire points (2012–2024, excluding 2017). In cases where the month was not directly available, visual and manual comparison supplemented the analysis. For each month, the total number of occurrences and the total burned area were calculated, to which a Principal Component Analysis (PCA) was applied.

The first principal component (PC1) was then utilized as a fire intensity index. Subsequently, the PC1 scores for each month were submitted to the Scott–Knott mean clustering test. This method is a hierarchical clustering analysis that partitions a set of means into statistically distinct and homogeneous groups, ensuring no overlap between them (Jelihovschi et al., 2014; Scott and Knott, 1974).

2.2.3 Fire Return Interval (FRI) Analysis

To incorporate the dynamics of post-fire vegetation regeneration, the Fire Return Interval (FRI) was analyzed for each Land Use and Cover (LUC) class within each of the four geoclimatic zones, using the historical fire record spanning from 1990 to 2024.

The method consisted of identifying all reburn events, defined as fire overlaps in distinct years covering an area greater than 1 hectare. For each event, the FRI was calculated and associated with the LUC class of the first fire. Subsequently, the 10th percentile (P10) of the FRI distribution was adopted for every unique combination of LUC and geoclimatic zone. This threshold was empirically selected following preliminary tests (not shown) that compared the P10, P25, and the median, where the P10 resulted in the highest predictive power (AUC) for the fitted models, indicating that it is the most effective indicator of the minimum fuel recovery time.

To test the hypothesis that this fuel limitation improves prediction, a 'No-Hazard Mask' was created for the year 2019. In its construction, all pixels whose age (time since the last fire) was lower than their specific FRI threshold (P10) were classified as 'no hazard', based on the assumption that they lacked sufficient fuel to sustain a new fire. Finally, this binary mask was applied to adjust the seasonal and overall hazard maps.

2.3 Wildfire Hazard Modeling

2.3.1 Preprocessing and Standardization of Predictors

The hazard modeling was based on a set of predictive variables (Table 1), which were processed and standardized to a 30 m spatial resolution and aligned to the same coordinate system and extent as the study area. These variables were divided into two groups. The first group, comprising static factors, included geomorphometric and climatic variables; the latter were represented by long-term climatological normals and were therefore treated as invariant over the study period. The second group comprised variables subject to temporal changes, namely land use and cover, firefighter density, population density, and Euclidean distance from agricultural areas. However, these factors were treated as static components within the modeling framework, utilizing a single snapshot from the year 2015. This specific year was selected as the temporal midpoint of the calibration period because the variations in these drivers between 2012–2015 and 2015–2018 were considered negligible, allowing the 2015 data to serve as a reliable baseline for the entire period.

Table 1. Geospatial explanatory variables applied in wildfire hazard modeling.

Name	Acronym (Unit)	Description	Scale/Resolution	Source
Aspect	ASP	Slope orientation according to cardinal points	500 m	(ASF, 2024)
Slope	SLP (∘)	Inclination of the relief (or: terrain inclination)	10 m	(ASF, 2024)
Elevation	ELV (m)	Altitude relative to sea level	Cartographic unit ha / Minimum Distance (among isolines) / Scale: 1:25,000	(ASF, 2024)
Solar Radiation	RAD (Wh m−2)	Incident solar radiation per point	10 m	(ASF, 2024)

Average Wind Speed	AWS (m/s)	Average Wind Speed measured at 10 m height	10 m	(Costa and Estanqueiro, 2023)
Euclidean distance from agricultural areas	EDA (km)	Euclidean distance from agricultural areas	10 m	(DGTerritório, 2022b)
Land Use and Cover	LUC	Type of cover or land use	100 m	(DGTerritório, 2022b)
Population Density	POP (inhab/ha)	Number of inhabitants per hectare	Frequency Level	(INE, 2022)
Number of days with T>25∘C	T25(days)	Number of days per year with temperature above 25∘C	Cartographic unit ha / Minimum Distance (between isolines) / Scale: 1:25,000	(IPMA, 2009d)
Mean Maximum Summer Temperature	TMAX(∘C)	Mean maximum temperature of each summer day	100 m	(IPMA, 2009a)
Number of days per year with P>10mm	NDP10 (days)	Number of days per year with precipitation >10mm	100 m	(IPMA, 2009c)
Accumulated Annual Precipitation	PREC (mm)	Accumulated precipitation per year	100 m	(IPMA, 2009b)
Firefighter Density	FFD (unit/ha)	Number of firefighters per hectare	Frequency Level	(PORDATA, 2025)

The pairwise correlations and potential multicollinearity among these predictor variables were previously evaluated by Santana Neto et al. (2025). Their analysis demonstrated that, with the exception of expected climatological interactions — such as a positive correlation between accumulated precipitation and days with P > 10 mm, and a negative correlation with maximum temperature —, the variables generally exhibit weak linear associations, confirming their suitability for joint inclusion in the spatial modeling framework.

2.3.2 Frequency-Based Hazard Weighting

The fire frequency analysis commenced with rigorous preprocessing to standardize the geometry of the 13 predictive variables. The 11 continuous variables—excluding Land Use and Cover (LUC) and Aspect — were subsequently discretized into up to eight quantile-based classes (Table 2). Due to the nature of their data distributions, the Population Density (POP) and Euclidean Distance from Agricultural Areas (EDA) variables exhibited a high frequency of identical values, consequently yielding fewer than eight classes.

Table 2. Quantile-based class boundaries for the continuous predictor variables.

EDA (km)	FFD (unit/ha)	POP (inhab/ha)	ELV (m)	SLP (°)
0.00 - 30.00	0.00 - 8.07e-04	0.00 - 2.34e-03	0.00 - 64.72	0.00 - 0.96
30.00 - 60.00	8.07e-04 - 1.39e-03	2.34e-03 - 7.74e-03	64.72 - 141.72	0.96 - 2.36
60.00 - 123.69	1.39e-03 - 2.00e-03	7.74e-03 - 0.02	141.72 - 235.54	2.36 - 4.02
123.69 - 218.40	2.00e-03 - 2.59e-03	0.02 - 0.08	235.54 - 327.68	4.02 - 6.17
218.40 - 381.84	2.59e-03 - 3.46e-03	0.08 - 1.05	327.68 - 427.14	6.17 - 9.12
381.84 - 680.15	3.46e-03 - 4.11e-03	1.05 - 764.86	427.14 - 551.91	9.12 - 13.30
680.15 - 11365.25	4.11e-03 - 5.86e-03		551.91 - 735.00	13.30 - 19.40
	5.86e-03 - 0.05		735.00 – 1,990.00	19.40 - 82.34

NDP10	NDT25	PREC (mm)	RAD (Wh/m²)	TMAX (°C)	AWS (m/s)
13.90 - 23.75	6.42 - 57.41	14.00 - 41.20	118,485 – 446,086	15.99 - 24.01	2.74 - 3.50
23.75 - 26.13	57.41 - 73.71	41.20 - 48.64	446,086 – 457,755	24.01 - 25.08	3.50 - 3.73
26.13 - 28.81	73.71 - 85.33	48.64 - 54.45	457,755 – 462,169	25.08 - 25.99	3.73 - 3.92
28.81 - 32.31	85.33 - 96.34	54.45 - 60.86	462,169 – 468,650	25.99 - 26.72	3.92 - 4.11

32.31 - 35.49	96.34 - 103.62	60.86 - 68.42	468,650 – 475,762	26.72 - 27.55	4.11 - 4.34
35.49 - 38.17	103.62 - 110.78	68.42 - 76.17	475,762 – 482,992	27.55 - 28.36	4.34 - 4.57
38.17 - 43.18	110.78 - 120.26	76.17 - 90.43	482,992 – 493,783	28.36 - 29.85	4.57 - 4.91
43.18 - 57.91	120.26 - 140.53	90.43 - 193.92	493,783 – 583,158	29.85 - 33.71	4.91 - 6.51

Where: EDA (Euclidean Distance from Agricultural Areas, km); FFD (Firefighter Density, unit/ha); POP (Population Density, inhab/ha); ELV (Elevation, m); SLP (Slope, °); NDP10 (Number of Days with Precipitation > 10 mm, days); T25 (Number of Days with T > 25 °C, days); PTOTAL (Total Precipitation, mm); RAD (Solar Radiation, Wh/m2); TMAX (Maximum Temperature, °C); AWS (Average Wind Speed, m/s).

To determine the fire propensity, the base burning ratio for each class was first established as the proportion between its burned area and its total area $BA_{v,c}/TA_{v,c}$. From this ratio, two distinct metrics were calculated: a relative score $R_{v,c}$ to evaluate the internal hierarchy of the variable, and a global score $S_{v,c}$ used for the final modeling.

The Relative Hazard Score $R_{v,c}$ was designed to weigh the classes within the same variable. It was calculated by normalizing the burning ratio of each class against the maximum burning ratio observed strictly within that specific variable, assigning a maximum score of 10 to the most fire-prone class, as shown in Equation 1:

$$R_{v,c} = \frac{\left(\frac{BA_{v,c}}{TA_{v,c}}\right)}{\max\left(\frac{BA_v}{TA_v}\right)} \times 10 \qquad \text{(Equation 1)}$$

Where:

- $R_{v,c}$ is the Burning Ratio for class c of variable v.
- $BA_{v,c}$ is the Total Burned Area of class c of variable v.
- $TA_{v,c}$ is the Total Area of class c of variable v
- $\max\left(\frac{BA_v}{TA_v}\right)$ is the highest burning ratio observed among all classes exclusively within variable v.

Conversely, the Global Hazard Score $S_{v,c}$ was established to allow direct comparison across different variables during the spatial modeling process. This metric normalized the burning ratio of each class against the absolute maximum burning ratio found across all classes of all variables combined, as expressed in Equation 2:

$$S_{v,c} = \frac{\left(\frac{BA_{v,c}}{TA_{v,c}}\right)}{\max\left(\frac{BA}{TA}\right)_{global}} \times 10 \qquad \text{(Equation 2)}$$

Where:

- $S_{v,c}$ is the Global Hazard Score for class c of variable v
- $BA_{v,c}$ is the Total Burned Area of class c of variable v.
- $TA_{v,c}$ is the Total Area of class c of variable v
- $\max\left(\frac{BA}{TA}\right)_{global}$ is the absolute maximum burning ratio observed across all classes of all 13 variables.

This global $S_{v,c}$ value was subsequently adopted as the definitive mathematical weight for each class in the map algebra to generate the final hazard maps.

2.3.3 Development of the RFE-Optimized Overall Hazard Model

The modeling process commenced with the generation of "score rasters" for each of the 13 variables, substituting the class values with their calculated Sv,c. To identify the subset of predictors with the highest generalization capacity, a Recursive Feature Elimination (RFE) technique with a backward elimination approach was implemented.

The iterative process was designed to optimize model performance on future and independent data (fires from 2019–2024). In each iteration, the method systematically evaluates the impact of removing each variable. The variable permanently discarded was the one whose absence resulted in the greatest performance gain, quantified by the increase in the Area Under the Curve (AUC) value.

The AUC, which synthesizes the Receiver Operating Characteristic (ROC) (Bradley, 1997), was selected as a robust metric that attests to the quality of the model. It indicates the probability that effectively burned areas will exhibit higher hazard values than unburned areas (Nunes and Lourenço, 2017; Santana Neto et al., 2025, 2023, 2022). AUC values are typically classified according to the following scale of adequacy: Poor (<0.6), Moderate (0.7–0.8), Good (0.8–0.9), or Excellent (>0.9) (Akıncı et al., 2024; Shang et al., 2020).

The subset of variables that produced the highest AUC was identified as the optimal model. The final hazard map was then generated by taking the simple average of the score rasters from this optimal set, applying the scores (calculated using 2015 data) to the 2018 dynamic variables. This year (2018) was utilized because it immediately precedes the validation period (2019–2024), thereby representing the most current landscape condition for the predictive test.

2.3.4 Development of Seasonal Hazard Models

Based on the fire seasons defined in Section 2.2.2, and to evaluate whether specific models enhance predictive performance, a hazard map was constructed for each defined fire season. The process involved recalculating the hazard scores ($S_{v,c}$) specific to each period. Crucially, the same subset of variables (defined by the RFE of the overall model) was maintained across all seasonal models. This decision, far from contradicting the hypothesis that factor importance varies across seasons, is essential for testing it: by holding the predictor set constant, any alteration observed in the $S_{v,c}$ values and predictive performance (AUC) can be directly attributed to the effect of seasonality, rather than to a change in the set of predictors itself. The season-specific hazard maps were generated using a data-driven Spatial Multi-Criteria Evaluation (SMCE) approach. Through GIS-based map algebra, the original environmental variables (utilizing 2018 data for dynamic factors) were reclassified based on their respective Global Scores $S_{v,c}$ derived from the baseline susceptibility model. Finally, a Simple Additive Weighting (SAW) method was applied to calculate the unweighted mean of these reclassified layers, yielding the final hazard index for each pixel.

2.4 Post-Processing Hazard Maps with FRI Dynamics

To test the hypothesis that vegetation regeneration dynamics enhance predictive capability, a post-processing stage was conducted. The generated hazard maps were refined using the 'no-hazard mask' (derived in Section 2.2.3). Application of this mask assigned a hazard value of zero to all pixels classified as 'no hazard,' based on the principle of insufficient fuel, resulting in a new suite of temporally adjusted maps.

2.5 Model Validation and Performance Assessment

The final stage involved a rigorous comparative validation of all maps developed, leveraging an independent, future fire dataset (2019–2024) as the reference. The analysis was structured to quantify model performance across two distinct scenarios: the original model (Baseline - BL) and the adjusted model (Temporally-Adjusted - TA).

Prior to validation, hazard maps were normalized to a 0-to-1 scale. To ensure the preservation of the relative value scale, this normalization was initially applied only to pixels exhibiting a hazard score greater than zero. Subsequently, the null areas from the FRI mask were reincorporated with a score of 0. The resultant maps were then compared against the actual burned areas observed during 2019–2024.

For each of the two scenarios (BL and TA), a specific "ground truth" map was created by rasterizing the 2019–2024 fires corresponding to the model's scope (overall or seasonal). Performance was subsequently assessed using two primary methods:

1. Coherence Analysis by Hazard Classes: The normalized hazard maps were reclassified into five ordinal classes (Very Low, Low, Moderate, High, and Very High) using equidistant intervals.
2. ROC Curve and AUC Analysis: The discriminatory capacity of each model was quantified via the Area Under the Curve (AUC).

3. Spatial Correlation Analysis: To evaluate the spatial congruence and divergence among the distinct hazard profiles, a pixel-wise Pearson correlation analysis was conducted. The correlation coefficient (r) was calculated pairwise across the normalized overall and season-specific hazard maps.

3 Results

3.1 Spatiotemporal Characterization of Fire Regimes

The clustering analysis stratified the study area into four distinct geoclimatic zones: East, West, South, and Central/North (Figure 2). During the analyzed period (excluding the extreme 2017 fire season), fire activity predominated in the Central/North and East regions, with moderate incidence observed in the South.

For the temporal analysis, the Principal Component Analysis (PCA) demonstrated that the first principal component (PC1) accounted for 83.5% of the combined variation in fire number and burned area. The subsequent Scott–Knott test, applied to this index, grouped the months into three statistically distinct fire seasons: August and September were classified as high-activity months, July as medium-activity, and the remaining nine months as low-activity (Annex A).

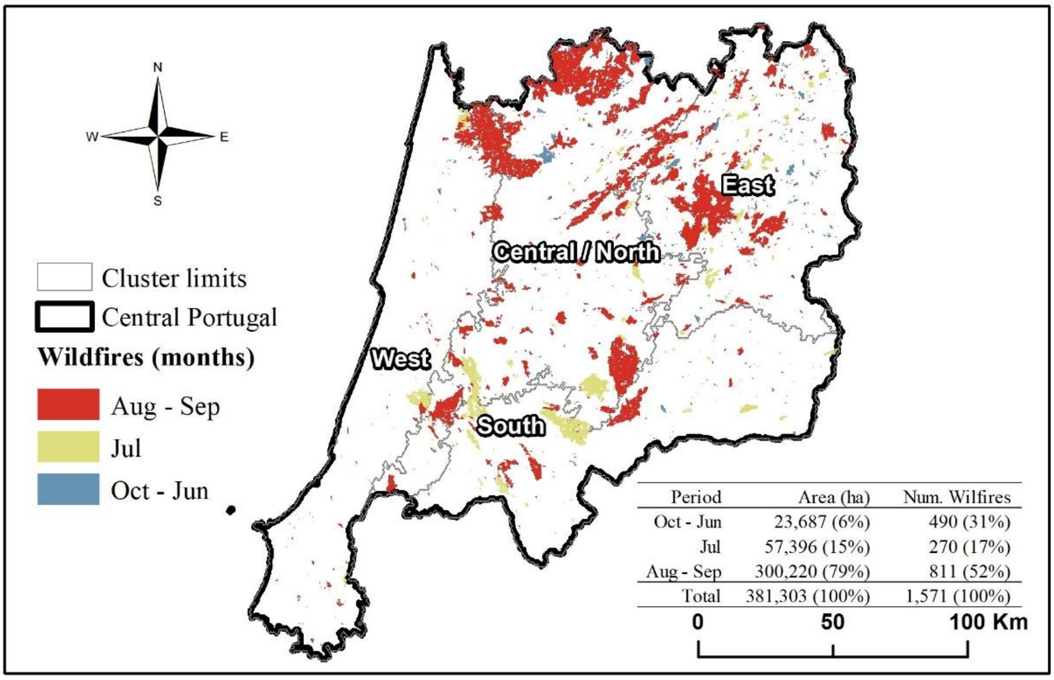

Figure 2. Map of the geoclimatic stratifications in the Central Region of Portugal. The superimposed colors represent burned areas between 2012–2024 (excluding 2017), classified according to the fire season. The inset table in the lower right corner summarizes the burned area and the number of fires for each period.

The Fire Return Interval (FRI) analysis revealed distinct regional patterns across the geoclimatic clusters (Annex B). The East cluster was characterized by the lowest FRI values overall. The West and Central/North clusters exhibited greater internal variation, with records spanning from the study's longest recurrence intervals (e.g., resinous forests in the West) to the shortest. The South cluster, conversely, presented higher P10 values than the East for the majority of land use classes.

The regional exception was found in the classes "Pastures, Agroforestry Systems (SAFs), Cork Oaks, Holm Oaks, and Bare Land" and "Shrublands," which consistently maintained the lowest P10 values across all four regions.

3.2 Wildfire Hazard Modeling

Recursive Feature Elimination (RFE) identified a parsimonious subset of six critical predictors for the hazard models: Aspect, Euclidean Distance from Agricultural Areas (EDA), Elevation (ELV), Slope (SLP), Number of Days with Precipitation > 10 mm (NDP10), and Maximum Temperature (TMAX). Figure 3 illustrates the specific class or quantile within each of these variables that exhibited the highest Global Score $S_{v,c}$, alongside their respective coefficient of variation (CV%) across the overall and seasonal models. The detailed quantitative scoring for each class is provided in Annex C.

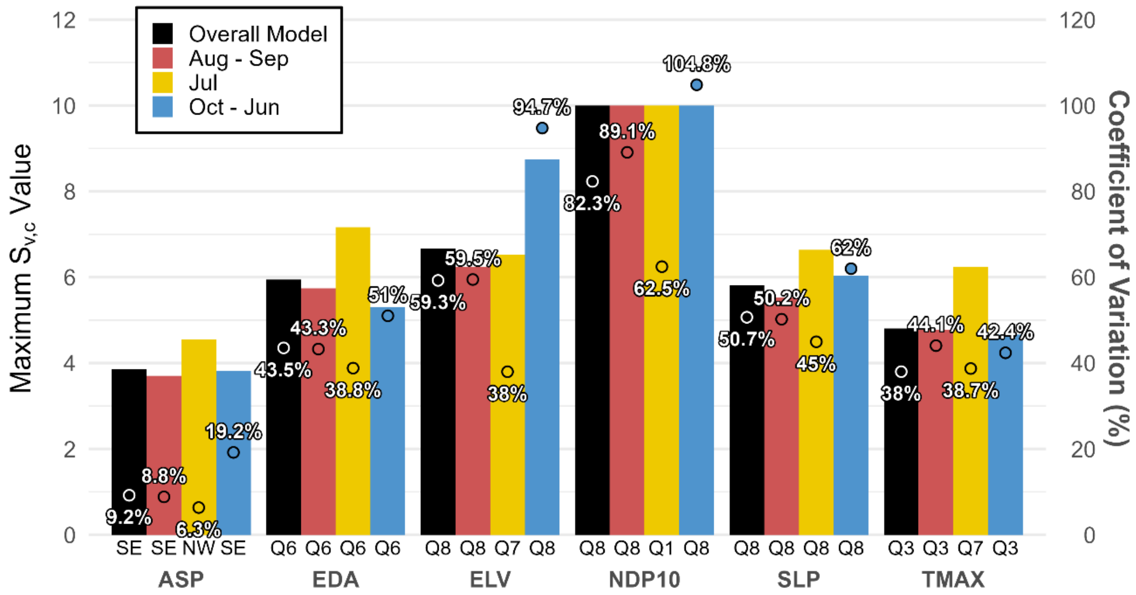

Figure 3. Synthesis of the maximum normalized index values ($S_{v,c}$) and Coefficient of Variation (CV) for predictor variables across the four hazard models. The bar chart (left axis) depicts the peak score for each variable, with the x-axis labels specifying the class where the maximum occurred; the superimposed points (right axis) illustrate the corresponding Coefficient of Variation (%).

Data analysis (Annex C) elucidates distinct functional relationships among the variables. A positive relationship was observed between fire hazard and Slope (SLP) across all models; a similar trend was evident for Elevation (ELV), with the notable exception of the July model. Regarding Aspect, while southeastern exposures consistently exhibited the highest hazard propensity, the low magnitude of $S_{v,c}$ and CV values (6.3%–19.2%) suggests this variable exerts a moderate and spatially homogeneous influence.

Euclidean Distance from Agricultural Areas (EDA) displayed a non-linear pattern, with hazard peaking at intermediate-to-high intervals (Quantiles 5 and 6). The most pronounced seasonal divergence was driven by Precipitation (NDP10), which demonstrated a marked behavioral inversion: the lowest precipitation class (Quantile 1) became the dominant driver in the July model—a shift reflected in its exceptionally high CV (62.5%–104.8%). Conversely, Maximum Temperature (TMAX) appeared as a secondary driver, characterized by moderate variability and the absence of a distinct directional pattern.

Pearson correlation analysis statistically substantiated this seasonal dichotomy. The Overall, Aug–Sep, and Oct–Jun models exhibited strong inter-correlation (r ranging from 0.89 to 0.99), whereas the July model displayed a weak correlation with the others (r ranging from 0.35 to 0.43), thereby confirming its unique hazard profile. This divergence is further manifested in the spatial distribution of hazard (Figure 4).

The Overall, Aug–Sep, and Oct–Jun scenarios are characterized by three distinct high-hazard nuclei in the central and northern sectors, spatially coincident with rugged terrain and higher NDP10 values. In sharp contrast, the July hazard map reveals a spatial shift, concentrating high-risk areas in the extreme northeast, southeast, and south—regions defined by lower precipitation regimes and elevated maximum temperatures. The application of the FRI mask notably results in a substantial exclusion of hazard areas within the central region, reflecting fuel-limited conditions (Figure 4).

Although a general pattern of lower hazard persists in the western coastal region, the spatial distribution varies significantly across the models. In the Overall, Aug–Sep, and Oct–Jun scenarios, high-hazard zones are concentrated in three nuclei within the central and northern sectors, spatially associated with higher elevations, steeper slopes, and increased NDP10. In contrast, the July map displays hazard concentrated in the extreme northeast, southeast, and south—areas characterized by lower NDP10 and higher maximum temperatures (TMAX). Notably, the application of the FRI mask reveals a widespread absence of hazard in the central region (Figure 4).

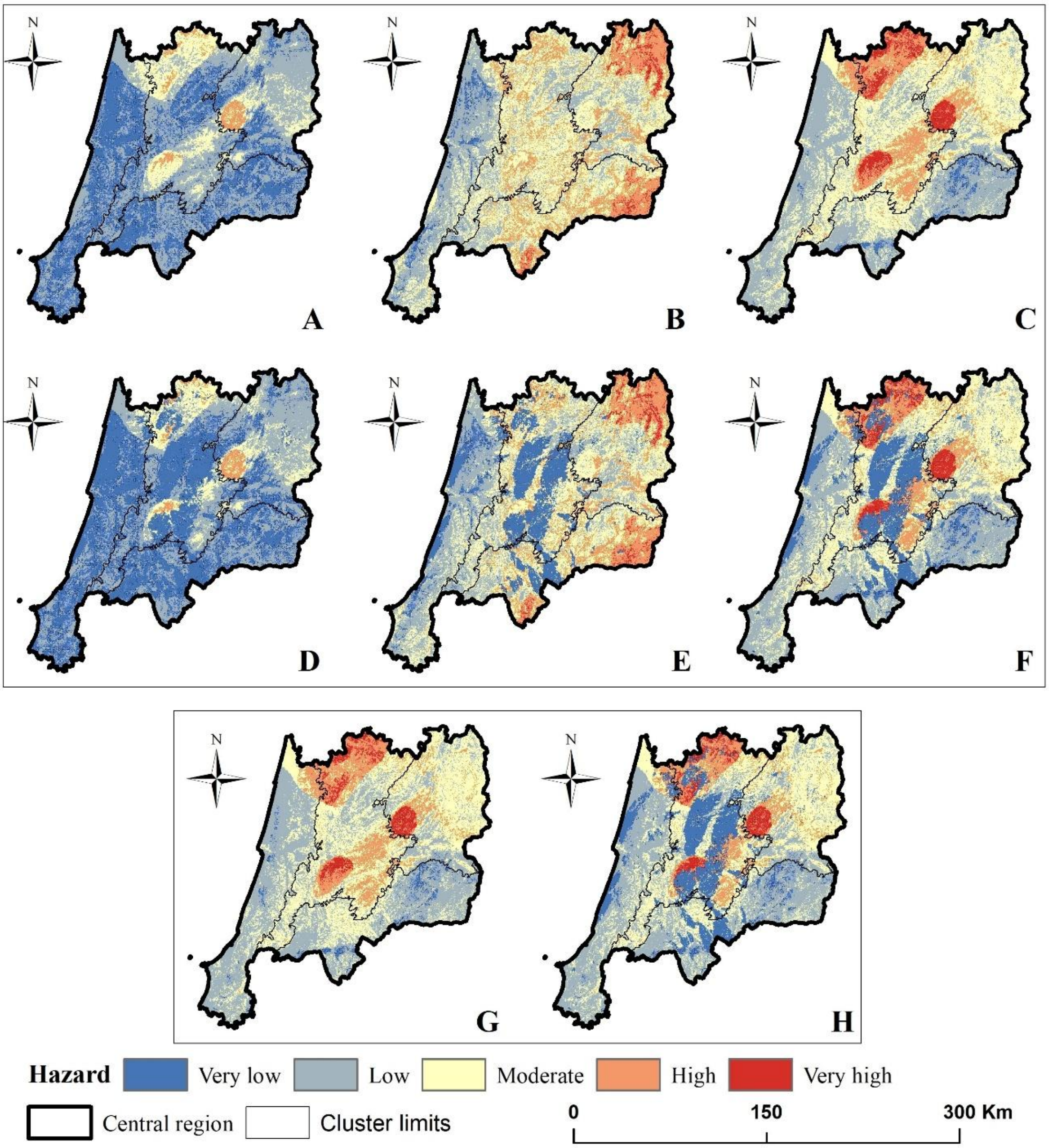

Figure 4. Fire hazard maps for the Central Region of Portugal. For the seasonal models, the Baseline maps (A: Aug–Sep; B: Jul; C: Oct–Jun) are positioned directly above their respective Temporally-Adjusted versions (D, E, F). The results for the Overall Model are displayed at the bottom, with the Baseline map (G) on the left and the Temporally-Adjusted version (H) on the right.

Both the Overall and Aug–Sep models exhibited a consistent positive relationship between fire behavior and hazard classes (Figure 5a). Conversely, the remaining models displayed a more subdued pattern, characterized by a less pronounced increase in the percentage of burned area across rising hazard classes, with values nearing zero in the Very High hazard category. The application of the FRI mask enhanced the coherence of the distribution within the Moderate to Very High classes; however, it compromised performance in the 'Very Low' category (particularly in the Aug–Sep and Overall models), which registered an anomalous increase in the percentage of burned area.

Contrary to the initial hypothesis, the implementation of FRI masking resulted in a reduction of AUC values for the Overall and Aug–Sep models, whereas the remaining models achieved a marginal improvement (Figure 5b).

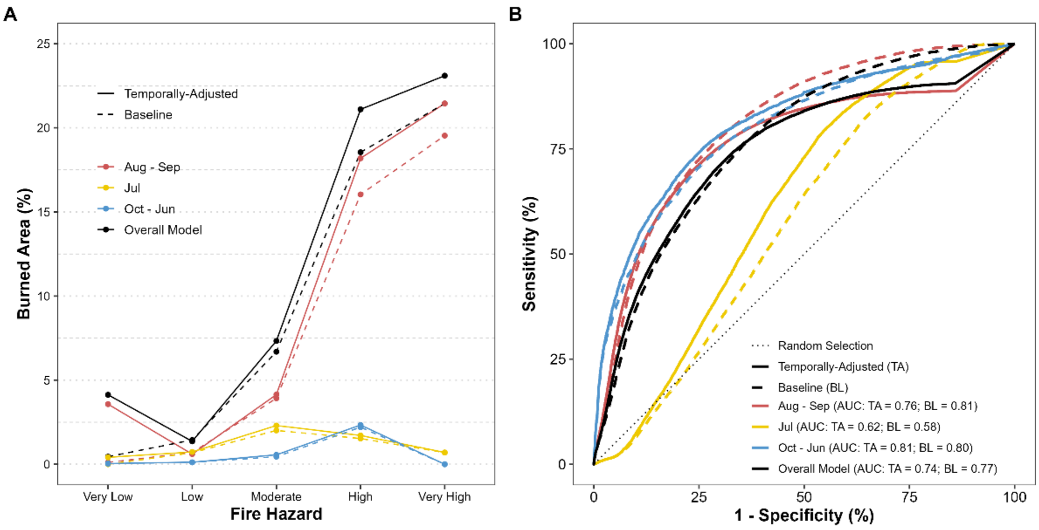

Figure 5. Model performance evaluation using two distinct methods: (A) coherence analysis, and (B) ROC curve analysis including respective AUC values. In both panels, Baseline models are depicted by solid lines, while Temporally-Adjusted models are indicated by dashed lines.

Significantly, the AUC-based validation (Figure 5b) further corroborated the superiority of the seasonal stratification strategy. The Baseline models for the Aug–Sep (AUC = 0.81) and Oct–Jun (AUC = 0.80) periods outperformed the Overall Model (AUC = 0.77). In marked contrast, the July model (AUC = 0.58) demonstrated limited predictive capacity.

4 Discussion

Spatial and temporal analysis of wildfires in Central Portugal confirms a dynamic fire regime (Bergonse et al., 2022), yet reveals that the well-known spatial dichotomy between the interior and the coast (Nunes et al., 2016; Santana Neto et al., 2025) obscures an even more critical temporal transition. While existing literature focuses on how fixed geographic features (such as the drier climate of the South or the altitude of the East) define fire regimes (Bergonse et al., 2023), the results demonstrate that the very hierarchy of hazard-controlling factors shifts drastically throughout the fire season.

This transition refines pyrogeographical theory (Batllori et al., 2013; Pausas and Ribeiro, 2013), which posits distinct regimes of moisture limitation (where fuel is abundant but wet) versus fuel limitation (where the climate is conducive but fuel is scarce). The present study, however, provides empirical evidence that this pyrogeographical transition also operates temporally within the same landscape, evolving from a regime limited by fuel availability to one dominated by topographic propagation. Such a seasonal shift is best exemplified by the statistical distinction of July as a period of moderate activity, functioning as a transitional phase (Annex A).

This distinction, fundamental to the seasonal analysis (Annex A), captures the precise moment when the paradoxical dual role of water (Bergonse et al., 2022) manifests itself. Hazard in this month is governed by NDP10, remaining high at both extremes of the variable. On one hand, areas with low NDP10 (chronic dryness) reflect an aridity-limited regime, reaching critical flammability earlier due to summer drought (Littell et al., 2016). On the other hand, areas with high NDP10 also exhibit high hazard, reflecting a productivity-limited regime. In these locations, greater annual water availability fosters higher fuel production (Romano and Ursino, 2020; Turco et al., 2017), thereby increasing vegetation load and continuity (Abatzoglou et al., 2018).

July is, therefore, the transitional period where fuel availability (due to flash drought) and high fuel load (due to annual productivity) coexist as critical factors, creating an explosive scenario where structural factors (load) and conjunctural factors (climate) align (Calheiros et al., 2022).

However, it is during the peak of the season (August–September) that their importance is exponentially amplified. During these periods, although NDP10 remains the most influential variable by determining fuel load, topography—specifically slope and elevation—emerges as the primary factor governing propagation, dictating fire intensity and rate of spread (Carmo et al., 2011; Costa et al., 2011; Leuenberger et al., 2018; Oliveira and Zêzere, 2020; Tran et al., 2024), and influencing microclimates and fuel characteristics (Iban and Sekertekin, 2022; Jaafari et al., 2018; Tran et al., 2024; Bergonse et al., 2021b).

The strong correlation between the Aug–Sep and Overall models is expected, as the Overall model is numerically dominated by this peak period, which accounts for the overwhelming majority of the burned area. Such spatial consistency is not exclusive to the peak; the high predictive performance (AUC = 0.80) and strong correlation observed with the low-activity period (Oct–Jun) suggest that this topography-driven template represents a permanent structural baseline of hazard. This stability further underscores July's role as the true seasonal outlier, marking the only phase where the landscape shifts from productivity- to aridity-driven constraints.

The dominance of this shared structural pattern is reflected in the spatial manifestation of the models: maps for these scenarios concentrate hazard foci in mountainous nuclei, aligned with topographic control, consistent with other studies (Bergonse et al., 2021b, 2021a; Marques et al., 2011; Nunes et al., 2023a; Oliveira and Zêzere, 2020). It is important to highlight, however, that this generalization may lead to hazard overestimation in high-altitude areas with specific microclimates, such as the *Serra da Estrela*, which reaches a maximum elevation of 1993 meters.

The peak in hazard at intermediate distances from agriculture (EDA) suggests an "interface zone," analogous to Wildland-Urban Interfaces (WUI) or Rural-Urban Interfaces (RUI), where the intersection of human development and vegetation naturally heightens ignition risk due to anthropogenic pressure (Barros and Pereira, 2014; Oliveira et al., 2021; Santana Neto et al., 2025), this intermediate zone is uniquely hazardous because it superimposes this high anthropogenic ignition potential onto a landscape with lower fragmentation, thereby preserving fuel continuity and facilitating fire spread (Calviño-Cancela et al., 2016).

In comparison, Aspect exhibited a secondary role; although theoretically linked to fuel heating and desiccation (Santana Neto et al., 2023; Sayad et al., 2019), its failure to enhance model performance in this study mirrors other recent findings (Iban and Sekertekin, 2022; Oliveira et al., 2021).

Parallel to seasonal dynamics, fire history (FRI) exerts a fundamental control. The legacy of fire exclusion, a policy historically entrenched in suppression (Calkin et al., 2021; Stratton, 2020), has precipitated a "fire deficit" (Baron et al., 2022; Parks et al., 2025). This deficit drives fuel accumulation and the densification of understory vegetation (Merriam et al., 2022; Parks et al., 2025).

The FRI analysis revealed that, while partially reflecting climate, this metric is strongly dictated by fuel type (Baron et al., 2022; Feurdean et al., 2020). Classes such as shrublands, frequently identified as the most fire-susceptible cover (Santana Neto et al., 2025), along with pastures and agroforestry systems (SAFs), exhibited the shortest return intervals. This suggests that biomass characteristics and human management practices are stronger determinants of recurrence than regional climatic gradients (Moreira et al., 2010a).

Analysis of fire history in classes typically considered less prone to fire, such as artificial territories and wetlands (Santana Neto et al., 2025), indicates that fire in these zones operates as an "interface phenomenon" (Moreira et al., 2011), concentrated at the margins where flammable vegetation meets the rural landscape. The long return interval (10 years) in southern wetlands (the driest region) implies that only exceptional droughts trigger ignition (Fernandes et al., 2012), whereas the short recurrence time (2 years) in the East (high frequency) indicates that adjacent pressure renders these interfaces rapidly vulnerable (Ferreira Leite et al., 2011). This high recurrence, where the interval between fires is insufficient for canopy maturation (Agne et al., 2022), may generate a vicious cycle, converting forests into more flammable shrublands which, in turn, burn more readily (Ferreira Leite et al., 2011; Moreira et al., 2011).

The analyses reinforce the ecological "memory" of FRI as a control mechanism. To test its predictive power, a "no-hazard mask" was applied, based on the premise that hazard is negligible immediately following a burn (Agne et al., 2022; Fernandes and Rego, 1998). The application of the mask yielded mixed results: in models for lower-activity seasons (July and Oct–Jun), the mask improved performance, confirming that fire can have a self-limiting effect (Davim et al., 2021) when meteorological conditions are moderate (Moreira et al., 2011; Moritz, 2003).

However, the most revealing finding was the performance decline in the peak (Aug–Sep) and Overall models. This result exposes the failure of the mask under extreme meteorological conditions. Fires occurring within masked areas demonstrate that critical winds and low humidity override historical recurrence patterns and fuel limitation (Davim et al., 2021; Moritz, 2003). Under such circumstances, fire selectivity regarding fuel type or age is drastically reduced (Barros and Pereira, 2014; Fernandes et al., 2012), Under such circumstances, fire selectivity regarding fuel type or age is drastically reduced.

The implications for management are profound, highlighting the necessity for more dynamic and seasonally aware strategies (Gonzalez-Mathiesen et al., 2021; Mockrin et al., 2020). First, management must be seasonally adaptive, targeting ignitions (July) or critical topography (Aug–Sep) that drives propagation (Calkin et al., 2021; Stratton, 2020). Second, "repeat offenders" such as shrublands and pastures, which demonstrate critically low FRIs, require policies to break the fire-regeneration-fire cycle (Moreira et al., 2010b) that precipitates fuel type transition (Oliveira et al., 2023). Finally, the mask's failure in extreme scenarios mandates dynamic planning (Stratton, 2020) that integrates current stand structure (Botequim et al., 2017), rather than relying exclusively on historical patterns—alongside short-term forecasting (Calkin et al., 2021).

Despite the robustness of the results, it is important to acknowledge the study's boundaries. A primary limitation is the use of climatological normals (1971–2000) to define the reference climate. While this approach captures average long-term hazard patterns, relying on historical baselines can be problematic under progressive climate change, as traditional climatological normals may become obsolete and fail to reflect recent shifts in extreme weather patterns (Turco et al., 2019). Under a warming climate, the ideal approach would integrate more recent and dynamic meteorological data to capture contemporary environmental alterations (Calheiros et al., 2022). Furthermore, this long-term average approach does not incorporate short-term extreme meteorological events ('weather'). As the failure of the FRI mask demonstrated, it is precisely these 'weather' conditions that supersede historical fuel patterns during peak seasons.

Other limitations include spatial resolution constraints and the historical fire database's limited temporal span, as precise monthly data is only available from 2012 onwards. This restricted the training data volume, largely explaining July's low predictive performance (AUC = 0.58 without the hazard mask, and 0.62 with it). Machine learning models require substantial datasets to capture complex environmental interactions and avoid data noise (Sayad et al., 2019). Consequently, relying on just five years of July data significantly reduced the model's ability to generalize robust spatial patterns (Tonbul et al., 2024), particularly because July operates as a highly variable transitional phase. These constraints ultimately define the scope of the results.

This study, however, paves the way for future investigations. Conclusions regarding the dual role of precipitation, for example, reinforce the need to incorporate direct estimates of fuel load, a capability that will become increasingly feasible with data from sensors such as GEDI and Sentinel-1, as well as future missions like NISAR and BIOMASS (ESA, 2025; European Comission, 2024; Hancock et al., 2019; Kellogg et al., 2020; Quegan et al., 2019), as demonstrated by Leite et al**.** (2022), using GEDI to model canopy fuels in conjunction with radar data. Future work could replicate this methodology using more dynamic datasets and integrate hazard models into comprehensive risk assessments. Finally, applying this seasonal framework to other Mediterranean regions represents a crucial step toward validating and generalizing the regimes identified here.

5 Conclusions

This study validates the core premise that wildfire hazard in Central Portugal is dynamically driven by seasonally distinct factors, thereby highlighting the inadequacy of static, aggregated annual models. Statistical analysis confirmed the stratification of the fire year into three distinct regimes—High (August–September), Moderate (July), and Low (October–June)—each governed by a unique hierarchy of environmental controls. While the high and low activity seasons were dominated by structural factors (topography) and fuel availability (precipitation), the July transitional period exhibited a unique profile driven primarily by aridity. Consequently, the seasonal models developed for the peak (Aug–Sep, AUC=0.81) and low-activity (Oct–Jun, AUC=0.80) periods significantly outperformed the reference Overall Model (AUC=0.77). However, the limited predictive success of the July model (AUC=0.58) signals that, while distinct, this transitional window requires a specialized set of predictors not fully captured in standard datasets.

Conversely, the hypothesis that incorporating fire history via a Fire Return Interval (FRI) mask would enhance predictive accuracy was refuted for the most critical fire scenarios. The application of the FRI mask degraded the performance of both the Overall and August–September models. This failure provides compelling evidence that under the extreme meteorological conditions characteristic of the peak season, the protective effect of younger vegetation is effectively overridden; in these scenarios, fire propagates regardless of recent burning history. The FRI adjustment yielded only marginal gains during the less severe conditions of the low and moderate activity periods. Ultimately, we conclude that while accounting for seasonality is essential to decipher the changing drivers of fire hazard, relying on historical recurrence metrics to predict fuel limitation is insufficient during the catastrophic peak of the fire season.

6 Acknowledgements

The authors are grateful to Drs. Alexandre Simões Lorenzon and Fausto Weimar Acerbi Junior for their valuable insights and contributions to enhancing the quality of this research.

7 Funding

This study was financed in part by the Coordenação de Aperfeiçoamento de Pessoal de Nível Superior - Brasil (CAPES) - Finance Code 001. This work also received support from The Centre of Studies in Geography and Spatial Planning (CEGOT), funded by national funds through the Foundation for Science and Technology (FCT) under the reference UIDP/GEO/04084/2020_UC.

8 References

Abatzoglou, J.T., Williams, A.P., Boschetti, L., Zubkova, M., Kolden, C.A., 2018. Global patterns of interannual climate–fire relationships. Global Change Biology 24, 5164–5175. https://doi.org/10.1111/gcb.14405

AGIF, 2025. Relatório anual de atividades do Sistema de Gestão Integrada de Fogos Rurais.

Agne, M.C., Fontaine, J.B., Enright, N.J., Harvey, B.J., 2022. Fire interval and post-fire climate effects on serotinous forest resilience. fire ecol 18, 22. https://doi.org/10.1186/s42408-022-00145-4

ASF, A.S.F., 2024. ASF Data Search [WWW Document]. URL https://search.asf.alaska.edu (accessed 3.1.24).

Bachmann, A., Allgöwer, B., 2001. A consistent wildland fire risk terminology is needed! Fire Management Today 61, 28–33.

Barbero, R., Abatzoglou, J.T., Pimont, F., Ruffault, J., Curt, T., 2020. Attributing Increases in Fire Weather to Anthropogenic Climate Change Over France. Front. Earth Sci. 8. https://doi.org/10.3389/feart.2020.00104

Baron, J.N., Gergel, S.E., Hessburg, P.F., Daniels, L.D., 2022. A century of transformation: fire regime transitions from 1919 to 2019 in southeastern British Columbia, Canada. Landsc Ecol 37, 2707–2727. https://doi.org/10.1007/s10980-022-01506-9

Barros, A.M.G., Pereira, J.M.C., 2014. Wildfire selectivity for land cover type: Does size matter? PLoS ONE 9. https://doi.org/10.1371/journal.pone.0084760

Batllori, E., Parisien, M., Krawchuk, M.A., Moritz, M.A., 2013. Climate change-induced shifts in fire for Mediterranean ecosystems. Global Ecology and Biogeography 22, 1118–1129. https://doi.org/10.1111/geb.12065

Bergonse, R., Oliveira, S., Gonçalves, A., Nunes, S., da Câmara, C., Zêzere, J.L., 2021a. A combined structural and seasonal approach to assess wildfire susceptibility and hazard in summertime. Natural Hazards 106, 2545–2573. https://doi.org/10.1007/s11069-021-04554-7

Bergonse, R., Oliveira, S., Gonçalves, A., Nunes, S., DaCamara, C., Zêzere, J.L., 2021b. Predicting burnt areas during the summer season in Portugal by combining wildfire susceptibility and spring meteorological conditions. Geomatics, Natural Hazards and Risk 12, 1039–1057. https://doi.org/10.1080/19475705.2021.1909664

Bergonse, R., Oliveira, S., Zêzere, J.L., Moreira, F., Ribeiro, P.F., Leal, M., Lima e Santos, J.M., 2022. Biophysical controls over fire regime properties in Central Portugal. Science of the Total Environment 810, 152314. https://doi.org/10.1016/j.scitotenv.2021.152314

Bergonse, R., Oliveira, S., Zêzere, J.L., Moreira, F., Ribeiro, P.F., Leal, M., Santos, J.M.L., 2023. Differentiating Fire Regimes and Their Biophysical Drivers in Central Portugal. Fire 6, 112. https://doi.org/10.3390/fire6030112

Botequim, B., Fernandes, P.M., Garcia-Gonzalo, J., Silva, A., Borges, J.G., 2017. Coupling fire behaviour modelling and stand characteristics to assess and mitigate fire hazard in a maritime pine landscape in Portugal. Eur J Forest Res 136, 527–542. https://doi.org/10.1007/s10342-017-1050-7

Bowman, D.M.J.S., Balch, J., Artaxo, P., Bond, W.J., Cochrane, M.A., D'Antonio, C.M., DeFries, R., Johnston, F.H., Keeley, J.E., Krawchuk, M.A., Kull, C.A., Mack, M., Moritz, M.A., Pyne, S., Roos, C.I., Scott, A.C., Sodhi, N.S., Swetnam, T.W., 2011. The human dimension of fire regimes on Earth. Journal of Biogeography 38, 2223–2236. https://doi.org/10.1111/j.1365-2699.2011.02595.x

Bradley, A.P., 1997. The use of the area under the ROC curve in the evaluation of machine learning algorithms. Pattern Recognition 30, 1145–1159. https://doi.org/10.1016/S0031-3203(96)00142-2

Calheiros, T., Benali, A., Pereira, M., Silva, J., Nunes, J., 2022. Drivers of extreme burnt area in Portugal: fire weather and vegetation. Natural Hazards and Earth System Sciences 22, 4019–4037. https://doi.org/10.5194/nhess-22-4019-2022

Calkin, D., O'Connor, C., Thompson, M., Stratton, R., 2021. Strategic Wildfire Response Decision Support and the Risk Management Assistance Program. Forests 12, 1407. https://doi.org/10.3390/f12101407

Calviño-Cancela, M., Chas-Amil, M.L., García-Martínez, E.D., Touza, J., 2016. Wildfire risk associated with different vegetation types within and outside wildland-urban interfaces. Forest Ecology and Management 372, 1–9. https://doi.org/10.1016/j.foreco.2016.04.002

Camargo, A.C.L., Barrio, R.O.L., de Camargo, N.F., Mendonça, A.F., Ribeiro, J.F., Rodrigues, C.M.F., Vieira, E.M., 2018. Fire affects the occurrence of small mammals at distinct spatial scales in a neotropical savanna. European Journal of Wildlife Research 64. https://doi.org/10.1007/s10344-018-1224-8

Carmo, M., Ferreira, J., Mendes, M., Silva, Á., Silva, P., Alves, D., Reis, L., Novo, I., Xavier Viegas, D., 2022. The climatology of extreme wildfires in Portugal, 1980–2018: Contributions to forecasting and preparedness. International Journal of Climatology 42, 3123–3146. https://doi.org/10.1002/joc.7411

Carmo, M., Moreira, F., Casimiro, P., Vaz, P., 2011. Land use and topography influences on wildfire occurrence in northern Portugal. Landscape and Urban Planning 100, 169–176. https://doi.org/10.1016/j.landurbplan.2010.11.017

Costa, A. das G., Torres, F.T.P., Lima, G.S., de Melo, F.R., Rodrigues, V.B., Neto, V.P.S., Fernandes, T.V., Costa, A. das G., Torres, F.T.P., Lima, G.S., de Melo, F.R., Rodrigues, V.B., Santana Neto, V.P., Fernandes, T.V., 2022. Fire influence on the ants community in savanic and forest environments of the Cerrado biome. Floresta e Ambiente 29, 1–10. https://doi.org/10.1590/2179-8087-FLORAM-2022-0025

Costa, L., Thonicke, K., Poulter, B., Badeck, F., 2011. Sensitivity of Portuguese forest fires to climatic, human, and landscape variables: Subnational differences between fire drivers in extreme fire years and decadal averages. Regional Environmental Change 11, 543–551. https://doi.org/10.1007/s10113-010-0169-6

Costa, P.S., Estanqueiro, A., 2023. Mapa do Atlas do Potencial Eólico Onshore de Portugal Continental. Laboratório Nacional de Energia e Geologia, I.P. (LNEG).

DaCamara, C.C., 2024. The Signature of Climate in Annual Burned Area in Portugal. Climate 12, 143. https://doi.org/10.3390/cli12090143

Davim, D.A., Rossa, C.G., Fernandes, P.M., 2021. Survival of prescribed burning treatments to wildfire in Portugal. Forest Ecology and Management 493, 119250. https://doi.org/10.1016/j.foreco.2021.119250

DGTerritório, 2022a. Carta de Perigosidade de Incêndio Rural [WWW Document]. URL https://www.dgterritorio.gov.pt/paisagem/ptp/carta-perigosidade-incendio-rural (accessed 10.15.25).

DGTerritório, 2022b. Especificações técnicas da Carta de uso e Ocupação do Solo de Portugal Continental para 1995, 2007, 2010, 2015 e 2018, Relatório Técnico. Direção-Geral do Território.

Doerr, S.H., Santín, C., 2016. Global trends in wildfire and its impacts: perceptions versus realities in a changing world. Philosophical Transactions of the Royal Society B: Biological Sciences 371, 20150345. https://doi.org/10.1098/rstb.2015.0345

Elia, M., Giannico, V., Lafortezza, R., Sanesi, G., 2019. Modeling fire ignition patterns in Mediterranean urban interfaces. Stochastic Environmental Research and Risk Assessment 33, 169–181. https://doi.org/10.1007/s00477-018-1558-5

ESA, 2025. European Space Agency [WWW Document]. URL https://www.esa.int/ (accessed 5.15.25).

European Comission, 2024. Copernicus Programme [WWW Document]. URL https://www.copernicus.eu/ (accessed 10.16.24).

Fernandes, P.M., Loureiro, C., Magalhães, M., Ferreira, P., Fernandes, M., 2012. Fuel age, weather and burn probability in Portugal. Int. J. Wildland Fire 21, 380. https://doi.org/10.1071/WF10063

Fernandes, P.M., Rego, F.C., 1998. Changes in fuel structure and fire behaviour with heathland aging in Northern Portugal. Presented at the Proceedings of the 13th Conference on Fire and Forest Meteorology, Lorne, Australia, pp. 433–436.

Ferreira Leite, F., Bento Gonçalves, A., Vieira, A., 2011. The recurrence interval of forest fires in Cabeço da Vaca (Cabreira Mountain—northwest of Portugal). Environmental Research 111, 215–221. https://doi.org/10.1016/j.envres.2010.05.007

Feurdean, A., Vannière, B., Finsinger, W., Warren, D., Connor, S.C., Forrest, M., Liakka, J., Panait, A., Werner, C., Andrič, M., Bobek, P., Carter, V.A., Davis, B., Diaconu, A.-C., Dietze, E., Feeser, I., Florescu, G., Gałka, M., Giesecke, T., Jahns, S., Jamrichová, E., Kajukało, K., Kaplan, J., Karpińska-Kołaczek, M., Kołaczek, P., Kuneš, P., Kupriyanov, D., Lamentowicz, M., Lemmen, C., Magyari, E.K., Marcisz, K., Marinova, E., Niamir, A., Novenko, E., Obremska, M., Pędziszewska, A., Pfeiffer, M., Poska, A., Rösch, M., Słowiński, M., Stančikaitė, M., Szal, M., Święta-Musznicka, J., Tanţău, I., Theuerkauf, M., Tonkov, S., Valkó, O., Vassiljev, J., Veski, S., Vincze, I., Wacnik, A., Wiethold, J., Hickler, T., 2020. Fire hazard modulation by long-term dynamics in land cover and dominant forest type in eastern and central Europe. Biogeosciences 17, 1213–1230. https://doi.org/10.5194/bg-17-1213-2020

Fidalgo, A., Fernandes, A.S., 2023. Efeito dos incêndios florestais no ecossistema: revisão integrativa. Territorium 5–13. https://doi.org/10.14195/1647-7723_30-2_1

Frost, C.C., 1998. Presettlement fire frequency regimes of the United States: a first approximation., in: Fire in Ecosystem Management: Shifting the Paradigm from Suppression to Prescription, Tall Timbers Fire Ecology Conference Proceedings. Tall Timbers Research Station, Tallahassee, FL, pp. 70–81.

Gonzalez-Mathiesen, C., Ruane, S., March, A., 2021. Integrating wildfire risk management and spatial planning – A historical review of two Australian planning systems. International Journal of Disaster Risk Reduction 53, 101984. https://doi.org/10.1016/j.ijdrr.2020.101984

Haas, O., Keeping, T., Gomez-Dans, J., Prentice, I.C., Harrison, S.P., 2024. The global drivers of wildfire. Front. Environ. Sci. 12. https://doi.org/10.3389/fenvs.2024.1438262

Hancock, S., Armston, J., Hofton, M., Sun, X., Tang, H., Duncanson, L.I., Kellner, J.R., Dubayah, R., 2019. The GEDI Simulator: A Large-Footprint Waveform Lidar Simulator for Calibration and Validation of Spaceborne Missions. Earth and Space Science 6, 294–310. https://doi.org/10.1029/2018EA000506

Iban, M.C., Sekertekin, A., 2022. Machine learning based wildfire susceptibility mapping using remotely sensed fire data and GIS: A case study of Adana and Mersin provinces, Turkey. Ecological Informatics 69, 101647. https://doi.org/10.1016/j.ecoinf.2022.101647

ICNF, 2024. Territórios ardidos [WWW Document]. URL https://sig.icnf.pt/portal/home/item.html?id=983c4e6c4d5b4666b258a3ad5f3ea5af (accessed 10.16.24).

INE, I.N. de E., 2022. Base Geográfica de Referenciação da Informação de Portugal [WWW Document]. URL https://mapas.ine.pt/download/metadados/bgri.html (accessed 2.27.24).

IPMA, 2009a. Média Temperatura Máxima do Ar, Verão, normal 1971-2000 [WWW Document]. URL https://snig.dgterritorio.gov.pt/rndg/srv/por/catalog.search#/metadata/PT100-ho19712000-jja-avgr-txavgr-cdg (accessed 2.27.24).

IPMA, 2009b. Precipitação Total, Verão, normal 1971-2000 [WWW Document]. URL https://snig.dgterritorio.gov.pt/rndg/srv/por/catalog.search#/metadata/PT100-ho19712000-jja-avgr-pravgr-cdg?tab=responsible (accessed 2.27.24).

IPMA, 2009c. Número de dias com Precipitação ≥10mm, normal 1971-2000 [WWW Document]. URL https://snig.dgterritorio.gov.pt/rndg/srv/por/catalog.search#/metadata/PT100-ho19712000-aaa-avgr-prna10-cdg (accessed 2.27.24).

IPMA, 2009d. Número de dias Temperatura Máxima do Ar ≥25ºC, normal 1971-2000 [WWW Document]. URL https://snig.dgterritorio.gov.pt/rndg/srv/por/catalog.search#/metadata/PT100-ho19712000-aaa-avgr-txna25-cdg (accessed 2.27.24).

Jaafari, A., Zenner, E.K., Pham, B.T., 2018. Wildfire spatial pattern analysis in the Zagros Mountains, Iran: A comparative study of decision tree based classifiers. Ecological Informatics 43, 200–211. https://doi.org/10.1016/j.ecoinf.2017.12.006

Januário, R.R., Minuzzi, R.B., 2020. Risco de incêndio sazonal em área descampada e de floresta para diferentes cenários climáticos no município de Águas Mornas. Geosul 35, 580–597. https://doi.org/10.5007/1982-5153.2020v35n75p580

Jappiot, M., Gonzalez-Olabarria, J.R., Lampin-Maillet, C., Borgniet, L., 2009. Assessing Wildfire Risk in Time and Space. EUROPEAN FOREST INSTITUTE, p. 41.

Jelihovschi, E.G., Faria, J.C., Allaman, I.B., 2014. ScottKnott: a package for performing the Scott-Knott clustering algorithm in R. TEMA (São Carlos) 15, 3–17. https://doi.org/10.5540/tema.2014.015.01.0003

Jones, M.W., Abatzoglou, J.T., Veraverbeke, S., Andela, N., Lasslop, G., Forkel, M., Smith, A.J.P., Burton, C., Betts, R.A., Van Der Werf, G.R., Sitch, S., Canadell, J.G., Santín, C., Kolden, C., Doerr, S.H., Le Quéré, C., 2022. Global and Regional Trends and Drivers of Fire Under Climate Change. Reviews of Geophysics 60, e2020RG000726. https://doi.org/10.1029/2020RG000726

Kellogg, K., Hoffman, P., Standley, S., Shaffer, S., Rosen, P., Edelstein, W., Dunn, C., Baker, C., Barela, P., Shen, Y., Guerrero, A.M., Xaypraseuth, P., Sagi, V.R., Sreekantha, C.V., Harinath, N., Kumar, R., Bhan, R., Sarma, C.V.H.S., 2020. NASA-ISRO Synthetic Aperture Radar (NISAR) Mission, in: 2020 IEEE Aerospace Conference. Presented at the 2020 IEEE Aerospace Conference, IEEE, Big Sky, MT, USA, pp. 1–21. https://doi.org/10.1109/AERO47225.2020.9172638

Leite, R.V., Silva, C.A., Broadbent, E.N., Amaral, C.H.D., Liesenberg, V., Almeida, D.R.A.D., Mohan, M., Godinho, S., Cardil, A., Hamamura, C., Faria, B.L.D., Brancalion, P.H.S., Hirsch, A., Marcatti, G.E., Dalla Corte, A.P., Zambrano, A.M.A., Costa, M.B.T.D., Matricardi, E.A.T., Silva, A.L.D., Goya, L.R.R.Y., Valbuena, R., Mendonça, B.A.F.D., Silva Junior, C.H.L., Aragão, L.E.O.C., García, M., Liang, J., Merrick, T., Hudak, A.T., Xiao, J., Hancock, S., Duncason, L., Ferreira, M.P., Valle, D., Saatchi, S., Klauberg, C., 2022. Large scale multi-layer fuel load characterization in tropical savanna using GEDI spaceborne lidar data. Remote Sensing of Environment 268, 112764. https://doi.org/10.1016/j.rse.2021.112764

Leuenberger, M., Parente, J., Tonini, M., Pereira, M.G., Kanevski, M., 2018. Wildfire susceptibility mapping: Deterministic vs. stochastic approaches. n 101, 194–203. https://doi.org/10.1016/j.envsoft.2017.12.019

Littell, J.S., Peterson, D.L., Riley, K.L., Liu, Y., Luce, C.H., 2016. A review of the relationships between drought and forest fire in the United States. Global Change Biology 22, 2353–2369. https://doi.org/10.1111/gcb.13275

Luu, C., Forino, G., Yorke, L., Ha, H., Bui, Q.D., Tran, H.H., Nguyen, D.Q., Duong, H.C., Kervyn, M., 2024. Integrating susceptibility maps of multiple hazards and building exposure distribution: a case study of wildfires and floods for the province of Quang Nam, Vietnam. Natural Hazards and Earth System Sciences 24, 4385–4408. https://doi.org/10.5194/nhess-24-4385-2024

Marques, S., Borges, J.G., Garcia-Gonzalo, J., Moreira, F., Carreiras, J.M.B., Oliveira, M.M., Cantarinha, A., Botequim, B., Pereira, J.M.C., 2011. Characterization of wildfires in Portugal. European Journal of Forest Research 130, 775–784. https://doi.org/10.1007/s10342-010-0470-4

Mateus, P., Fernandes, P.M., 2014. Forest Fires in Portugal: Dynamics, Causes and Policies, in: Reboredo, F. (Ed.), Forest Context and Policies in Portugal, World Forests. Springer International Publishing, Cham, pp. 97–115. https://doi.org/10.1007/978-3-319-08455-8_4

Merriam, K.E., Meyer, M.D., Coppoletta, M., Butz, R.J., Estes, B.L., Farris, C.A., North, M.P., 2022. Reestablishing natural fire regimes to restore forest structure in California's red fir forests: The importance of regional context. Forest Ecology and Management 503, 119797. https://doi.org/10.1016/j.foreco.2021.119797

Mihajlovski, B., Zhiyanski, M., 2025. Global Forest Fire Assessment Methods: A Comparative Analysis of Hazard, Susceptibility, and Vulnerability Approaches in Different Landscapes. Fire 8, 380. https://doi.org/10.3390/fire8100380

Mockrin, M.H., Fishler, H.K., Stewart, S.I., 2020. After the fire: Perceptions of land use planning to reduce wildfire risk in eight communities across the United States. International Journal of Disaster Risk Reduction 45, 101444. https://doi.org/10.1016/j.ijdrr.2019.101444

Moreira, F., Catry, F.X., Rego, F., Bacao, F., 2010a. Size-dependent pattern of wildfire ignitions in Portugal: When do ignitions turn into big fires? Landscape Ecology 25, 1405–1417. https://doi.org/10.1007/s10980-010-9491-0

Moreira, F., Catry, F.X., Rego, F., Bacao, F., 2010b. Size-dependent pattern of wildfire ignitions in Portugal: when do ignitions turn into big fires? Landscape Ecol 25, 1405–1417. https://doi.org/10.1007/s10980-010-9491-0

Moreira, F., Viedma, O., Arianoutsou, M., Curt, T., Koutsias, N., Rigolot, E., Barbati, A., Corona, P., Vaz, P., Xanthopoulos, G., Mouillot, F., Bilgili, E., 2011. Landscape – wildfire interactions in southern Europe: Implications for landscape management. Journal of Environmental Management 92, 2389–2402. https://doi.org/10.1016/j.jenvman.2011.06.028

Moritz, M.A., 2003. Spatiotemporal Analysis of Controls on Shrubland Fire Regimes: Age Dependency and Fire Hazard. Ecology 84, 351–361. https://doi.org/10.1890/0012-9658(2003)084%255B0351:SAOCOS%255D2.0.CO;2

Murtagh, F., Legendre, P., 2014. Ward's Hierarchical Agglomerative Clustering Method: Which Algorithms Implement Ward's Criterion? J Classif 31, 274–295. https://doi.org/10.1007/s00357-014-9161-z

NASA Science, 2025. Wildfires and Climate Change [WWW Document]. URL https://science.nasa.gov/earth/explore/wildfires-and-climate-change/ (accessed 10.14.25).

Nunes, A.N., Figueiredo, A., Pinto, C., Lourenço, L., 2023a. Assessing Wildfire Hazard in the Wildland–Urban Interfaces (WUIs) of Central Portugal. Forests 14. https://doi.org/10.3390/f14061106

Nunes, A.N., Figueiredo, A., Pinto, C.D., Lourenço, L., 2023b. An Evaluation of Wildfire Vulnerability in the Wildland–Urban Interfaces of Central Portugal Using the Analytic Network Process. Fire 6. https://doi.org/10.3390/fire6050194

Nunes, A.N., Lourenço, L., 2017. Increased vulnerability to wildfires and post fire hydro-geomorphic processes in Portuguese mountain regions: what has changed? Open Agriculture 2, 70–82. https://doi.org/10.1515/opag-2017-0008

Nunes, A.N., Lourenço, L., Meira, A.C.C., 2016. Exploring spatial patterns and drivers of forest fires in Portugal (1980–2014). Science of the Total Environment 573, 1190–1202. https://doi.org/10.1016/j.scitotenv.2016.03.121

Nunes, L.J.R., Raposo, M.A.M., Pinto Gomes, C.J., 2021. A Historical Perspective of Landscape and Human Population Dynamics in Guimarães (Northern Portugal): Possible Implications of Rural Fire Risk in a Changing Environment. Fire 4, 49. https://doi.org/10.3390/fire4030049

Oliveira, E., Fernandes, P.M., 2023. Pastoral Burning and Its Contribution to the Fire Regime of Alto Minho, Portugal. Fire 6, 210. https://doi.org/10.3390/fire6050210

Oliveira, S., Gonçalves, A., Zêzere, J.L., 2021. Reassessing wildfire susceptibility and hazard for mainland Portugal. Science of The Total Environment 762, 143121. https://doi.org/10.1016/j.scitotenv.2020.143121

Oliveira, S., Zêzere, J.L., 2020. Assessing the biophysical and social drivers of burned area distribution at the local scale. Journal of Environmental Management 264. https://doi.org/10.1016/j.jenvman.2020.110449

Parente, J., Pereira, M.G., 2016. Structural fire risk: The case of Portugal. Science of the Total Environment 573, 883–893. https://doi.org/10.1016/j.scitotenv.2016.08.164

Parks, S.A., Guiterman, C.H., Margolis, E.Q., Lonergan, M., Whitman, E., Abatzoglou, J.T., Falk, D.A., Johnston, J.D., Daniels, L.D., Lafon, C.W., Loehman, R.A., Kipfmueller, K.F., Naficy, C.E., Parisien, M.-A., Portier, J., Stambaugh, M.C., Williams, A.P., Wion, A.P., Yocom, L.L., 2025. A fire deficit persists across diverse North American forests despite recent increases in area burned. Nat Commun 16, 1493. https://doi.org/10.1038/s41467-025-56333-8

Pausas, J.G., Ribeiro, E., 2013. The global fire–productivity relationship. Global Ecology and Biogeography 22, 728–736. https://doi.org/10.1111/geb.12043

Pereira, M., Calado, T., DaCamara, C., Calheiros, T., 2013. Effects of regional climate change on rural fires in Portugal. Clim. Res. 57, 187–200. https://doi.org/10.3354/cr01176

PORDATA, 2025. Inquérito ao Ambiente - Ações dos Corpos de Bombeiros (até 2010) | Inquérito às Entidades Detentoras de Corpos de Bombeiros (a partir de 2011) [WWW Document]. URL https://www.pordata.pt/municipios/numero+de+bombeiros-39 (accessed 9.23.25).

Quegan, S., Le Toan, T., Chave, J., Dall, J., Exbrayat, J.-F., Minh, D.H.T., Lomas, M., D'Alessandro, M.M., Paillou, P., Papathanassiou, K., Rocca, F., Saatchi, S., Scipal, K., Shugart, H., Smallman, T.L., Soja, M.J., Tebaldini, S., Ulander, L., Villard, L., Williams, M., 2019. The European Space Agency BIOMASS mission: Measuring forest above-ground biomass from space. Remote Sensing of Environment 227, 44–60. https://doi.org/10.1016/j.rse.2019.03.032

Reid, C.E., Brauer, M., Johnston, F.H., Jerrett, M., Balmes, J.R., Elliott, C.T., 2016. Critical Review of Health Impacts of Wildfire Smoke Exposure. Environ Health Perspect 124, 1334–1343. https://doi.org/10.1289/ehp.1409277

Romano, N., Ursino, N., 2020. Forest fire regime in a mediterranean ecosystem: Unraveling the mutual interrelations between rainfall seasonality, soil moisture, drought persistence, and biomass dynamics. Fire 3, 1–20. https://doi.org/10.3390/fire3030049

Santana Neto, V.P., Leite, R.V., dos Santos, V.J., Castro, J.D.S., Torres, F.T.P., Calijuri, M.L., 2022. Burning Susceptibility Modeling to Reduce Wildfire Impacts: A GIS and Multivariate Statistics Approach. Floresta e Ambiente 29, 1–12. https://doi.org/10.1590/2179-8087-FLORAM-2021-0078

Santana Neto, V.P., Nunes, A. de J.N., Torres, F.T.P., Gleriani, J.M., Cosenza, D.N., 2025. Assessing wildfire susceptibility and driving variables in Portugal using machine learning approach. Journal for Nature Conservation 86, 126956. https://doi.org/10.1016/j.jnc.2025.126956

Santana Neto, V.P., Soares, D.M., Silva, T.C. da, Torres, F.T.P., 2023. Assessment of two methods on zoning wildfire propagation in Itacolomi State Park, Minas Gerais State, Brazil. Pesquisa Florestal Brasileira 43, 1–12. https://doi.org/10.4336/2023.pfb.43e202102227

Santos, L., Lopes, V., Baptista, C., 2022. MDIR Monthly Ignition Risk Maps, an Integrated Open-Source Strategy for Wildfire Prevention. Forests 13, 408. https://doi.org/10.3390/f13030408

Sayad, Y.O., Mousannif, H., Al Moatassime, H., 2019. Predictive modeling of wildfires: A new dataset and machine learning approach. Fire Safety Journal 104, 130–146. https://doi.org/10.1016/j.firesaf.2019.01.006

Scott, A.J., Knott, M., 1974. A Cluster Analysis Method for Grouping Means in the Analysis of Variance. Biometrics 30, 507–512. https://doi.org/10.2307/2529204

Shen, Z., Giljohann, K., Liu, Z., Pausas, J., Rogers, B., 2025. Novel wildfire regimes under climate change and human activity: patterns, driving mechanisms and ecological impacts. Philosophical Transactions of the Royal Society B: Biological Sciences 380, 20230446. https://doi.org/10.1098/rstb.2023.0446

Silva, P., Carmo, M., Rio, J., Novo, I., 2023. Changes in the Seasonality of Fire Activity and Fire Weather in Portugal: Is the Wildfire Season Really Longer? Meteorology 2, 74–86. https://doi.org/10.3390/meteorology2010006

Stratton, R.D., 2020. The Path to Strategic Wildland Fire Management Planning, in: Wildfire. pp. 24–31.

Tonbul, H., 2024. Integrating ensemble machine learning and explainable AI for enhanced forest fire susceptibility analysis and risk assessment in Türkiye's Mediterranean region. Earth Sci Inform. https://doi.org/10.1007/s12145-024-01480-7

Tonini, M., Parente, J., Pereira, M.G., 2018. Global assessment of rural-urban interface in Portugal related to land cover changes. Natural Hazards and Earth System Sciences 18, 1647–1664. https://doi.org/10.5194/nhess-18-1647-2018

Torres, F.T.P., Pancieri, S.D., Santana Neto, V.P., Rodrigues, V.B., 2024. Fire danger in the supply areas of hydroelectric reservoirs under the restoration process in the south of Minas Gerais, Brazil. Revista Árvore 48, 1–11. https://doi.org/10.53661/1806-9088202448263762

Tran, T.T.K., Janizadeh, S., Bateni, S.M., Jun, C., Kim, D., Trauernicht, C., Rezaie, F., Giambelluca, T.W., Panahi, M., 2024. Improving the prediction of wildfire susceptibility on Hawai'i Island, Hawai'i, using explainable hybrid machine learning models. Journal of Environmental Management 351, 119724. https://doi.org/10.1016/j.jenvman.2023.119724

Trucchia, A., Meschi, G., Fiorucci, P., Provenzale, A., Tonini, M., Pernice, U., 2023. Wildfire hazard mapping in the eastern Mediterranean landscape. Int. J. Wildland Fire 32, 417–434. https://doi.org/10.1071/WF22138

Turco, M., von Hardenberg, J., AghaKouchak, A., Llasat, M.C., Provenzale, A., Trigo, R.M., 2017. On the key role of droughts in the dynamics of summer fires in Mediterranean Europe. Sci Rep 7, 81. https://doi.org/10.1038/s41598-017-00116-9

U.S. National Park Service, 2018. Wildfire Causes and Evaluations [WWW Document]. URL https://www.nps.gov/articles/wildfire-causes-and-evaluation.htm (accessed 10.14.25).

Verde, J.C., Zêzere, J.L., 2010. Assessment and validation of wildfire susceptibility and hazard in Portugal. Natural Hazards and Earth System Science 10, 485–497. https://doi.org/10.5194/nhess-10-485-2010

Wang, W., Zhao, F., Wang, Y., Huang, X., Ye, J., 2023. Seasonal differences in the spatial patterns of wildfire drivers and susceptibility in the southwest mountains of China. Science of The Total Environment 869, 161782. https://doi.org/10.1016/j.scitotenv.2023.161782

Yue, W., Gao, Y., Ma, Y., Ye, Z., Zhang, Y., 2025. Wildfire risk assessment in Sichuan Province, China: hazard modeling approach considering different combinations of classification criteria and connection values of factor attributes. Int. J. Wildland Fire 34. https://doi.org/10.1071/WF25089

Zigner, K., Carvalho, L.M.V., Jones, C., Benoit, J., Duine, G.J., Roberts, D., Fujioka, F., Moritz, M., Elmquist, N., Hazard, R., 2022. Wildfire Risk in the Complex Terrain of the Santa Barbara Wildland–Urban Interface during Extreme Winds. Fire 5. https://doi.org/10.3390/fire5050138

SUPLEMENTARY MATERIAL

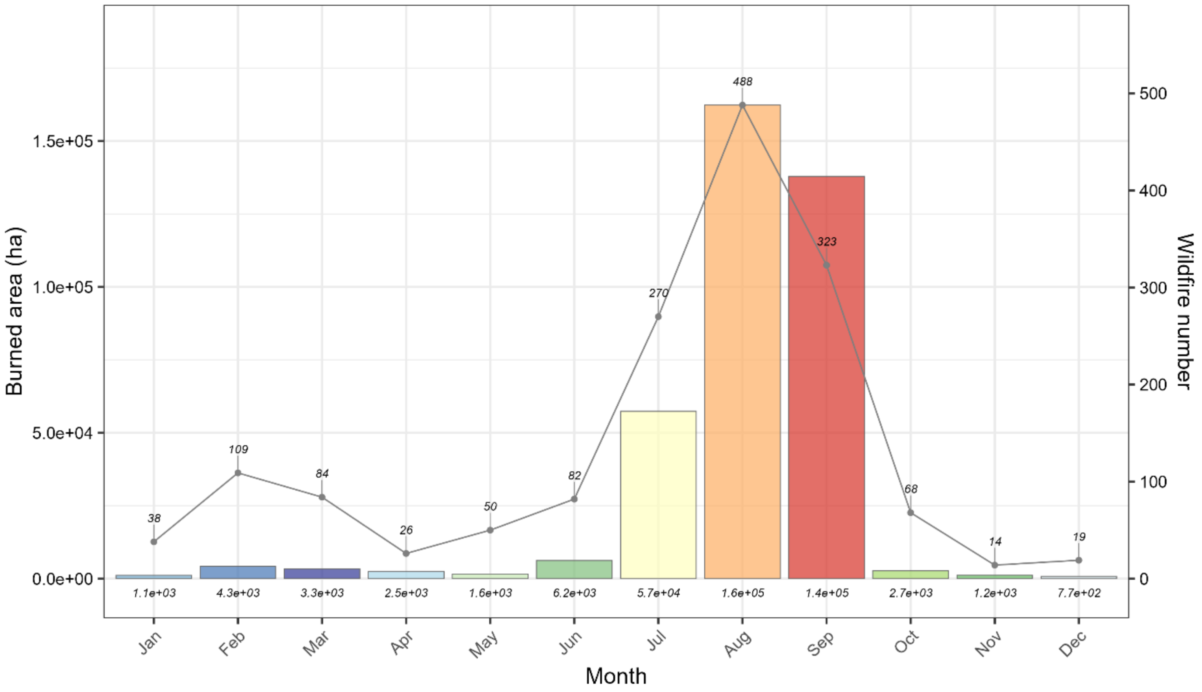

Annex A. Monthly distribution of fire activity, juxtaposing Total Burned Area (ha) against the Total Number of Fires. The bars illustrate the burned area (left axis), with total values in hectares displayed at the base. The superimposed gray line depicts the total number of occurrences (right axis), with the exact counts provided above each data point.

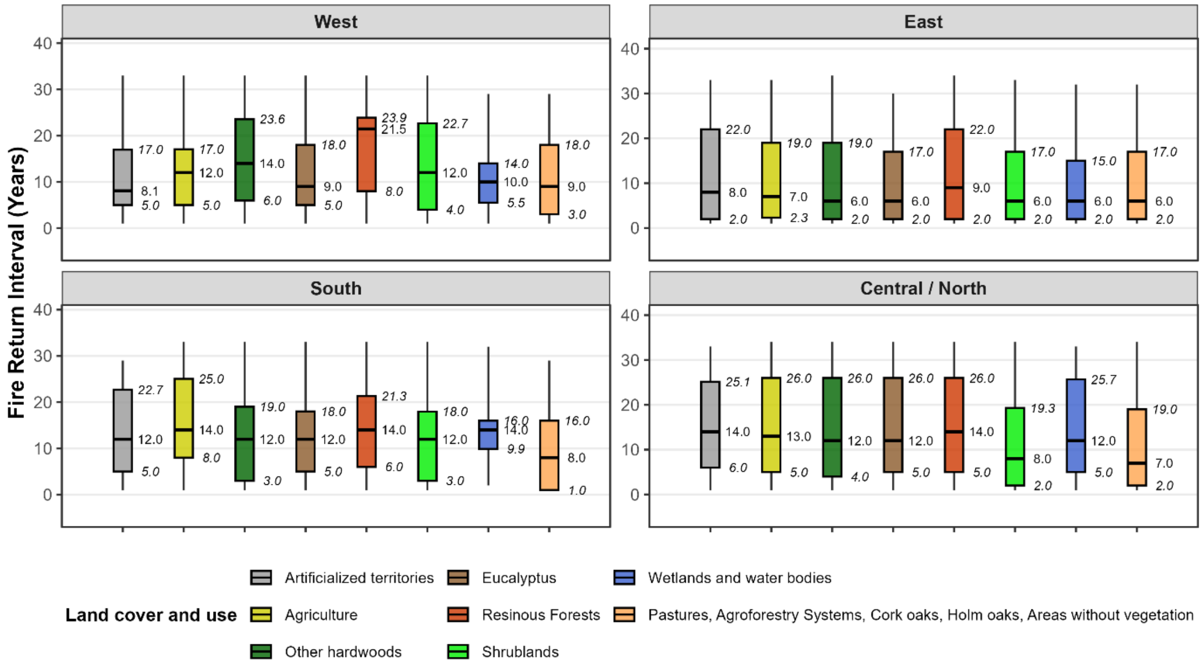

Annex B. Distribution of the Fire Return Interval (FRI) stratified by Land Use and Cover (LUC) class and geoclimatic cluster (West, East, South, and Central/North) for the 1990–2024 period. Vertical whiskers extend across the full data range (minimum to maximum). The colored band for each category delineates the 80% inter-percentile range (spanning from the 10th to the 90th percentile). The black horizontal line within the band represents the median (50th Percentile). Numeric labels indicate, from top to bottom, the 90th percentile, the median, and the 10th percentile.

Annex C. Detailed statistics for the predictor variables across the four hazard models (Overall, Aug–Sep, Jul, and Oct–Jun). The tables present, for each class/quantile of every variable, the total area, burned area, burning ratio $R_{v,c}$, and the corresponding normalized score $S_{v,c}$, as defined by Equations 1 and 2.

Model: Overall						
Variable	Class Name	TA (ha)	BA (ha)	BA/TA	$R_{v,c}$	$S_{v,c}$
LUC	Artificial Territories	153,075	1,282	0.008	0.57	0.45
LUC	Agriculture	650,124	11,844	0.018	1.23	0.97
LUC	Pastures. Agroforestry Systems. Cork Oaks. Holm Oaks. and Bare Land	293,073	11,936	0.041	2.75	2.17
LUC	Other Broadleaves	186,378	15,060	0.081	5.45	4.3
LUC	Eucalyptus	458,197	40,513	0.088	5.97	4.7
LUC	Resinous Forests	670,258	42,104	0.063	4.24	3.34
LUC	Shrublands	372,928	55,268	0.148	10	7.88
LUC	Wetlands and Water Bodies	35,898	227	0.006	0.43	0.34
ASP	North	267,867	15,166	0.057	7.8	3.01
ASP	Northeast	317,824	19,188	0.06	8.31	3.21
ASP	East	322,657	20,841	0.065	8.89	3.44
ASP	Southeast	375,717	27,285	0.073	10	3.86

ASP	South	319,978	20,866	0.065	8.98	3.47
ASP	Southwest	379,721	23,619	0.062	8.57	3.31
ASP	West	374,562	22,697	0.061	8.34	3.22
ASP	Northwest	387,681	24,709	0.064	8.78	3.39
ASP	Flat	72,008	3,764	0.052	7.2	2.78
EDA (km)	Quantile 1	897,778	20,567	0.023	2.05	1.22
EDA (km)	Quantile 2	187,371	8,373	0.045	4	2.38
EDA (km)	Quantile 3	342,012	20,473	0.06	5.36	3.18
EDA (km)	Quantile 4	340,285	27,247	0.08	7.17	4.26
EDA (km)	Quantile 5	350,662	34,877	0.099	8.9	5.29
EDA (km)	Quantile 6	349,603	39,064	0.112	10	5.94
EDA (km)	Quantile 7	352,220	27,634	0.078	7.02	4.17
FFD (ffd/ha)	Quantile 1	467,663	13,258	0.028	1.67	1.51
FFD (ffd/ha)	Quantile 2	260,087	13,873	0.053	3.15	2.84
FFD (ffd/ha)	Quantile 3	353,962	22,690	0.064	3.78	3.41
FFD (ffd/ha)	Quantile 4	360,605	16,578	0.046	2.71	2.45

FFD (ffd/ha)	Quantile 5	356,364	60,394	0.169	10	9.02
FFD (ffd/ha)	Quantile 6	320,105	14,949	0.047	2.76	2.48
FFD (ffd/ha)	Quantile 7	358,689	13,044	0.036	2.15	1.93
FFD (ffd/ha)	Quantile 8	344,953	23,608	0.068	4.04	3.64
POP (inhab/ha)	Quantile 1	1,058,331	83,507	0.079	9.76	4.2
POP (inhab/ha)	Quantile 2	351,978	21,715	0.062	7.63	3.28
POP (inhab/ha)	Quantile 3	352,280	28,471	0.081	10	4.3
POP (inhab/ha)	Quantile 4	352,382	27,392	0.078	9.62	4.14
POP (inhab/ha)	Quantile 5	352,469	13,331	0.038	4.68	2.01
POP (inhab/ha)	Quantile 6	352,491	3,820	0.011	1.34	0.58
ELV (m)	Quantile 1	352,380	4,016	0.011	0.91	0.61
ELV (m)	Quantile 2	352,429	12,923	0.037	2.93	1.95
ELV (m)	Quantile 3	352,414	17,973	0.051	4.07	2.71

ELV (m)	Quantile 4	352,311	18,520	0.053	4.2	2.8
ELV (m)	Quantile 5	352,407	16,197	0.046	3.67	2.45
ELV (m)	Quantile 6	352,346	27,059	0.077	6.14	4.09
ELV (m)	Quantile 7	353,220	37,544	0.106	8.49	5.65
ELV (m)	Quantile 8	351,535	44,002	0.125	10	6.66
SLP (°)	Quantile 1	352,231	5,742	0.016	1.49	0.87
SLP (°)	Quantile 2	352,231	10,422	0.03	2.71	1.57
SLP (°)	Quantile 3	352,231	15,675	0.045	4.07	2.37
SLP (°)	Quantile 4	352,232	20,681	0.059	5.37	3.12
SLP (°)	Quantile 5	352,232	25,022	0.071	6.5	3.78
SLP (°)	Quantile 6	352,249	29,195	0.083	7.59	4.41
SLP (°)	Quantile 7	352,212	32,938	0.094	8.56	4.98
SLP (°)	Quantile 8	352,230	38,477	0.109	10	5.81
NDP10	Quantile 1	351,639	19,443	0.055	2.94	2.94
NDP10	Quantile 2	351,474	7,663	0.022	1.16	1.16
NDP10	Quantile 3	351,560	12,134	0.035	1.84	1.84

NDP10	Quantile 4	351,629	13,796	0.039	2.09	2.09
NDP10	Quantile 5	351,559	18,907	0.054	2.86	2.86
NDP10	Quantile 6	351,532	22,723	0.065	3.44	3.44
NDP10	Quantile 7	351,568	17,363	0.049	2.63	2.63
NDP10	Quantile 8	351,473	66,063	0.188	10	10
T25 (°C)	Quantile 1	351,591	16,970	0.048	4.28	2.57
T25 (°C)	Quantile 2	351,543	21,527	0.061	5.44	3.26
T25 (°C)	Quantile 3	351,594	19,425	0.055	4.9	2.94
T25 (°C)	Quantile 4	351,572	28,465	0.081	7.19	4.31
T25 (°C)	Quantile 5	351,491	39,596	0.113	10	5.99
T25 (°C)	Quantile 6	351,555	18,739	0.053	4.73	2.84
T25 (°C)	Quantile 7	351,628	23,638	0.067	5.97	3.58
T25 (°C)	Quantile 8	351,460	9,730	0.028	2.46	1.47
PREC (mm)	Quantile 1	351,606	6,242	0.018	1.02	0.94
PREC (mm)	Quantile 2	351,543	12,196	0.035	1.99	1.85
PREC (mm)	Quantile 3	351,594	12,349	0.035	2.01	1.87

PREC (mm)	Quantile 4	351,562	14,798	0.042	2.41	2.24
PREC (mm)	Quantile 5	351,535	20,884	0.059	3.4	3.16
PREC (mm)	Quantile 6	351,544	22,714	0.065	3.7	3.44
PREC (mm)	Quantile 7	351,527	27,536	0.078	4.49	4.17
PREC (mm)	Quantile 8	351,524	61,372	0.175	10	9.29
RAD (Whm2)	Quantile 1	352,381	29,768	0.084	7.13	4.49
RAD (Whm2)	Quantile 2	352,384	15,530	0.044	3.72	2.34
RAD (Whm2)	Quantile 3	352,377	9,360	0.027	2.24	1.41
RAD (Whm2)	Quantile 4	352,380	15,523	0.044	3.72	2.34
RAD (Whm2)	Quantile 5	352,380	19,265	0.055	4.61	2.91
RAD (Whm2)	Quantile 6	352,381	20,203	0.057	4.84	3.05
RAD (Whm2)	Quantile 7	352,380	26,829	0.076	6.43	4.05
RAD (Whm2)	Quantile 8	352,380	41,755	0.118	10	6.3
TMAX (°C)	Quantile 1	351,605	29,404	0.084	9.25	4.45
TMAX (°C)	Quantile 2	351,540	18,926	0.054	5.96	2.86
TMAX (°C)	Quantile 3	351,527	31,765	0.09	10	4.81

TMAX (°C)	Quantile 4	351,620	28,004	0.08	8.81	4.24
TMAX (°C)	Quantile 5	351,482	22,730	0.065	7.16	3.44
TMAX (°C)	Quantile 6	351,556	20,105	0.057	6.33	3.04
TMAX (°C)	Quantile 7	351,565	22,524	0.064	7.09	3.41
TMAX (°C)	Quantile 8	351,540	4,634	0.013	1.46	0.7
AWS (m/s)	Quantile 1	350,821	19,671	0.056	6.75	2.98
AWS (m/s)	Quantile 2	350,780	19,992	0.057	6.86	3.03
AWS (m/s)	Quantile 3	350,801	17,236	0.049	5.91	2.61
AWS (m/s)	Quantile 4	350,795	17,265	0.049	5.92	2.62
AWS (m/s)	Quantile 5	350,807	25,486	0.073	8.74	3.87
AWS (m/s)	Quantile 6	350,782	29,157	0.083	10	4.42
AWS (m/s)	Quantile 7	350,798	26,506	0.076	9.09	4.02
AWS (m/s)	Quantile 8	350,793	22,246	0.063	7.63	3.37

Model: Aug - Sep

Variable	Class Name	TA (ha)	BA (ha)	BA/TA	$R_{v,c}$	$S_{v,c}$
LUC	Artificial Territories	153,075	1,023	0.007	0.56	0.43
LUC	Agriculture	650,124	9,402	0.014	1.22	0.93

LUC	Pastures. Agroforestry Systems. Cork Oaks. Holm Oaks. and Bare Land	293,073	8,872	0.03	2.55	1.95
LUC	Other Broadleaves	186,378	11,341	0.061	5.13	3.91
LUC	Eucalyptus	458,197	33,384	0.073	6.15	4.69
LUC	Resinous Forests	670,258	34,015	0.051	4.28	3.26
LUC	Shrublands	372,928	44,198	0.119	10	7.62
LUC	Wetlands and Water Bodies	35,898	177	0.005	0.42	0.32
ASP	North	267,867	12,296	0.046	7.98	2.95
ASP	Northeast	317,824	15,225	0.048	8.33	3.08
ASP	East	322,657	16,487	0.051	8.88	3.29
ASP	Southeast	375,717	21,620	0.058	10	3.7
ASP	South	319,978	16,695	0.052	9.07	3.36
ASP	Southwest	379,721	18,951	0.05	8.67	3.21
ASP	West	374,562	18,061	0.048	8.38	3.1
ASP	Northwest	387,681	19,970	0.052	8.95	3.31
ASP	Flat	72,008	3,017	0.042	7.28	2.69
EDA (km)	Quantile 1	897,778	16,485	0.018	2.06	1.18

EDA (km)	Quantile 2	187,371	6,766	0.036	4.04	2.32
EDA (km)	Quantile 3	342,012	16,433	0.048	5.38	3.09
EDA (km)	Quantile 4	340,285	21,771	0.064	7.16	4.11
EDA (km)	Quantile 5	350,662	27,745	0.079	8.86	5.09
EDA (km)	Quantile 6	349,603	31,222	0.089	10	5.74
EDA (km)	Quantile 7	352,220	21,991	0.062	6.99	4.02
FFD (ffd/ha)	Quantile 1	467,663	8,094	0.017	1.21	1.11
FFD (ffd/ha)	Quantile 2	260,087	10,693	0.041	2.87	2.64
FFD (ffd/ha)	Quantile 3	353,962	19,009	0.054	3.75	3.45
FFD (ffd/ha)	Quantile 4	360,605	11,308	0.031	2.19	2.02
FFD (ffd/ha)	Quantile 5	356,364	50,975	0.143	10	9.2
FFD (ffd/ha)	Quantile 6	320,105	10,531	0.033	2.3	2.12
FFD (ffd/ha)	Quantile 7	358,689	10,438	0.029	2.03	1.87
FFD (ffd/ha)	Quantile 8	344,953	21,507	0.062	4.36	4.01
POP (inhab/ha)	Quantile 1	1,058,331	66,038	0.062	9.52	4.01

POP (inhab/ha)	Quantile 2	351,978	15,884	0.045	6.89	2.9
POP (inhab/ha)	Quantile 3	352,280	23,081	0.066	10	4.21
POP (inhab/ha)	Quantile 4	352,382	22,758	0.065	9.86	4.15
POP (inhab/ha)	Quantile 5	352,469	11,469	0.033	4.97	2.09
POP (inhab/ha)	Quantile 6	352,491	3,183	0.009	1.38	0.58
ELV (m)	Quantile 1	352,380	2,664	0.008	0.78	0.49
ELV (m)	Quantile 2	352,429	10,210	0.029	2.99	1.86
ELV (m)	Quantile 3	352,414	14,298	0.041	4.19	2.61
ELV (m)	Quantile 4	352,311	14,856	0.042	4.35	2.71
ELV (m)	Quantile 5	352,407	12,777	0.036	3.74	2.33
ELV (m)	Quantile 6	352,346	23,220	0.066	6.8	4.24
ELV (m)	Quantile 7	353,220	30,310	0.086	8.85	5.52
ELV (m)	Quantile 8	351,535	34,077	0.097	10	6.23
SLP (°)	Quantile 1	352,231	4,343	0.012	1.44	0.79

SLP (°)	Quantile 2	352,231	8,334	0.024	2.76	1.52
SLP (°)	Quantile 3	352,231	12,761	0.036	4.22	2.33
SLP (°)	Quantile 4	352,232	16,820	0.048	5.56	3.07
SLP (°)	Quantile 5	352,232	20,270	0.058	6.7	3.7
SLP (°)	Quantile 6	352,249	23,460	0.067	7.76	4.28
SLP (°)	Quantile 7	352,212	26,112	0.074	8.64	4.77
SLP (°)	Quantile 8	352,230	30,240	0.086	10	5.52
NDP10	Quantile 1	351,639	12,739	0.036	2.33	2.33
NDP10	Quantile 2	351,474	2,192	0.006	0.4	0.4
NDP10	Quantile 3	351,560	9,288	0.026	1.7	1.7
NDP10	Quantile 4	351,629	11,034	0.031	2.02	2.02
NDP10	Quantile 5	351,559	17,098	0.049	3.13	3.13
NDP10	Quantile 6	351,532	20,002	0.057	3.66	3.66
NDP10	Quantile 7	351,568	15,294	0.044	2.8	2.8
NDP10	Quantile 8	351,473	54,654	0.156	10	10
T25 (°C)	Quantile 1	351,591	12,257	0.035	3.52	2.24

T25 (°C)	Quantile 2	351,543	15,874	0.045	4.55	2.9
T25 (°C)	Quantile 3	351,594	14,802	0.042	4.25	2.71
T25 (°C)	Quantile 4	351,572	24,712	0.07	7.09	4.52
T25 (°C)	Quantile 5	351,491	34,859	0.099	10	6.38
T25 (°C)	Quantile 6	351,555	14,122	0.04	4.05	2.58
T25 (°C)	Quantile 7	351,628	18,863	0.054	5.41	3.45
T25 (°C)	Quantile 8	351,460	6,812	0.019	1.95	1.25
PREC (mm)	Quantile 1	351,606	3,294	0.009	0.65	0.6
PREC (mm)	Quantile 2	351,543	8,861	0.025	1.74	1.62
PREC (mm)	Quantile 3	351,594	9,949	0.028	1.95	1.82
PREC (mm)	Quantile 4	351,562	10,254	0.029	2.01	1.88
PREC (mm)	Quantile 5	351,535	15,773	0.045	3.1	2.89
PREC (mm)	Quantile 6	351,544	18,661	0.053	3.66	3.41
PREC (mm)	Quantile 7	351,527	24,549	0.07	4.82	4.49
PREC (mm)	Quantile 8	351,524	50,961	0.145	10	9.32
RAD (Whm2)	Quantile 1	352,381	23,919	0.068	7.22	4.37

RAD (Whm2)	Quantile 2	352,384	12,227	0.035	3.69	2.23
RAD (Whm2)	Quantile 3	352,377	7,228	0.021	2.18	1.32
RAD (Whm2)	Quantile 4	352,380	12,428	0.035	3.75	2.27
RAD (Whm2)	Quantile 5	352,380	15,440	0.044	4.66	2.82
RAD (Whm2)	Quantile 6	352,381	16,415	0.047	4.96	3
RAD (Whm2)	Quantile 7	352,380	21,629	0.061	6.53	3.95
RAD (Whm2)	Quantile 8	352,380	33,125	0.094	10	6.05
TMAX (°C)	Quantile 1	351,605	25,392	0.072	9.73	4.64
TMAX (°C)	Quantile 2	351,540	14,950	0.043	5.73	2.73
TMAX (°C)	Quantile 3	351,527	26,084	0.074	10	4.77
TMAX (°C)	Quantile 4	351,620	23,129	0.066	8.86	4.23
TMAX (°C)	Quantile 5	351,482	17,833	0.051	6.84	3.26
TMAX (°C)	Quantile 6	351,556	16,349	0.047	6.27	2.99
TMAX (°C)	Quantile 7	351,565	17,032	0.048	6.53	3.12
TMAX (°C)	Quantile 8	351,540	1,533	0.004	0.59	0.28
AWS (m/s)	Quantile 1	350,821	17,483	0.05	7.66	3.2

AWS (m/s)	Quantile 2	350,780	14,444	0.041	6.33	2.65
AWS (m/s)	Quantile 3	350,801	12,519	0.036	5.49	2.29
AWS (m/s)	Quantile 4	350,795	13,630	0.039	5.98	2.5
AWS (m/s)	Quantile 5	350,807	20,669	0.059	9.06	3.79
AWS (m/s)	Quantile 6	350,782	21,542	0.061	9.44	3.95
AWS (m/s)	Quantile 7	350,798	22,811	0.065	10	4.18
AWS (m/s)	Quantile 8	350,793	18,717	0.053	8.21	3.43

Model: Jul

Variable	Class Name	TA (ha)	BA (ha)	BA/TA	$R_{v,c}$	$S_{v,c}$
LUC	Artificial Territories	153,075	182	0.001	1.34	0.93
LUC	Agriculture	650,124	1,338	0.002	2.32	1.62
LUC	Pastures. Agroforestry Systems. Cork Oaks. Holm Oaks. and Bare Land	293,073	1,500	0.005	5.78	4.02
LUC	Other Broadleaves	186,378	1,345	0.007	8.14	5.67
LUC	Eucalyptus	458,197	3,909	0.009	9.63	6.7
LUC	Resinous Forests	670,258	3,607	0.005	6.07	4.23
LUC	Shrublands	372,928	3,304	0.009	10	6.96
LUC	Wetlands and Water Bodies	35,898	41	0.001	1.28	0.89

ASP	North	267,867	1,390	0.005	8.95	4.08
ASP	Northeast	317,824	1,839	0.006	9.99	4.55
ASP	East	322,657	1,797	0.006	9.61	4.38
ASP	Southeast	375,717	2,044	0.005	9.39	4.27
ASP	South	319,978	1,640	0.005	8.84	4.03
ASP	Southwest	379,721	1,910	0.005	8.68	3.95
ASP	West	374,562	2,011	0.005	9.26	4.22
ASP	Northwest	387,681	2,246	0.006	10	4.55
ASP	Flat	72,008	346	0.005	8.29	3.78
EDA (km)	Quantile 1	897,778	2,158	0.002	2.64	1.89
EDA (km)	Quantile 2	187,371	775	0.004	4.54	3.25
EDA (km)	Quantile 3	342,012	1,836	0.005	5.89	4.22
EDA (km)	Quantile 4	340,285	2,318	0.007	7.47	5.35
EDA (km)	Quantile 5	350,662	2,909	0.008	9.1	6.52
EDA (km)	Quantile 6	349,603	3,186	0.009	10	7.16
EDA (km)	Quantile 7	352,220	2,043	0.006	6.36	4.56

FFD (ffd/ha)	Quantile 1	467,663	3,576	0.008	8.06	6.01
FFD (ffd/ha)	Quantile 2	260,087	725	0.003	2.94	2.19
FFD (ffd/ha)	Quantile 3	353,962	1,560	0.004	4.64	3.46
FFD (ffd/ha)	Quantile 4	360,605	3,422	0.009	10	7.46
FFD (ffd/ha)	Quantile 5	356,364	2,267	0.006	6.7	5
FFD (ffd/ha)	Quantile 6	320,105	1,366	0.004	4.5	3.35
FFD (ffd/ha)	Quantile 7	358,689	807	0.002	2.37	1.77
FFD (ffd/ha)	Quantile 8	344,953	1,504	0.004	4.59	3.43
POP (inhab/ha)	Quantile 1	1,058,331	6,409	0.006	8.36	4.76
POP (inhab/ha)	Quantile 2	351,978	2,303	0.007	9.03	5.14
POP (inhab/ha)	Quantile 3	352,280	2,552	0.007	10	5.69
POP (inhab/ha)	Quantile 4	352,382	2,293	0.007	8.98	5.11
POP (inhab/ha)	Quantile 5	352,469	1,311	0.004	5.13	2.92

POP (inhab/ha)	Quantile 6	352,491	356	0.001	1.39	0.79
ELV (m)	Quantile 1	352,380	676	0.002	2.31	1.51
ELV (m)	Quantile 2	352,429	1,635	0.005	5.58	3.65
ELV (m)	Quantile 3	352,414	2,507	0.007	8.56	5.59
ELV (m)	Quantile 4	352,311	2,371	0.007	8.1	5.29
ELV (m)	Quantile 5	352,407	1,621	0.005	5.54	3.62
ELV (m)	Quantile 6	352,346	1,345	0.004	4.59	3
ELV (m)	Quantile 7	353,220	2,935	0.008	10	6.53
ELV (m)	Quantile 8	351,535	2,135	0.006	7.31	4.77
SLP (°)	Quantile 1	352,231	750	0.002	2.52	1.67
SLP (°)	Quantile 2	352,231	1,068	0.003	3.59	2.38
SLP (°)	Quantile 3	352,231	1,283	0.004	4.31	2.86
SLP (°)	Quantile 4	352,232	1,621	0.005	5.45	3.62
SLP (°)	Quantile 5	352,232	2,066	0.006	6.94	4.61
SLP (°)	Quantile 6	352,249	2,519	0.007	8.47	5.62
SLP (°)	Quantile 7	352,212	2,940	0.008	9.88	6.56

SLP (°)	Quantile 8	352,230	2,975	0.008	10	6.64
NDP10	Quantile 1	351,639	4,474	0.013	10	10
NDP10	Quantile 2	351,474	2,284	0.006	5.11	5.11
NDP10	Quantile 3	351,560	1,577	0.004	3.53	3.53
NDP10	Quantile 4	351,629	1,408	0.004	3.15	3.15
NDP10	Quantile 5	351,559	1,175	0.003	2.63	2.63
NDP10	Quantile 6	351,532	1,256	0.004	2.81	2.81
NDP10	Quantile 7	351,568	644	0.002	1.44	1.44
NDP10	Quantile 8	351,473	2,405	0.007	5.38	5.38
T25 (°C)	Quantile 1	351,591	2,047	0.006	6.93	4.58
T25 (°C)	Quantile 2	351,543	1,598	0.005	5.42	3.57
T25 (°C)	Quantile 3	351,594	895	0.003	3.03	2
T25 (°C)	Quantile 4	351,572	2,703	0.008	9.16	6.04
T25 (°C)	Quantile 5	351,491	1,002	0.003	3.4	2.24
T25 (°C)	Quantile 6	351,555	1,915	0.005	6.49	4.28
T25 (°C)	Quantile 7	351,628	2,952	0.008	10	6.6

T25 (°C)	Quantile 8	351,460	2,110	0.006	7.15	4.72
PREC (mm)	Quantile 1	351,606	2,027	0.006	7.86	4.53
PREC (mm)	Quantile 2	351,543	2,126	0.006	8.24	4.75
PREC (mm)	Quantile 3	351,594	1,359	0.004	5.27	3.04
PREC (mm)	Quantile 4	351,562	2,320	0.007	8.99	5.19
PREC (mm)	Quantile 5	351,535	2,579	0.007	10	5.77
PREC (mm)	Quantile 6	351,544	2,175	0.006	8.43	4.86
PREC (mm)	Quantile 7	351,527	940	0.003	3.64	2.1
PREC (mm)	Quantile 8	351,524	1,697	0.005	6.58	3.8
RAD (Whm2)	Quantile 1	352,381	2,921	0.008	10	6.51
RAD (Whm2)	Quantile 2	352,384	1,833	0.005	6.28	4.09
RAD (Whm2)	Quantile 3	352,377	1,197	0.003	4.1	2.67
RAD (Whm2)	Quantile 4	352,380	1,748	0.005	5.99	3.9
RAD (Whm2)	Quantile 5	352,380	1,993	0.006	6.82	4.45
RAD (Whm2)	Quantile 6	352,381	1,566	0.004	5.36	3.49
RAD (Whm2)	Quantile 7	352,380	1,854	0.005	6.35	4.14

RAD (Whm2)	Quantile 8	352,380	2,113	0.006	7.23	4.71
TMAX (°C)	Quantile 1	351,605	457	0.001	1.64	1.02
TMAX (°C)	Quantile 2	351,540	1,680	0.005	6.02	3.76
TMAX (°C)	Quantile 3	351,527	1,621	0.005	5.81	3.62
TMAX (°C)	Quantile 4	351,620	1,567	0.004	5.61	3.5
TMAX (°C)	Quantile 5	351,482	2,506	0.007	8.98	5.6
TMAX (°C)	Quantile 6	351,556	2,301	0.007	8.25	5.15
TMAX (°C)	Quantile 7	351,565	2,791	0.008	10	6.24
TMAX (°C)	Quantile 8	351,540	2,300	0.007	8.24	5.14
AWS (m/s)	Quantile 1	350,821	954	0.003	2.99	2.14
AWS (m/s)	Quantile 2	350,780	2,887	0.008	9.05	6.47
AWS (m/s)	Quantile 3	350,801	2,229	0.006	6.98	4.99
AWS (m/s)	Quantile 4	350,795	1,665	0.005	5.22	3.73
AWS (m/s)	Quantile 5	350,807	1,959	0.006	6.14	4.39
AWS (m/s)	Quantile 6	350,782	3,192	0.009	10	7.15
AWS (m/s)	Quantile 7	350,798	1,544	0.004	4.84	3.46

AWS (m/s)	Quantile 8	350,793	793	0.002	2.48	1.78
Model: Out - Jun						
Variable	Class Name	TA (ha)	BA (ha)	BA/TA	$R_{v,c}$	$S_{v,c}$
LUC	Artificial Territories	153,075	58	0	0.19	0.15
LUC	Agriculture	650,124	937	0.001	0.71	0.59
LUC	Pastures. Agroforestry Systems. Cork Oaks. Holm Oaks. and Bare Land	293,073	1,479	0.005	2.48	2.05
LUC	Other Broadleaves	186,378	2,322	0.012	6.13	5.07
LUC	Eucalyptus	458,197	3,093	0.007	3.32	2.75
LUC	Resinous Forests	670,258	4,336	0.006	3.18	2.63
LUC	Shrublands	372,928	7,580	0.02	10	8.27
LUC	Wetlands and Water Bodies	35,898	9	0	0.13	0.11
ASP	North	267,867	1,416	0.005	5.62	2.15
ASP	Northeast	317,824	2,019	0.006	6.76	2.59
ASP	East	322,657	2,456	0.008	8.1	3.1
ASP	Southeast	375,717	3,532	0.009	10	3.83
ASP	South	319,978	2,476	0.008	8.23	3.15
ASP	Southwest	379,721	2,665	0.007	7.47	2.86

ASP	West	374,562	2,494	0.007	7.08	2.71
ASP	Northwest	387,681	2,370	0.006	6.5	2.49
ASP	Flat	72,008	378	0.005	5.59	2.14
EDA (km)	Quantile 1	897,778	1,705	0.002	1.46	0.77
EDA (km)	Quantile 2	187,371	787	0.004	3.22	1.71
EDA (km)	Quantile 3	342,012	2,087	0.006	4.68	2.48
EDA (km)	Quantile 4	340,285	3,018	0.009	6.81	3.61
EDA (km)	Quantile 5	350,662	4,123	0.012	9.02	4.79
EDA (km)	Quantile 6	349,603	4,556	0.013	10	5.3
EDA (km)	Quantile 7	352,220	3,538	0.01	7.71	4.09
FFD (ffd/ha)	Quantile 1	467,663	1,581	0.003	1.74	1.38
FFD (ffd/ha)	Quantile 2	260,087	2,330	0.009	4.61	3.65
FFD (ffd/ha)	Quantile 3	353,962	2,077	0.006	3.02	2.39
FFD (ffd/ha)	Quantile 4	360,605	1,840	0.005	2.63	2.08
FFD (ffd/ha)	Quantile 5	356,364	6,918	0.019	10	7.9
FFD (ffd/ha)	Quantile 6	320,105	2,886	0.009	4.64	3.67

FFD (ffd/ha)	Quantile 7	358,689	1,737	0.005	2.49	1.97
FFD (ffd/ha)	Quantile 8	344,953	460	0.001	0.69	0.54
POP (inhab/ha)	Quantile 1	1,058,331	10,800	0.01	10	4.15
POP (inhab/ha)	Quantile 2	351,978	3,426	0.01	9.54	3.96
POP (inhab/ha)	Quantile 3	352,280	2,651	0.008	7.37	3.06
POP (inhab/ha)	Quantile 4	352,382	2,219	0.006	6.17	2.56
POP (inhab/ha)	Quantile 5	352,469	489	0.001	1.36	0.56
POP (inhab/ha)	Quantile 6	352,491	230	0.001	0.64	0.27
ELV (m)	Quantile 1	352,380	531	0.002	0.7	0.61
ELV (m)	Quantile 2	352,429	1,057	0.003	1.4	1.22
ELV (m)	Quantile 3	352,414	1,132	0.003	1.5	1.31
ELV (m)	Quantile 4	352,311	1,273	0.004	1.68	1.47
ELV (m)	Quantile 5	352,407	1,661	0.005	2.19	1.92

ELV (m)	Quantile 6	352,346	2,419	0.007	3.2	2.79
ELV (m)	Quantile 7	353,220	4,188	0.012	5.52	4.83
ELV (m)	Quantile 8	351,535	7,553	0.021	10	8.74
SLP (°)	Quantile 1	352,231	614	0.002	1.18	0.71
SLP (°)	Quantile 2	352,231	926	0.003	1.77	1.07
SLP (°)	Quantile 3	352,231	1,529	0.004	2.93	1.77
SLP (°)	Quantile 4	352,232	2,116	0.006	4.05	2.45
SLP (°)	Quantile 5	352,232	2,552	0.007	4.89	2.95
SLP (°)	Quantile 6	352,249	3,075	0.009	5.88	3.55
SLP (°)	Quantile 7	352,212	3,769	0.011	7.21	4.36
SLP (°)	Quantile 8	352,230	5,225	0.015	10	6.04
NDP10	Quantile 1	351,639	2,189	0.006	2.53	2.53
NDP10	Quantile 2	351,474	2,994	0.009	3.47	3.47
NDP10	Quantile 3	351,560	1,219	0.003	1.41	1.41
NDP10	Quantile 4	351,629	1,250	0.004	1.45	1.45
NDP10	Quantile 5	351,559	595	0.002	0.69	0.69

NDP10	Quantile 6	351,5 32	1,46 6	0.00 4	1. 7	1. 7
NDP10	Quantile 7	351,5 68	1,43 6	0.00 4	1. 66	1. 66
NDP10	Quantile 8	351,4 73	8,63 6	0.02 5	10	10
T25 (°C)	Quantile 1	351,5 91	2,63 0	0.00 7	6. 57	3. 04
T25 (°C)	Quantile 2	351,5 43	4,00 2	0.01 1	10	4. 63
T25 (°C)	Quantile 3	351,5 94	3,53 9	0.01	8. 84	4. 1
T25 (°C)	Quantile 4	351,5 72	1,06 0	0.00 3	2. 65	1. 23
T25 (°C)	Quantile 5	351,4 91	3,54 5	0.01	8. 86	4. 1
T25 (°C)	Quantile 6	351,5 55	2,70 2	0.00 8	6. 75	3. 13
T25 (°C)	Quantile 7	351,6 28	1,57 7	0.00 4	3. 94	1. 83
T25 (°C)	Quantile 8	351,4 60	730	0.00 2	1. 82	0. 84
PREC (mm)	Quantile 1	351,6 06	818	0.00 2	0. 98	0. 95
PREC (mm)	Quantile 2	351,5 43	1,11 1	0.00 3	1. 33	1. 29
PREC (mm)	Quantile 3	351,5 94	1,00 1	0.00 3	1. 19	1. 16
PREC (mm)	Quantile 4	351,5 62	2,22 4	0.00 6	2. 65	2. 57
PREC (mm)	Quantile 5	351,5 35	2,50 2	0.00 7	2. 99	2. 9

PREC (mm)	Quantile 6	351,544	1,755	0.005	2.1	2.03
PREC (mm)	Quantile 7	351,527	1,996	0.006	2.38	2.31
PREC (mm)	Quantile 8	351,524	8,377	0.024	10	9.7
RAD (Whm2)	Quantile 1	352,381	2,871	0.008	4.52	3.32
RAD (Whm2)	Quantile 2	352,384	1,381	0.004	2.18	1.59
RAD (Whm2)	Quantile 3	352,377	841	0.002	1.32	0.97
RAD (Whm2)	Quantile 4	352,380	1,284	0.004	2.02	1.48
RAD (Whm2)	Quantile 5	352,380	1,748	0.005	2.75	2.02
RAD (Whm2)	Quantile 6	352,381	2,115	0.006	3.33	2.44
RAD (Whm2)	Quantile 7	352,380	3,227	0.009	5.08	3.73
RAD (Whm2)	Quantile 8	352,380	6,347	0.018	10	7.33
TMAX (°C)	Quantile 1	351,605	3,365	0.01	8.36	3.89
TMAX (°C)	Quantile 2	351,540	2,173	0.006	5.4	2.52
TMAX (°C)	Quantile 3	351,527	4,025	0.011	10	4.66
TMAX (°C)	Quantile 4	351,620	3,177	0.009	7.89	3.68
TMAX (°C)	Quantile 5	351,482	2,228	0.006	5.54	2.58

TMAX (°C)	Quantile 6	351,556	1,453	0.004	3.61	1.68
TMAX (°C)	Quantile 7	351,565	2,561	0.007	6.36	2.96
TMAX (°C)	Quantile 8	351,540	801	0.002	1.99	0.93
AWS (m/s)	Quantile 1	350,821	1,103	0.003	2.59	1.28
AWS (m/s)	Quantile 2	350,780	2,654	0.008	6.24	3.08
AWS (m/s)	Quantile 3	350,801	2,507	0.007	5.89	2.91
AWS (m/s)	Quantile 4	350,795	1,803	0.005	4.23	2.09
AWS (m/s)	Quantile 5	350,807	2,799	0.008	6.57	3.25
AWS (m/s)	Quantile 6	350,782	4,257	0.012	10	4.94
AWS (m/s)	Quantile 7	350,798	2,097	0.006	4.92	2.43
AWS (m/s)	Quantile 8	350,793	2,519	0.007	5.92	2.92

GENERAL CONCLUSIONS

The present thesis aimed to advance the understanding of wildfire dynamics in Central Portugal by integrating static spatial susceptibility models with dynamic, season-specific hazard assessments. Together, the findings underscore the complexity of Mediterranean fire regimes, which are governed by highly intertwined environmental, climatic, and socio-economic factors.

Through the evaluation of wildfire susceptibility (Chapter 1), this research highlighted the crucial support provided by environmental variables in predictive modeling, while also revealing a strong correlation between firefighter presence and rural depopulation. Topography plays a determining role in spatial vulnerability, with higher elevation areas exhibiting significantly greater fire susceptibility. Furthermore, the analysis of climatic drivers demonstrated that lower thresholds—specifically, the number of days with temperatures above 25 °C and precipitation over 10 mm—are more relevant predictors than general aggregated means or accumulated precipitation. Spatially, the highest susceptibility remains heavily concentrated in the northern and inland sections of the study area. This points to a critical need for targeted fire suppression and prevention efforts in less populous, higher-elevation regions dominated by shrublands, particularly within the districts of Guarda, Viseu, and Santarém.

Building upon this spatial foundation, the assessment of temporal fire hazard (Chapter 2) validated the core premise that wildfire dynamics are driven by seasonally distinct factors, rendering static, aggregated annual models inadequate. Statistical analyses confirmed the stratification of the fire year into three distinct regimes: High (August–September), Moderate (July), and Low (October–June). The seasonal models developed for the peak (AUC = 0.81) and low-activity (AUC = 0.80) periods—which are primarily governed by structural factors (topography) and fuel availability (precipitation)—significantly outperformed the reference overall annual model (AUC = 0.77). Conversely, the transitional July period (AUC = 0.58) exhibited a unique profile driven primarily by aridity, indicating that this specific window requires specialized predictors not fully captured by standard datasets.

A pivotal finding of this thesis challenges traditional assumptions regarding fuel memory and landscape resilience. The hypothesis that incorporating fire history via a Fire Return Interval (FRI) mask would enhance predictive accuracy was refuted for the most critical fire scenarios. The application of the FRI mask actually degraded the performance of both the overall and the peak-season (August–September) models. This failure provides compelling evidence that, under the extreme meteorological conditions characteristic of the peak season, the protective effect of younger vegetation is effectively overridden; fire propagates regardless of recent burning history. While the FRI adjustment yielded marginal gains during the less severe conditions of the low and moderate activity periods, relying on historical recurrence metrics to predict fuel limitation is insufficient during the catastrophic peak of the fire season.

Ultimately, these consolidated results offer vital insights for future fire management and landscape planning. Effective wildfire mitigation requires periodic model updates that incorporate higher-resolution data, seasonality, and complex socio-economic and cultural factors. Strategic interventions must be prioritized in depopulated inland regions where the hazard is most pronounced. Furthermore, acknowledging pyrobiocultural territories and integrating local fire management practices will be essential to foster sustainable, resilient landscapes capable of withstanding extreme fire events that bypass natural fuel barriers.